Line element and variational methods for color difference metrics

Dibakar Raj Pant

Line Element and Variational Methods for Color Difference Metrics

Dibakar Raj Pant

Doctoral School ED SIS 488

University Jean Monnet in collaboration with Gjøvik University College

A thesis submitted to The Jean Monnet University, Saint Etienne in conformity with the requirements for the degree of

PhilosophiæDoctor (PhD) in Images, Vision and Signal

2012

Lignes géodésiques et méthodes différentielles pour les métriques de différence couleur

Dibakar Raj PANT

Thèse présentée pour obtenir le grade de docteur
Laboratoire Hubert Curien UMR CNRS 5516
Université Jean Monnet-Saint Etienne

This thesis work was conducted in Gjøvik University College, Norway and co-supervised by

1) Professor Alain Treméau
Laboratoire Hubert Curien
University Jean Monnet, Saint-etienne, France
2) Associate Professor Ivar Farup
Faculty of Computer and Media Technology
Gjøvik University College, Norway
Date: February, 2012

PhD committee:

Professor Manuel Melgosa, Department of Optics, University of Granada, Spain
Professor Christine Fernandez-Maloigne, Laboratoire: signal - image - communications, University of Poitiers, France
Professor Rune Hjelsvold, The Media Technology Laboratory, Gjøvik University College, Norway
Professor Jon Yngve Hardeberg, The Norwegian Color Research Laboratory, Gjøvik University College, Norway

Abstract

Visual sensitivity to small color difference is an important factor for precision color matching. Small color differences can be measured by the line element theory in terms of color distances between a color point and neighborhoods of points in a color space. This theory gives a smooth positive definite symmetric metric tensor which describes threshold of color differences by ellipsoids in three dimensions and ellipses in two dimensions. The metric tensor is also known as the Riemannian metric tensor. In regard to the color differences, there are many color difference formulas and color spaces to predict visual difference between two colors but, it is still challenging due to the nonexistence of a perfect uniform color space. In such case, the Riemannian metric tensor can be used as a tool to study the performance of various color spaces and color difference metrics for measuring the perceptual color differences. It also computes the shortest length or the distance between any two points in a color space. The shortest length is called a geodesic. According to Schrödinger's hypothesis geodesics starting from the neutral point of a surface of constant brightness correspond to the curves of constant hue. The chroma contours are closed curves at constant intervals from the origin measured as the distance along the constant hue geodesics. This hypothesis can be utilized to test the performance of color difference formulas to predict perceptual attributes (hue and chroma) and distribution of color stimulus in any color space. In this research work, a method to formulate line element models of color difference formulas the ΔE^*_{ab} , the ΔE^*_{uv}, the OSA-UCS ΔE_E and infinitesimal approximation of CIEDE2000 (ΔE_{00}) is presented. The Jacobian method is employed to transfer their Riemannian metric tensors in other color spaces. The coefficients of such metric tensors are used to compute ellipses in two dimensions. The performance of these four color difference formulas is evaluated by comparing computed ellipses

with experimentally observed ellipses in different chromaticity diagrams. A method is also developed for comparing the similarity between a pair of ellipses. The technique works by calculating the ratio of the area of intersection and the area of union of a pair of ellipses. Similarly, at a fixed value of lightness L^*, hue geodesics originating from the achromatic point and their corresponding chroma contours of the above four formulas in the CIELAB color space are computed by solving the Euler-Lagrange equations in association with their Riemannian metrics. They are compared with with the Munsell chromas and hue circles at the Munsell values 3, 5 and 7. The result shows that neither formulas are fully perfect for matching visual color difference data sets. However, Riemannized ΔE_{00} and the ΔE_E formulas measure the visual color differences better than the ΔE^*_{ab} and the ΔE^*_{uv} formulas at local level. It is interesting to note that the latest color difference formulas like the OSA-UCS ΔE_E and the Riemannized ΔE_{00} do not show better performance to predict hue geodesics and chroma contours than the conventional CIELAB and CIELUV color difference formulas and none of these formulas fit the Munsell data accurately.

Résumé

Afin de pouvoir apparier de manière précise les couleurs il est essential de prendre en compte la sensibilité visuelle à percevoir de petites différences de couleur. Les petites différences de couleur peuvent être mesurées par des ellipses qui décrivent les différences justes observables (just noticeable difference - JND). Ces ellipses décrivent la faculté du Système Visuel Humain à discriminer des couleurs très peu différentes. D'un point de vue mathématique, ces ellipses peuvent être modélisées par une fonction différentielle positive de forme quadratique, caractéristique de ce que l'on appelle communément une métrique Riemannienne. La métrique Riemannienne peut être considérée comme un outil utile pour évaluer l'adéquation, la robustesse et la précision, d'un espace couleur ou d'une métrique couleur, à décrire, à mesurer, correctement les différences de couleur telles qu'elles sont perçues par le Système Visuel Humain. L'un des particularités de cette métrique est qu'elle modélise la plus petite distance qui sépare deux couleurs dans un espace couleur par une ligne géodésique. Selon l'hypothèse de Schrödinger les lignes géodésiques qui partent d'un point neutre d'une surface de luminosité constante décrivent des courbes de teinte constante. Les contours de chrominance (chroma) forment alors des courbes fermées à intervalles constants à partir de ce point neutre situées à une distance constante des lignes géodésiques associées à ces teintes constances. Cette hypothèse peut être utilisée pour tester la robustesse, la précision, des formules mathématiques utilisées pour mesurer des différences couleur (color difference formulas) et pour prédire quelle valeurs peuvent prendre tel ou tel attribut perceptuel, ex. la teinte et la saturation (hue and chroma), ou telle distribution de stimulus couleur, dans n'importe quel espace couleur. Dans cette thèse, nous présentons une méthode qui permet de modéliser les éléments de ligne (lignes géodésiques), correspondants aux formules

mathématiques Delta $E*ab$, Delta $E*uv$, OSA-UCS Delta E_E utilisées pour mesurer des différences couleur, ainsi que les éléments de ligne correspondants à l'approximation infinitésimales du CIEDE2000. La pertinence de ces quatre formules mathématiques a été évaluée par comparaison, dans différents plans de représentation chromatique, des ellipses prédites et des ellipses expérimentalement obtenues par observation visuelle. Pour chacune de ces formules mathématiques, nous avons également testé l'hypothèse de Schrödinger, en calculant à partir de la métrique Riemannienne, les lignes géodésiques de teinte et les contours de chroma associés, puis en comparant les courbes calculées dans l'espace couleur CIELAB avec celles obtenues dans le système Munsell. Les résultats que nous avons obtenus démontrent qu'aucune de ces formules mathématiques ne prédit précisément les différences de couleur telles qu'elles sont perçues par le Système Visuel Humain. Ils démontrent également que les deux dernières formules en date, OSA-UCS Delta E_E et l'approximation infinitésimale du CIEDE2000, ne sont pas plus précises que les formules conventionnelles calculées à partir des espaces couleur CIELAB et CIELUV, quand on se réfère au système Munsell (Munsell color order system).

I would like to dedicate this thesis
to my parents.

Acknowledgements

I would like to give sincere thanks to my supervisor associate Prof. Dr. Ivar Farup (Gjøvik University College) who has given continuous and incredible guidance to me for completing this research work, otherwise this work would not have been possible. Like wise, I would like to give many thanks to my thesis director Professor Alain Tremeau (Universite Jean Monnet, Saint Etienne) for his help, support and advice while pursuing this research work. The next important person is Professor Jon Yngve Hardeberg (Head, The Norwegian Color Research Laboratory, Gjøvik University college) to whom I am greatly indebted for his encouragement, help and advice during my three years research time.

Dr. Marius Pedresen, my great friend of the Norwegian Color Research Laboratory who never tired to help me for solving latex generated errors as well as in many practical matters, so how do I acknowledge you? many many thanks! Every member in the Norwegian Color Research Laboratory is great and helpful, I salute to associate Prof. Dr. Peter Nussbaum, Gabriele Simone, Arne Magnus Bakke, Aditya Sole, Raju, Steven le Moan and others.

Many of the faculties in the IMT, Gjøvik University College are co-operative and friendly and in particular, I would like to thank Associate Prof. Hans Petter Hornæs, Associate Prof. Dr. Patrick A.H. Bours (Head NISLAB), Prof. Katrin Franke, Associate Prof. Terje Stafseng(Head Media lab), Associate Prof. Dr. Faouzi Alaya Cheikh and others. I would like to thank the leaders of HIG, Rector Jørn Wroldsen, IMT Dean Morten Irgens, Director Inge Moen and all members of HIG.

Special thanks also goes to Hilde Bakke, Kathrine Huke and Helene GOODSIR (Administration and Development Coordinator of CIMET, Jean Mon-

net University) for their co-operation and assistance. I acknowledge all my IMT friends for their supporting hands.

I am also grateful to Dr. Michael Brill (Datacolor, US) for his insightful comments and discussions on this research work.

My parents and my family are super marvelous to me and their inspiration makes me work hard.

Contents

List of Figures

LIST OF FIGURES

Chapter 1

Introduction

1.1 Motivation

Many color spaces and color difference formulas have been developed over the past decades to predict visual color perception as far as possible. But, it is not happening because of the complex human visual system.

Riemann [49] described from his differential geometry that colors and the positions of objects of sense constitute a non-Euclidean manifold. Helmholtz [60] on the basis of Riemannian geometry presented a line element to describe how distance in a color space specifies pairs of color stimuli that give a particular constant perceptual difference in the RGB color space. This quantitative mathematical analysis has progressed further in the color vision by Schrödinger [50], Stiles [56] and Vos and Walraven [65]. JJ Vos [63] presented a pictorial outline about the implementation of line element as well as its importance in the color vision system (see Figure 1.1). He described 'Lower color metrics' for the laws of color mixture as exhibit in the trichromatic color space and 'Higher color metrics' for the line element in the sense that it builds on the fundamentals of lower color metrics. His concluding remarks of extended modelling of line elements for paradoxical effects of luminance and saturation on color discrimination deserve the renewed interest for color science researchers.

MacAdam [34] successfully implemented the line element theory in a two dimensional space that have the Riemannian form for his experimental data to measure the visual sensitivity to color differences. He derived just noticeable difference (JND) ellipses from the metric tensor g_{ik} and plotted them in the xy chromaticity diagram to

Figure 1.1: Outline of the events leading from lower to higher color metrics - figure reproduced from the article [63].

describe the threshold of color matches about a color center [33]. Many other threshold and in recent supra threshold color matching data sets have been developed and established [3, 5, 31, 66, 69]. All these data sets are represented in terms of variability ellipses in color spaces and they are derived from the Riemannian metric. These data sets are the basis for the many color difference formulas developed so far by the Commission Internationale de l Éclairage (CIE) and others. It shows an integral relationship between color difference formulas and the line element theory.

With respect to color differences, the main objective of color difference formulas is to give quantitative color difference value (ΔE) that should represent the visual color difference perceived by the human visual system (color difference obtained from the psychophysical experiment). Many color difference formulas like the ΔE^*_{ab} [8] and the ΔE_{00} [32] of the CIELAB space, the ΔE^*_{uv} of the CIELUV space [8], the ΔE_E of the log compressed OSA-UCS space [44] and so on have been developed to fulfill such an objective. Unfortunately, all these formulas so far developed do not have perfect uniform color spaces. It means they are unable to to measure the visual perception of color differences sufficiently [11, 12, 20, 27, 38]. Theoretically in a perfect uniform color space, the color matching ellipses should become circles. Figures 1.2 and 1.3 show MacAdam's ellipses transformed into the CIELAB and the CIELUV color spaces and they appeared again ellipses which indicate non-uniform color spaces.

Figure 1.2: MacAdam's ellipses in the CIELAB color space - Enlarged 10 times.

These existing formulas are optimized to predict certain set of visual data. It can not be assured that such formulas are able to predict other sets of visual data which

Figure 1.3: MacAdam's ellipses in the CIELUV color space - Enlarged 10 times.

are obtained under different experimental conditions. On the other hand, color and imaging industries have a continuous demand to know which color difference formula or color space should be used for a specific application. This crucial fact necessitates to evaluate the performance of color difference formulas for measuring the visual color difference data. Mathematical modelling of color difference formulas to calculate small color differences by applying the line element theory could be one option. Further, many color difference formulas use the Euclidean distance to measure color differences between two color points in a color space. But, color researchers have found that the small color difference calculation using the Euclidean distance does not agree sufficiently with the perceptual color difference due to the curvilinear nature of the color space [12, 19, 25, 29, 51, 53, 58]. The beauty of line element theory for assessing color differences is that it can deal with the Euclidean as well as non-Euclidean color perception space at a time where as the color difference formulas in nearly every case assume that color perception is Euclidean.

Line element is also used to study the perceptual attributes hue, chroma and lightness by computing the appropriate geometrical quantities which correlates in some way with these attributes [70]. The geometrical quantities imply hue geodesics and chroma contours originating from a point representing an achromatic stimulus on a surface of constant brightness. This conjecture can be applied to color difference formulas to know how well they predict such attributes in comparison to the experimentally observed the Munsell like color order system in a color space because there is no analytical expression to convert the CIE system to the Munsell system.

1.2 Aims

The first aim of this research study is to implement the line element theory based on the Riemannian geometry for the color difference formulas to evaluate their performances for measuring the visual color difference data. Four color difference formulas the ΔE^*_{ab}, the the ΔE^*_{uv}, the ΔE_{00} and the OSA-UCS based ΔE_E are chosen to study because of their symmetrical nature and specific importance in the color vision. Implementation of the line element model for these four formulas to accomplish the above task consist following steps:

- Formulation of the line element distance of above color difference formulas by converting color coordinates into color vectors.
- Computation of the Riemannian metric tensors g_{ik} of the formulas.
- Computation of the equidistance (threshold) ellipses in a color space.
- Formulation of a pair of ellipses comparison method.
- Comparison of the computed ellipses of the formulas with the experimentally observed standard data sets.

The second aim is to compute hue geodesics and chroma contours of these formulas in the CIELAB color space to study the distribution of their color stimuli with respect to the Munsell color order system. Such computations allow us to evaluate how well they predict perceptual attributes defined in terms of hue, chroma and lightness. The following steps should be carried out in order to complete this aim:

- Formulation of the Euler-Lagrange equations of above color difference formulas.
- Computation of the Christoffel symbols defined in terms Riemannian metric tensors g_{ik} of the formulas in the CIELAB color space.
- Comparison of the computed hue geodesics and chroma contours of the formulas with the the Munsell color system.

1.3 Research Methodology

The nature of this research study is based on theoretical consideration of the Riemannian form regarding the functioning of color difference formulas coupled with certain threshold and supra threshold experimental data sets. Therefore, the author has used mathematical and statistical methods to carry out this research. Jacobian coordinate transfer method is used to transfer the metric coefficients from one color space to other. Statistical the sign test is adopted to evaluate the significance of the results come from comparing pairs of ellipses. Graphical methods like histogram plots, box plots and cumulative distribution function plots are also used to show the research results. Likewise, to compute hue geodesics and chroma contours, the Runge-Kutta and the central difference numerical techniques are applied.

1.4 Chapter Introduction

The intent of chapter 2 is to provide relatively simple concept of color theory development and state of the art used in this research work. Section 2.1 describes historical background of the color theory and overview of the line element model for the color discrimination. Section 2.2 includes basic colorimetry with emphasized on the CIE 1931 and 1964 system, tristimulus values and chromaticity coordinates. Visual color difference data and its type are described in section 2.3. The next section 2.4 gives brief description of the CIELAB, the CIELUV, and the OSA-UCS color spaces as well as color difference formulas associated with theses space. The color order system and the Munsell system which describe three classical attributes (value, hue and chroma) in color perception are presented in section 2.5 and subsection 2.5.1. The prime focused topic Riemannian geometry and the line element for color space is described clearly in section 2.6. Different historical line element models for the color space are summarized in section 2.7. Analysis of color difference formulas by the line element model also require color space transformation and it is described in section 2.8. Finally, this chapter ends in section 2.9 with deriving geodesic equations.

Chapter 3 is the main important part of this thesis where the key achievement of this research work published in different conferences and journal is summarized. Chapter 4 is the discussion over the obtained results and chapter 5 gives concluding remarks of this work.

Chapter 2

Background and State of the Art

2.1 Historical Background and Overview

A theory of color vision is based on a set of assumptions or postulates about the visual system. Newton [41] was the first to explain color theory from his color matching experiments with light. He also introduced geometric concept of complementary colors using the color circle. The scientist, Thomas Young [71] suggested the three fold model of color perception in 1802. He speculated that there were three different types of photo receptors in the eyes for color vision. He also developed equilateral triangle for exhibiting in theory, all possible shades of colors which is known as Young's trichromatic theory. In the 1860, James Clerk Maxwell [37] explored the use of three primary colors and realized that no additive combination of three primary colors can cover the entire perceivable hues. He showed that the set of primaries was not unique, but that spectral primaries more widely separated in wavelength could be used to produce a wider range of perceived hues. Maxwell recognized that the chromaticity (hue and saturation) of a colored surface is relatively insensitive to the brightness. Maxwell's work could be considered to be the basis for modern colorimetry [30]. Helmholtz [60] described Young's trichromatic nature of color space on a more quantitative basis which came to be known as the Young-Helmholtz theory of color vision. This theory was postulated on the basis of additive and associative laws of color mixture developed by Grassman [21]. Right after Grassman, a German mathematician, Riemann [49] remarked significantly that the colors and the positions of the objects of sense constitute a non-Euclidean manifold. Helmholtz was the first to define a line element in terms of Riemannian

geometry on the color space which would measure the perceptual difference between any two colors. In 1920, Schrödinger [50] modified Helmholtz line element stating that the additivity of brightness is essential to formulate line element. He further described that in the Riemannian space, shortest distances between colors of equal intensity form geodesics which can be calculated from line elements. His pioneer efforts give a solid footing about the geometry of color space. In 1946, Stiles [56] did simple modification of Helmholtz's line element by introducing different constant factors in each coordinate of three dimensional color space. The latest and most advanced contribution along this line, is the zone-fluctuation line element of Vos and Walraven [65]. The Riemannian space based line element can still be used as color vision models.

Along with the theoretical color vision models, it is necessary to do color stimulus measurement defining standard observers and a colorimetric system. To recommend internationally standardized colorimetric system, Commission Internationale delÉclairage (CIE) set up color matching functions based on the experimental color matching data of Guild [22] and Wright [68]. The CIE also defined three tristimulus values X, Y and Z implying a three dimensional color space as well as a horseshoe- shaped outline called the CIE chromaticity diagram.

For expressing the relative sensitivity of the visual system to small color differences, psychophysical experiment is done which gives a color difference threshold. Such threshold values are called just noticeable differences (JNDs). MacAdam [34] was the first to derive JND thresholds for small color differences throughout the CIE xy chromaticity diagram in terms of ellipses. These are now known as MacAdam's JND ellipses. After MacAdam, many other color researchers also derived chromaticity difference data sets based on JND ellipses. The latest data sets are BFD-Perceptibility(BFD-P) [31], RIT-DuPont [3], Witt [66]and others. They are known as supra threshold color difference data. The color difference formulas like CIELAB, CIELUV, CIEDE2000 and so on are derived from supra threshold color difference data. These empirical color difference formulas can be evaluated by applying the line element model in a postulated color space.

The attributes of color based on principles of color perception are described with Color order systems. Geometrically, the attributes hue, chroma and lightness represent three coordinates of a color order system and they are orthogonal to each other. A set of color standard materials (patches) are selected to represent scales of constant

hue, chroma and lightness with the aim of perceptual uniformity. An example of such kind is the Munsell Color order System [40] and they are analogous to the Riemannian coordinate system in Schrödinger's interpretation[28]. Using the Riemannian metric as a tool, geodesics of color difference formulas can be calculated which can be compared with the Munsell color order system for evaluating their perceptual uniformity and distribution of color stimulus in any color space.

2.2 Colorimetry

Colorimetry is concerned with an observer's perception for small color differences. It also explains color quantitatively using standard experimental data and the empirical laws of color matching properties of additive mixtures of color stimuli. The CIE colorimetric system builds on these empirical laws which describes color perception specifying the color matching functions of standard observers as functions of wavelength.

2.2.1 The CIE 1931 System

In 1931, the CIE specified color matching functions of standard observers in terms of $\bar{x}(\lambda)$, $\bar{y}(\lambda)$ and $\bar{z}(\lambda)$ in the wavelength range $\lambda = 380$ to 780 nm. These color matching functions represent the chromatic response of the average human viewing through a 2° angle [1]. This system is also known as the CIE 1931 2° Standard Observer. It is suitable for application to matching fields of between one and four degree angular subtense. The plot of $\bar{x}(\lambda)$, $\bar{y}(\lambda)$ and $\bar{z}(\lambda)$ as a function of wavelength is shown in Figure (2.1). The CIE 1931 standard observer is based on two independent color matching experiments performed by Guild (1931) and Wright (1928-29) for a total of 17 observers and the relative luminance of the colors of the spectrum averaged for about 100 observers.

2.2.2 The CIE 1964 System

The CIE 1931 system is not appropriate for the larger-field (greater than 4°) visual color matching [15]. Its inadequacy at short-wavelengths is well known, and is often taken into account in colorimetric and photometric applications [61]. In 1964, the CIE standardized a large field colorimetric system based on the visual color matching observations of Stiles at el. [55] and Speranskaya [54] with a 10° field of view. This system

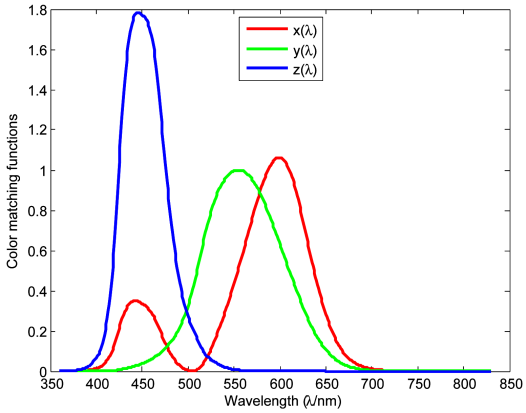

Figure 2.1: The CIE 1931 Standard Colorimetric Observer - CIE31 Color matching functions.

is defined as the CIE 1964 10° Standard Observer. Its color matching functions are noted as $\bar{x_{10}}(\lambda)$, $\bar{y_{10}}(\lambda)$ and $\bar{z_{10}}(\lambda)$. Figure (2.2) shows 1964 color matching functions of standard colorimetric observer in the wavelength from 360 nm to 830nm. The subscript 10 is used to distinguish the 10° data from the original 1931 standard 2° observer data.

Figure 2.2: The CIE 1964 Standard Colorimetric Observer - CIE64 Color matching functions.

2.2.3 Tristimulus Values and Chromaticity Coordinates

The CIE created a special set of mathematical primaries (imaginary primaries) X,Y and Z to replace the actual red, green and blue (RGB) primaries for simplifying color

calculations. All real colors can be matched using positive proportion of three imaginary primaries. The values of X,Y and Z are known as the CIE 1931 tristimuls values which specify the color stimulus. The Y tristimulus value is equal to the curve that indicates the human eye's response to the total power of a light source. It is also called relative luminance. The Y tristimulus value roughly represents the lightness of a sample. The CIE tristmuls values for object colors are calculated by adding the product of the spectral power distribution of the illuminant, the spectral reflectance factor of the object and the color matching functions of the observer at each wave length of the visible spectrum [36]. According to the CIE recommendation, following equations are used to calculate the tristimulus values of an object.

$$\begin{aligned} X &= k \sum_{\lambda} P(\lambda)\, \bar{x}(\lambda)\, R(\lambda) \\ Y &= k \sum_{\lambda} P(\lambda)\, \bar{y}(\lambda)\, R(\lambda) \\ Z &= k \sum_{\lambda} P(\lambda)\, \bar{z}(\lambda)\, R(\lambda) \\ k &= \frac{100}{\sum_{\lambda} P(\lambda)\, \bar{y}(\lambda)} \end{aligned} \tag{2.1}$$

where, $P(\lambda)$ is the value of the spectral power distribution of the illuminant at wave length λ , $R(\lambda)$ is the reflectance factor of the sample at the wavelength λ. The factor k normalizes the tristimulus values so that Y will have a value of 100 for the perfect white diffuser - a theoretical material that reflects 100 percent of the incident light. In the CIE XYZ system, the curve for the Y tristimulus value is equal to the curve of the human eye's response to the total power of a light source.

2.2.4 Chromaticity Coordinates and Diagram

To describe visual attributes of colors in terms of hue and chroma, the CIE XYZ tristimulus values are used to formulate a new set of chromaticity coordinates that are denoted by xyz. The chromaticity coordinates xyz are obtained by taking the ratio of

the tristimulus values to their sum $X + Y + Z$ as given by the equations below:

$$\begin{aligned} x &= \frac{X}{X+Y+Z} \\ y &= \frac{Y}{X+Y+Z} \\ z &= \frac{Z}{X+Y+Z} \\ 1 &= x + y + z \end{aligned} \tag{2.2}$$

Mathematically, x and y are formulated by the projective transformation of the tristimulus values into a two-dimensional plane. The derived color space specified by x, y, and Y is known as the CIE xyY color space. The third dimension is indicated by the tristimulus value Y. The scale for Y extends from the white spot in a line perpendicular to the plane formed by x and y using a scale that goes from 0 to 100.

A plot of y against x is called a chromaticity diagram. Such a plot using the CIE XYZ and $X_{10}Y_{10}, Z_{10}$ is shown in Figure (2.2). The chromaticity diagram is a

Figure 2.3: The chromaticity diagram using the CIE 1931 and 1964 tristimulus values - The difference between CIE31 and 64 systems.

horseshoe shaped spectrum locus, purple line and the colors of the chromaticity diagram occupy a region of the real projective plane.

2.3 Visual Color Difference Data

Psychophysical experiments are done for measuring visual color differences. In general, observers matched a series of colors viewing through a bipartite field. The experimental

data gives color attributes in terms of hue, chroma and lightness for a color difference and is commonly known as the visual color difference data. This means chroma difference for a test color is produced keeping the lightness and hue constant and the same process is repeated to produce other two attributes. Color difference formulas are generally developed by using such a data set. There are several approaches to obtain visual color difference data set [47, 70]. Here, threshold and supra threshold data are mainly focused.

2.3.1 Threshold Color Difference Data

Threshold color difference data describes observers ability to discriminate two color stimuli by the just noticeable difference (JND) in terms of color attributes such as hue or chroma. The JND gives as a unit of sensation difference. It is also referred to the just-perceptible difference (JPD) that the visual differences are too small. MacAdam [34] first performed a psychophysical experiment to derive JND thresholds for chromaticity discrimination of 25 color samples. He used a bipartite comparison field of view that allowed very small variation in chromaticity until it matched the test color. The results were plotted as small areas in the 1931 CIE xy chromaticity diagram. These small discrimination areas in different directions represent visual color differences of different magnitudes and could be described by ellipses. They became known as MacAdam's JND ellipses (2.4). Although, this chromatic discrimination data set is based on the

Figure 2.4: MacAdam's JND ellipses in the CIE 1931 chromaticity diagram - enlarged 10 times.

standard deviation of color matches about a color center, MacAdam ellipses provide a

guideline about the color vision and how good they are at distinguishing between similar colors. Brown [5], Wyszecki and Fielder [69] and many other researchers also derived chromaticity difference data sets based on JND ellipses. Color difference formula like Friele-MacAdam-Chickering (FMC) [7] was developed using threshold color difference data.

2.3.2 Supra Threshold Color Difference Data

Supra threshold data are derived by discriminating visual color difference between two colors instead of determining just-noticeable color differences. The color differences presented to and matched by the observer are not necessarily small or of near threshold size, but can be many times JND threshold. The criterion of equality of color difference requires the observer's ability to discriminate between color differences of comparable size generated by pairs of color stimuli of different chromaticities [70]. Witzel at el. [67] also describes that supra threshold color differences are obtained from ratio judgments of visual color differences. This procedure is called perceptual color scaling in which a unit perceptual color ellipsoid can be described about a point in a color space more precisely than ones obtained by threshold color difference experiments. Perceptibility and acceptability measurements are done in supra threshold color differences [2].

Recent visual color difference data sets BFD-Perceptibility(BFD-P) [31], RIT-DuPont [3], Witt [66] and Leeds [27] are based on supra threshold color difference. Among the four data sets, BFD-P is the largest data set. The CIE technical committee I-47 on hue and lightness dependent correction accumulated the four data set and recommended 17 color centers for deriving color difference formulas [26]. A scaling factor was calculated for each data set to adjust different psychophysical methods used in various perceptibility experiments [31]. All these experimental data sets are expressed in terms of the chromatic ellipses. The distance between the center of an ellipse to any ellipse point represents more or less same visual difference. Luo and Rigg [31] accumulated and and plotted BFD-P data relating to small to medium color differences of surface colors in the CIE xy chromaticity diagram. Figure 2.5 shows BFD-P ellipses plotted in the CIE xy chromaticity diagram.

Figure 2.5: BFD-P ellipses in the CIE 1964 chromaticity diagram - 1.5 times enlarged.

2.4 Color Spaces and Color Metrics

A color space is an abstract mathematical model to describe color differences in three dimensions. It gives a quantitative measure of visual or perceptual color difference in terms of the color distance in a three dimensional space. Color spaces are important for color quality control in many applications such as image analysis, color reproduction, and so on. Many color space models are defined such as RGB, CMYK for different applications. Here, the CIE defined the CIELAB, the CIELUV and the OSA-UCS color space are discussed.

2.4.1 The CIELAB

In 1976, the CIE recommended the CIELAB [8] color space based on Adams-Nickerson [14, 17] color space. It is a rectangular color space defined by the three axes L^*, a^* and b^* as follows:

$$\begin{aligned} L^* &= 116\left(\frac{Y}{Y_r}\right)^{\frac{1}{3}} - 16 \\ a^* &= 500\left[\left(\frac{X}{X_r}\right)^{\frac{1}{3}} - \left(\frac{Y}{Y_r}\right)^{\frac{1}{3}}\right] \\ b^* &= 200\left[\left(\frac{Y}{Y_r}\right)^{\frac{1}{3}} - \left(\frac{Z}{Z_r}\right)^{\frac{1}{3}}\right] \end{aligned} \tag{2.3}$$

with the constraint that $\frac{X}{X_r}, \frac{Y}{Y_r}, \frac{Z}{Z_r} > 0.01$. Here, L^*, a^* and b^* correspond to the Lightness, the redness-greenness and the yellowness-blueness scales in the CIELAB color space. Similarly, X, Y, Z and X_r, Y_r, Z_r are the tristimulus values of the color stimuli and white reference respectively. If $\frac{X}{X_r}, \frac{Y}{Y_r}, \frac{Z}{Z_r}$ is less than 0.01, the following equations are used:

$$\begin{aligned} L^* &= 116\left[f\left(\frac{Y}{Y_r}\right) - \left(\frac{16}{116}\right)\right] \\ a^* &= 500\left[f\left(\frac{X}{X_r}\right) - f\left(\frac{Y}{Y_r}\right)\right] \\ b^* &= 200\left[f\left(\frac{Y}{Y_r}\right) - f\left(\frac{Z}{Z_r}\right)\right] \end{aligned} \tag{2.4}$$

where $f(Y/Y_n) = (Y/Y_n)^1/3$ for (Y/Y_n) greater than 0.008856 and $f(Y/Y_n = 7.787(Y/Y_n)+ 16/116$ for $Y/Y_n \leq 0.008856$; $f(X/X_n)$ and $f(Z/Z_n)$ are similarly defined. The CIELAB color space in Figure 2.6 is organized in the cube form which provides an approximately uniform color space. Basically, this color space provides a simplified lightness scale and an opponent color model in which compressed normalized CIE tristimulus values are subtracted from each other. The L^* axis values run from 0 (black) to 100 (white). The a^* and b^* axes have no numerical limits. On the a^* axis, positive value indicates red and negative value indicates green. On the b^* axis, positive is yellow and negative is blue, but for the both a^* and b^* axes, zero means neutral gray.

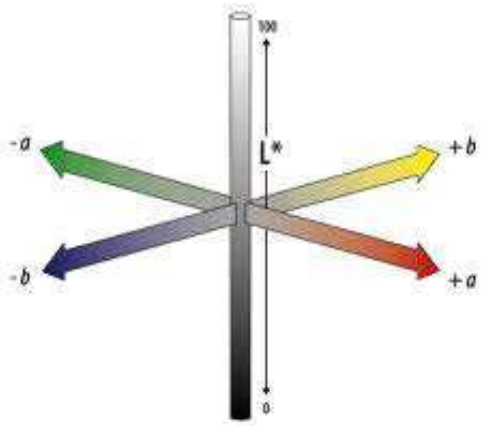

Figure 2.6: The CIELAB color space, taken from `http://dba.med.sc.edu/price/irf/Adobe_tg/models/cielab.html` **(visited,11/10/11)** - Permission is granted for personal use

The color difference, ΔE^*_{ab} between the color pair in the CIELAB color space is

defined as an Euclidean distance between the two points in the color space representing them. The color difference formula is written as:

$$\Delta E^*_{ab} = \sqrt{(\Delta L^*)^2 + (\Delta a^*)^2 + (\Delta b^*)^2}\,. \tag{2.5}$$

The CIELAB color difference formula can also be expressed in terms of lightness, chroma and hue as:

$$\Delta E^*_{ab} = \sqrt{(\Delta L^*)^2 + (\Delta c^*_{ab})^2 + (\Delta H^*_{ab})^2}\,. \tag{2.6}$$

Here, Δc^*_{ab} and ΔH^*_{ab} are the chroma and the differences in H as derived in Equation 2.7. They are computed for a color pair with subscripts 0 and 1 by following equations:

$$\begin{aligned}
\Delta C^*_{ab} &= C^*_{ab,1} - C^*_{ab,0} \\
\Delta H^*_{ab} &= 2(C^*_{ab,1} C^*_{ab,0})^{1/2}\, sin(\Delta h^*_{ab}) \\
\Delta h^*_{ab} &= h^*_{ab,1} - h^*_{ab,0} \\
C^*_{ab} &= (a^{*2} + b^{*2})^{1/2} \\
h_{ab} &= arctan(b^*/a^*).
\end{aligned} \tag{2.7}$$

In the CIELAB space, the rectangular coordinates are transferred into the polar coordinates to define hue as an angle and chroma as a radius. The hue angle h_{ab} as defined in Equation 2.7 is zero along the positive a^* axis. It increases counter clock wise with 90° for $+b^*$ direction, 180° for $-a^*$ direction and 270° for $-a^*$ direction [8].

2.4.2 The CIELUV

The CIE in 1976 also adopted the CIELUV color space based on the CIE1964 U^*, V^*, W^* by modifying the lightness and chromaticity scale [8]. It is also a rectangular color space defined by three quantities as:

$$\begin{aligned}
L^* &= 116 \left(\frac{Y}{Y_r}\right)^{\frac{1}{3}} - 16 \\
u^* &= 13L^* (u^{'} - u^{'}_r) \\
v^* &= 13L^* (v^{'} - v^{'}_r)
\end{aligned} \tag{2.8}$$

with the constraint that $\frac{Y}{Y_r} > 0.01$. The L^* corresponds lightness scale having the range from 0 to 100. u^* and v^* are the chromaticity scales. The quantities $u^{'}_r$ and $v^{'}_r$

are the $u^{'}$ and $v^{'}$ chromaticity coordinates of a the perfect reflecting diffuser [9]. These four quantities are calculated as follows:

$$\begin{aligned} u^{'} &= \frac{4X}{X + 15Y + 3Z} \\ v^{'} &= \frac{9Y}{X + 15Y + 3Z} \\ u^{'}_{r} &= \frac{4X_r}{X_r + 15Y_r + 3Z_r} \\ v^{'}_{r} &= \frac{9Y_r}{X_r + 15Y_r + 3Z_r}. \end{aligned} \tag{2.9}$$

The plot of $u^{'}$ and $v^{'}$ chromaticity coordinates in Figure (2.7) is known as the CIE 1976 uniform chromaticity scale diagram which measures the better visual color difference than the CIE xy chromaticity diagram.

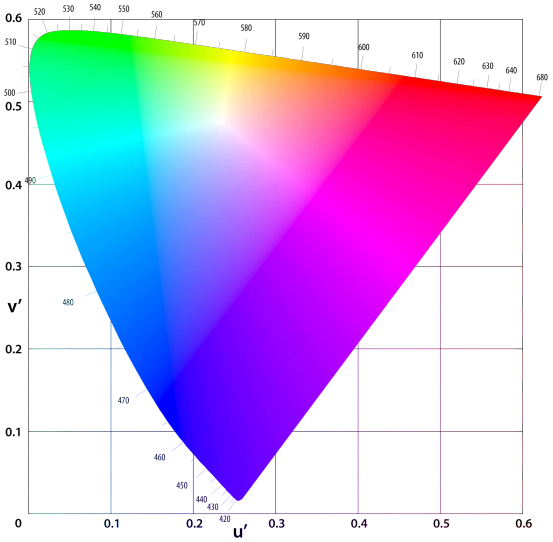

Figure 2.7: The CIELUV uniform chromaticity scale diagram, taken from `http://en.wikipedia.org/wiki/File:CIE_1976_UCS.png` - Permission is granted for personal use

In the CIELUV color space, the color difference, ΔE^{*}_{uv} can be calculated using the Euclidean distance of the L^{*}, u^{*} and v^{*} coordinates expressed as:

$$\Delta E^{*}_{uv} = \sqrt{(\Delta L^{*})^2 + (\Delta u^{*})^2 + (\Delta v^{*})^2}. \tag{2.10}$$

2.4.3 The CIEDE2000

The CIE in 2000 recommended a new color difference formula, the CIEDE2000 [12] for small to medium color difference evaluation. The formula is based upon the CIELAB color space and Luo at el. [32] described the methodology used for developing the formula from experimental color difference data. The CIEDE2000 formula is a complex formula than its predecessor color difference formulas like the CIELAB and the CIE94 [10]. It includes specific weighting functions known as lightness (S_L), chroma (S_C) and hue (S_H), parametric factors (k_L, k_C, k_H), the rotation term R_T to correct chroma and hue differences in the blue region and a scaling factor $(1 + G)$ for the CIELAB a^* to improve the performance for gray colors. The color difference, ΔE^*_{00} is calculated in the non-Euclidean form expressed as:

$$\Delta E_{00} = \left[\left(\frac{\Delta L'}{k_L S_L} \right)^2 + \left(\frac{\Delta C'}{k_C S_C} \right)^2 + \left(\frac{\Delta H'}{k_H S_H} \right)^2 + R_T \left(\frac{\Delta C'}{k_C S_C} \right) \cdot \left(\frac{\Delta H'}{k_H S_H} \right) \right]^{0.5} \tag{2.11}$$

In Equation (2.11), R_T is the rotation function and it is defined as:

$$\begin{aligned} R_T &= -\sin(2\Delta\theta) R_c \\ \Delta\theta &= 30 \cdot exp- \left(\frac{\bar{h}' - 275}{25} \right)^2 \\ R_c &= 2\sqrt{\frac{\bar{C}'^7}{\bar{C}'^7 + 25^7}} \end{aligned} \tag{2.12}$$

Similarly, the weighting functions are defined as:

$$\begin{aligned} S_L &= 1 + \frac{0.015(\bar{L}' - 50)^2}{\sqrt{20 + (\bar{L}' - 50)^2}} \\ S_C &= 1 + 0.045\bar{C}' \\ S_H &= 1 + 0.015\bar{C}'T \\ T &= 1 - 0.17\cos(\bar{h}' - 30^o) + 0.24\cos(2\bar{h}' + .32\cos(3\bar{h}' + 6^o) - 0.2\cos(4\bar{h}' - 63^o) \end{aligned} \tag{2.13}$$

Here, the lightness, the chroma and the hue are expressed taking the average of a pair of color samples. In equation form, we write:

$$\begin{aligned} \bar{L}' &= \frac{L_1^* + L_2^*}{2} \\ \bar{C}' &= \frac{C_1' + C_2'}{2} \\ \bar{h}' &= \frac{h_1' + h_2'}{2} \\ \Delta H &= 2\sqrt{C_1' C_2'} \sin \frac{\Delta h'}{2} \end{aligned} \tag{2.14}$$

The other terms used in the ΔE_{00}^* formula are also defined in the following way:

$$\begin{aligned} L' &= L^* \\ a' &= a^*(1+G) \\ b' &= b^* \\ C' &= \sqrt{a'^2 + b'^2} \\ h' &= \arctan \frac{b'}{a'} \\ G &= \frac{1}{2}\left(1 - \sqrt{\frac{C_{ab}^{*7}}{C_{ab}^{*7} + 25^7}}\right) \end{aligned} \tag{2.15}$$

C_{ab}^* is the average of the two samples in the color pair.

2.4.4 The OSA-UCS Color Space

In 1974, the committee on Uniform Color Scales of the Optical Society of America developed a color space (color appearance system) that is based on the regular rhombohedral lattice arrangement of color samples [18, 35]. The OSA-UCS system specifies color by three coordinates, the constant OSA lightness L_{OSA} and lattice coordinates (j, g). j defines yellowness-blueness and g represents greenness-redness and they are abstract parameters in the sense that a positive value of g will not indicate green; instead, this parameter separates the blue and green colors. Correspondingly, the negative values of j parameter separates blue from the violet region. The OSA L can have values from -7 to +5. Positive values for L_{OSA} mean a color which is brighter than the background, and negative values a color which is darker. The lattice points (L, j, g) of the OSA-UCS color space can be derived from the CIE 1964 tristimulus values.

Figure 2.8 shows the OSA-UCS color space. In such a structure, each color is surrounded by 12 neighboring colors and the distances between a color and the nearest neighbors at each point of the lattice are perceived as a uniform color-difference [13].

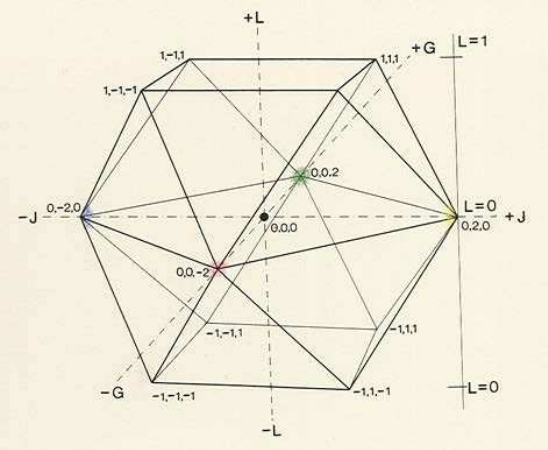

Figure 2.8: The OSA-UCS color space, taken from `http://www.colorsystem.com/?page_id=960&lang=en` **(visited,11/10/11)** - Permission is granted for personal use

2.4.5 The OSA-UCS ΔE_E

The OSA-UCS ΔE_E is a new Euclidean color-difference formula using log compression on the basis of the properties of the OSA-UCS color space [44]. Small and medium color-differences can be measured efficiently by a simple Euclidean distance in the log-compressed OSA-UCS space [42, 43] defined by the coordinates L_E, G_E and J_E as:

$$L_E = \left(\frac{1}{b_L}\right) \ln\left[1 + \frac{b_L}{a_L}(10L_{OSA})\right], \tag{2.16}$$

$$G_E = -C_E \cos(h), \tag{2.17}$$

$$J_E = C_E \sin(h), \tag{2.18}$$

$$C_E = \left(\frac{1}{b_c}\right) \ln\left[1 + \frac{b_c}{a_c}(10C_{OSA})\right], \tag{2.19}$$

$$\tag{2.20}$$

where, L_E, G_E, J_E and C_E are the log compressed lightness, chromaticity coordinates and chroma respectively. The constants are:

$$\begin{aligned} a_L &= 2.890, \\ b_L &= 0.015, \\ a_c &= 1.256, \\ b_c &= 0.050. \end{aligned} \tag{2.21}$$

In the OSA-UCS space, the chroma (C_{OSA}) and the hue angle (h) are derived from the coordinates J and G, which correspond to the empirical j and g of the OSA-UCS system as:

$$C_{OSA} = \sqrt{G^2 + J^2}, \tag{2.22}$$

$$h = \arctan(\frac{-J}{G}). \tag{2.23}$$

The CIE 1964 ($x_{10}\, y_{10}\, Y_{10}$) space to the OSA-UCS (L_{OSA}, J, G) is defined through a sequence of linear transformations and a logarithmic compression as follows:

$$\begin{aligned} L_{OSA} &= \left(5.9[(Y_0^{1/3} - \frac{2}{3}) + 0.042(Y_0 - 30)^{1/3}] - 14.4\right)\frac{1}{\sqrt{2}}, \\ Y_0 &= Y\left(4.4934x^2 + 4.3034y^2 - 4.2760xy - 1.3744x - 2.5643y + 1.8103\right). \end{aligned} \tag{2.24}$$

$$\begin{bmatrix} A \\ B \\ C \end{bmatrix} = \begin{bmatrix} 0.6597 & 0.4492 & -0.1089 \\ -0.3053 & 1.2126 & 0.0927 \\ -0.0374 & 0.4795 & 0.5579 \end{bmatrix} \begin{bmatrix} X \\ Y \\ Z \end{bmatrix}, \tag{2.25}$$

$$\begin{bmatrix} J \\ G \end{bmatrix} = \begin{bmatrix} S_J & 0 \\ 0 & S_G \end{bmatrix} \begin{bmatrix} -\sin\alpha & \cos\alpha \\ \sin\beta & -\cos\beta \end{bmatrix} \begin{bmatrix} \ln\left(\frac{A/B}{A_n/B_n}\right) \\ \ln\left(\frac{B/C}{B_n/C_n}\right) \end{bmatrix} \tag{2.26}$$

$$\begin{aligned} &= \begin{bmatrix} 2(0.5735L_{OSA} + 7.0892) & 0 \\ 0 & -2(0.764L_{OSA} + 9.2521) \end{bmatrix} \\ &\times \begin{bmatrix} 0.1792[\ln A - \ln(0.9366B)] + 0.9837[\ln B - \ln(0.9807C)] \\ 0.9482[\ln A - \ln(0.9366B)] - 0.3175[\ln B - \ln(0.9807C)] \end{bmatrix}. \end{aligned} \tag{2.27}$$

2.5 The Munsell Color Order System

In colorimetry, a color order system based on the principles of color perception describes a logical method to organize color perception consisting with the following properties:

- Have natural dimensions for hue, chroma and lightness
- Have perceptually uniform scales

Many color order systems have been developed [2, 24] and are in use for the scientific and industrial interests. Within the numerous color order systems [2, 70], the Munsell color system [40] is perhaps the best known and the most studied scientifically, because of its careful color scale formulation.

The Munsell color order system specifies colors in a three-dimensional space according the three color attributes Munsell hue, value and chroma. These attributes can be represented cylindrically and varied independently in three dimensions as shown in Figure 2.9. The neutral colors are placed along a vertical line, called the neutral axis

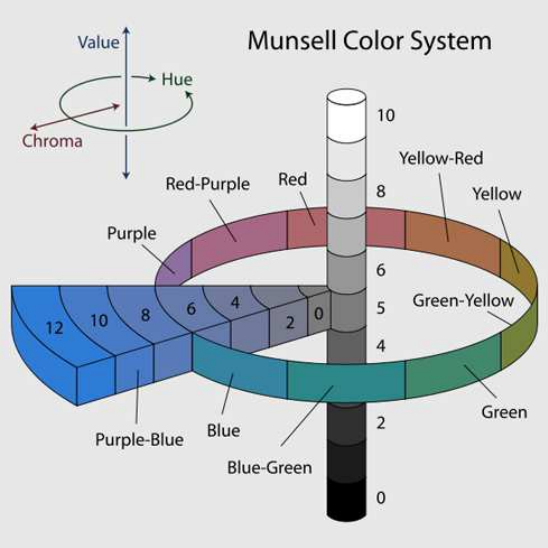

Figure 2.9: The Munsell color system, taken from `http://en.wikipedia.org/wiki/Munsell_color_system` (visited,14/10/11) - Permission is granted for personal use.

with black at the bottom, white at the top and all grays in between. The different hues are displayed at various angles around the neutral axis. The chroma scale is perpendicular to the axis, increasing outward. This three-dimensional arrangement of colors is called the Munsell color space where the perceptive distribution of color is uniform.

For the scientific study of the color spaces and color difference formulas, the Munsell data can be plotted into the different color spaces. Figure 2.10 shows an example of plotting the Munsell hue and chroma plotted in the xy chromaticity diagram of the CIE

xyY color space at the constant Munsell value 5. A closer inspection of the Munsell constant - hue lines show that most hue lines are curved starting from the achromatic origin.

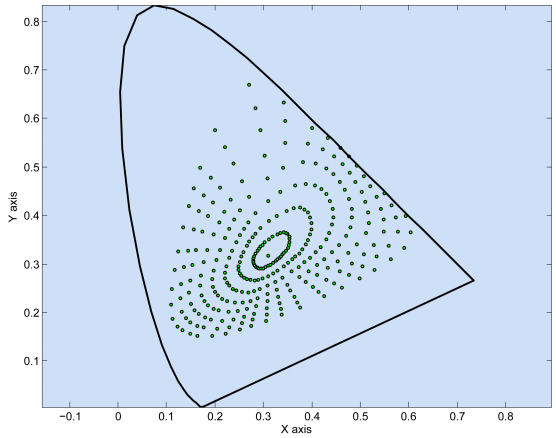

Figure 2.10: The Munsell hue and chroma in the CIE xy chromaticity diagram at the Munsell value - 5.

2.6 Riemannian Space and Line Element

Riemannian space describes curvature of a surface by smooth manifolds with a Riemannian metric tensor. It generalizes Euclidean geometry to spaces that are not necessarily flat, although they still resemble the Euclidean space at each point infinitesimally. In the Riemannian space, the distance between two points is measured by means of a smooth positive definite symmetric form. For example, the arc length of curves can be determined by the Riemannian metric tensors and analysis of differential equations that have been generalized to the setting of Riemannian manifolds. The formal definition of Riemannian space and mathematical details can be found in [4]. The Riemannian symmetric space can be applied as a tool to color spaces for measuring color difference distances.

Considering a color space as a Riemannian space, small color differences can be measured locally in terms of color distances between a color point and neighborhoods of points in that space. Such color difference distances represent threshold of color differences. They described by ellipsoids in three dimensions and ellipses in two dimensions. These representation of color differences can be mapped from one color space

to other color space due to the isometry between Riemannian spaces provided that the Gaussian curvatures at the corresponding points must be the same [25, 48]. This is also called a distance-preserving diffeomorphism between Riemannian spaces [6]. The isometry feature plays an important role to study the performance of various color spaces and color difference metrics for measuring the the perceptual color differences.

Helmholtz [60] did first attempt to define a line element and a Riemannian metric tensor for the color space to describe the mechanism of color vision. Basically, line elements are mathematical formulations in terms of first fundamental form in a color space defined as the Riemannian space in which perceptual or visual color differences are represented by color vectors. The application of the line element is to compute the shortest length or the distance between any two points in such a color space from the Riemannian metric. The shortest length is called a geodesic which is used to evaluate magnitude of their perceptual color differences. The geodesics are straight lines in a flat space but in the Riemannian space they are generally curved.

2.6.1 Formulation of the Line Element for Color Space

In this subsection, the mathematical form of the line element is described considering the CIE chromaticity color space xyY as the three dimensional Riemannian space. Suppose p_1 and p_2 are two points in such a color space with coordinates (x, y, Y) and $(x + dx, y + dy, Y + dY)$. The distance ds between these two points can be expressed in the following quadratic form:

$$ds^2 = g_{11}dx^2 + 2g_{12}dxdy + g_{22}dy^2 + 2g_{13}dxdY + 2g_{23}dydY + g_{33}dY^2. \tag{2.28}$$

Equation 2.28 in matrix form is:

$$ds^2 = \begin{bmatrix} dx & dy & dY \end{bmatrix} \begin{bmatrix} g_{11} & g_{12} & g_{13} \\ g_{21} & g_{22} & g_{23} \\ g_{31} & g_{32} & g_{33} \end{bmatrix} \begin{bmatrix} dx \\ dy \\ dY \end{bmatrix}, \tag{2.29}$$

with $g_{12} = g_{21}$ and $g_{23} = g_{32}$. The coefficients g_{ik} in Equation 2.29 is a positive definite symmetric metric tensor and it is known as the Riemannian metric. The distance ds is called the line element. At the constant ds, the Riemannian metric gives an ellipsoid at a color center. In a two dimensional color space, the metric g_{ik} has the following

form:

$$g_{ik} = \begin{bmatrix} g_{11} & g_{12} \\ g_{21} & g_{22} \end{bmatrix} \tag{2.30}$$

The metric represents the chromaticity difference of any two colors measured along the geodesic of the surface and it gives the chromaticity discrimination ellipses in terms of chromaticity coordinates (x, y) at constant luminance Y. MacAdam's ellipses in Figure 2.4 are the examples of chromaticity discrimination ellipses.

2.7 Line Element Models

In this section, the author will briefly discuss historical line element models based on color fundamentals R, G and B or cone fundamentals. In theses color spaces, color differences with increments have assumed to be based on the Weber-Fecher law.

2.7.1 Helmholtz Line Element Model

Helmholtz [60] assumed that all three R, G and B color vision processes are identical and satisfy the Weber-Fecher law:

$$\frac{dR}{R} = \frac{dG}{G} = \frac{dB}{B} = const \tag{2.31}$$

where, dR, dG, dB are the incremental changes in the processes. Assuming a Euclidean space, he purposed that with all three primaries in operation, the smallest perceptible difference is obtained by combining the fractional deviations for the three primaries. The line element consists following form:

$$ds = \left[\left(\frac{dR}{R}\right)^2 + \left(\frac{dG}{G}\right)^2 + \left(\frac{dB}{B}\right)^2 \right]^{1/2} \tag{2.32}$$

where ds is the threshold difference between two points in the R, G and B space. This line model possessed difficulties to fit experimental data of color discrimination [29]. As pointed out by Schrödinger [50], the Helmholtz line element does not have the same luminous efficiency curve as obtained from the directly observed $V(\lambda)$ curve.

2.7.2 Schrödinger Line Element Model

Schrödinger [50] proposed a more complex line element to correct the shortcomings of the Helmholtz line element of following form:

$$ds^2 = \frac{1}{I_R R + I_G G + I_B B}\left[\frac{I_R(dR)^2}{R} + \frac{I_G(dG)^2}{G} + \frac{I_B(dB)^2}{B}\right] \tag{2.33}$$

where I_R, I_G and I_B are the luminous efficiency functions of the three fundamental color vision processes. The factor $1/I_R R + I_G G + I_B B$ makes a surface of constant brightness plane in tristimulus space for this line element. The additivity of brightness considered by Schrödinger was a strong point of his line element because with a suitable choice of the relative values of the constants I_R, I_G and I_B, brightness deduced from the Schrödinger line element agree approximately with the luminances based on the experimentally determined $V(\lambda)$ curve. However, his line element did not get practical importance because of difficulties to calculate relative values of constants and it has not been studied intensively [70].

2.7.3 Stiles Line Element Model

Stiles [56] suggested a line element based on his two color thresholds experimental data. It has the following form:

$$ds^2 = \left[\frac{\zeta(R)}{\rho}(dR)\right]^2 + \left[\frac{\zeta(G)}{\gamma}(dG)\right]^2 + \left[\frac{\zeta(B)}{\beta}(dB)\right]^2 \tag{2.34}$$

where $\zeta(R) = 9/1 + 9R$, $\zeta(G) = 9/1 + 9G$ and $\zeta(B) = 9/1 + 9B$ are experimentally determined functions. ρ, γ and β are the Weber fractions with values 1.28, 1.65 and 7.25 respectively. Stiles line element was found good to fit visual experimental data than the above mentioned two line elements. The constant values indicates that "blue" vision process is less sensitive than "green" and "red". However, there remain experimental data that can not be predicted adequately [70].

2.7.4 Vos and Walraven Line Element Model

Vos and Walraven [65] line element is based on photon noise methodology in place of the empirical Weber-Frencher law. They consider the first the case in which the visual mechanism is stimulated by color stimuli of low luminances. The important

new concept introduced by Vos and Walraven to the notion of the line element is that the out put signals of the individual cone mechanism are integrated by combining two chromatic signals and one luminance signal, before a difference signal is transmitted to the brain [62]. According to their hypothesis, in the cone mechanism zone, the signal to noise output can then be treated in terms of standard Poisson statistics as given below:

$$\left[\frac{Signal}{Noise}\right]_{output} = \frac{dN}{\sqrt{N}} \tag{2.35}$$

where N is the average number of quanta absorbed per second. Vos and Walraven concluded that opponent processing does not play a role at the threshold level and they defined line element as follows:

$$\begin{aligned}(ds)^2 = &\left[\frac{dR}{[R(1+R/R_0+R^2/R_1^2)]^{0.5}}\right]^2 + \left[\frac{dG}{[G(1+G/G_0+G^2/G_1^2)]^{0.5}}\right]^2 \\ &+ \left[\frac{dB}{[B(1+B/B_0+B^2/B_1^2)]^{0.5}}\right]^2\end{aligned} \tag{2.36}$$

where $R\,G\,B$ are the responses of the three independently operating cone mechanisms. The subscript 0 indicates the number of quanta for which saturation occurs and subscript 1 the number of quanta for which supersaturation occurs. Thus, this model of line element can account for various level of saturation of the cone system. Vos and walraven find reasonable agreement between the line element prediction and experimental color discrimination data. This is the most elaborate line element which includes both Helmholtz and Schrödinger concepts.

2.8 Jacobian Method for Coordinates Transform

The first fundamental form ds^2 of Equation 2.28 can be mapped from one coordinate system to other coordinate system using the Jacobian method. Suppose, (x, y, Y) coordinates are related to (u, v, w) having new metric tensor g'_{ik}. The metric tensor g_{ik} of the (x, y, Y) coordinate system is also related to the new metric tensor g'_{ik} as follows:

$$\begin{bmatrix} g'_{11} & g'_{12} & g'_{13} \\ g'_{21} & g'_{22} & g'_{23} \\ g'_{31} & g'_{32} & g'_{33} \end{bmatrix} = \begin{bmatrix} \frac{\partial x}{\partial u} & \frac{\partial x}{\partial v} & \frac{\partial x}{\partial w} \\ \frac{\partial y}{\partial u} & \frac{\partial y}{\partial v} & \frac{\partial y}{\partial w} \\ \frac{\partial Y}{\partial u} & \frac{\partial Y}{\partial v} & \frac{\partial Y}{\partial w} \end{bmatrix}^T \begin{bmatrix} g_{11} & g_{12} & g_{13} \\ g_{21} & g_{22} & g_{23} \\ g_{31} & g_{32} & g_{33} \end{bmatrix} \begin{bmatrix} \frac{\partial x}{\partial u} & \frac{\partial x}{\partial v} & \frac{\partial x}{\partial w} \\ \frac{\partial y}{\partial u} & \frac{\partial y}{\partial v} & \frac{\partial y}{\partial w} \\ \frac{\partial Y}{\partial u} & \frac{\partial Y}{\partial v} & \frac{\partial Y}{\partial w} \end{bmatrix} \tag{2.37}$$

where the superscript T denotes the matrix transpose and the matrix

$$J = \frac{\partial(x, y, Y)}{\partial(u, v, w)} = \begin{bmatrix} \frac{\partial x}{\partial u} & \frac{\partial x}{\partial v} & \frac{\partial x}{\partial w} \\ \frac{\partial y}{\partial u} & \frac{\partial y}{\partial v} & \frac{\partial y}{\partial w} \\ \frac{\partial Y}{\partial u} & \frac{\partial Y}{\partial v} & \frac{\partial Y}{\partial w} \end{bmatrix} \tag{2.38}$$

is the Jacobian matrix for the coordinate transformation.

2.9 The Geodesic Equation

The line element in a color space can also be defined as:

$$ds^2 = g_{ik} dx^i dx^k. \tag{2.39}$$

where ds is the incremental distance between two points, dx^i and dx^k are differential coordinates.Here, Einstein's summation convention which indicates summation over repeated indices, $a^i b_i = \sum_i a^i b_i$ is used. If we consider two points p_0 and p_1, the distance between the two points along a given path is given by the line integral:

$$s = \int_{p_0}^{p_1} ds = \int_{p_0}^{p_1} (g_{ik} dx^i dx^k)^{\frac{1}{2}}. \tag{2.40}$$

The shortest distance between p_0 and p_1 can be obtained by minimizing s with respect to the path. This path is called the geodesic that represents the positive distance function in the color space. Let λ be a variable that parameterizes the path taken. So, let us define $x^i = x^i(\lambda)$. Equation 2.40 can be written as:

$$s = \int_{p_0}^{p_1} ds = \int_{\lambda_0}^{\lambda_1} \left(g_{ik} \frac{dx^i}{d\lambda} \frac{dx^k}{d\lambda} \right)^{\frac{1}{2}} d\lambda. \tag{2.41}$$

Using variational calculus approach and introducing the Lagrangian $L[dx^i/d\lambda, x^i] = \sqrt{g_{ik}\, dx^i/d\lambda\, dx^k/d\lambda}$, we can define:

$$\begin{aligned} \frac{dx^i}{d\lambda} &= \dot{x}^i \\ \frac{ds}{d\lambda} &= L \end{aligned} \tag{2.42}$$

Equation (2.40) in terms of the variation of distance s with path is

$$\begin{aligned}\delta s &= \int_{\lambda_0}^{\lambda_1} \delta L \, d\lambda \\ &= \int_{\lambda_0}^{\lambda_1} \left[\frac{\partial L}{\partial x^i} \delta x^i + \frac{\partial L}{\partial \dot{x}^i} \delta \dot{x}^i \right] d\lambda\end{aligned} \tag{2.43}$$

where

$$\delta \dot{x}^i = \delta \left(\frac{dx^i}{d\lambda} \right) = \frac{d}{d\lambda} (\delta x^i). \tag{2.44}$$

Integrating the second term by parts and using Equation (2.44), we get

$$\int_{\lambda_o}^{\lambda_1} \frac{\partial L}{\partial \dot{x}^i} \frac{d}{d\lambda} (\delta x^i) \, d\lambda = \frac{\partial L}{\partial \dot{x}^i} \delta x^i \Big|_{\lambda_0}^{\lambda_1} - \int_{\lambda_0}^{\lambda_1} \frac{d}{d\lambda} \left(\frac{\partial L}{\partial \dot{x}^i} \right) \delta x^i d\lambda. \tag{2.45}$$

In this case, every path starts at λ_0 and terminates at λ_1, there is no variation of the coordinates x^i at the endpoints and the integrated term in Equation (2.45) vanishes. We can write Equation (2.43) as:

$$\delta s = \int_{\lambda_0}^{\lambda_1} \left[\frac{\partial L}{\partial x^i} - \frac{d}{d\lambda} \left(\frac{\partial L}{\partial \dot{x}^i} \right) \delta x^i d\lambda \right] \delta x^i d\lambda. \tag{2.46}$$

The distance s will be minimum when $\delta s = 0$. From Equation (2.46) with the criteria of minima, we can obtain the Euler-Lagrange equation in the following form:

$$\frac{\partial L}{\partial x^i} - \frac{d}{d\lambda} \left(\frac{\partial L}{\partial \dot{x}^i} \right) = 0 \tag{2.47}$$

For the positive symmetric metric, we have $g_{ik} \neq g_{ik}(\dot{x}^j)$ and $\frac{\partial \dot{x}^m}{\partial \dot{x}^n} = \delta_n^m$ and the derivatives of Equation (2.47) are computed step by step. First, we find

$$\begin{aligned}\frac{\partial L}{\partial \dot{x}^i} &= \frac{1}{2L} g_{kj} \frac{\partial}{\partial \dot{x}^i} (\dot{x}^k \, \dot{x}^j) \\ &= \frac{1}{2L} g_{kj} \left(\delta_{ik} \dot{x}^j + \delta_{ij} \dot{x}^k \right) \\ &= \frac{1}{2L} \left(g_{ij} \dot{x}^j + g_{ki} \dot{x}^k \right) \\ &= \frac{1}{2L} \left(g_{ij} \frac{dx^j}{d\lambda} + g_{ki} \frac{dx^k}{d\lambda} \right)\end{aligned} \tag{2.48}$$

Here, j in the first term and k in the second term are dummy indices and Equation

(2.48) can be written as:

$$\frac{\partial L}{\partial \dot{x}^i} = \frac{1}{L}\left(g_{ik}\frac{dx^k}{d\lambda}\right) = g_{ik}\frac{dx^k}{ds}. \tag{2.49}$$

Therefore,

$$\frac{d}{d\lambda}\left(\frac{\partial L}{\partial \dot{x}^i}\right) = \frac{d}{ds}\left(g_{ik}\frac{dx^k}{ds}\right)\frac{ds}{d\lambda}. \tag{2.50}$$

Now, we compute first term of Equation (2.47) with $L = ds/d\lambda$

$$\frac{\partial L}{\partial x^i} = \frac{1}{2L}\frac{\partial g_{kj}}{\partial x^i}\frac{dx^k}{d\lambda}\frac{dx^j}{d\lambda} \quad = \frac{1}{2}\frac{\partial g_{kj}}{\partial x^i}\frac{dx^k}{ds}\frac{dx^j}{ds}\frac{ds}{d\lambda} \tag{2.51}$$

Combining Equations (2.51) and (2.50), the geodesic equation is:

$$\begin{aligned} \frac{1}{2}\frac{\partial g_{kj}}{\partial x^i}\frac{dx^k}{ds}\frac{dx^j}{ds}\frac{ds}{d\lambda} - \frac{d}{ds}\left(g_{ik}\frac{dx^k}{ds}\right)\frac{ds}{d\lambda} = 0 \\ \frac{1}{2}\frac{\partial g_{kj}}{\partial x^i}\frac{dx^k}{ds}\frac{dx^j}{ds} - \frac{d}{ds}\left(g_{ik}\frac{dx^k}{ds}\right) = 0. \end{aligned} \tag{2.52}$$

The second term of Equation (2.52) can be expanded as:

$$\begin{aligned} \frac{d}{ds}\left(g_{ik}\frac{dx^k}{ds}\right) &= g_{ik}\frac{d^2x^k}{ds^2} + \frac{dg_{ik}}{ds}\frac{dx^k}{ds} \\ &= g_{ik}\frac{d^2x^k}{ds^2} + \frac{\partial g_{ik}}{\partial x^j}\frac{dx^j}{ds}\frac{dx^k}{ds} \\ &= g_{ik}\frac{d^2x^k}{ds^2} + \frac{1}{2}\left(\frac{\partial g_{ik}}{\partial x^j} + \frac{\partial g_{ij}}{\partial x^k}\right)\frac{dx^k}{ds}\frac{dx^j}{ds} \end{aligned} \tag{2.53}$$

Here, the reindexing of repeated indices have done using the property of the symmetric metric. The Equation (2.52) becomes:

$$\begin{aligned} g_{ik}\frac{d^2x^k}{ds^2} &= \frac{1}{2}\frac{\partial g_{kj}}{\partial x^i}\frac{dx^k}{ds}\frac{dx^j}{ds} - \frac{1}{2}\left(\frac{\partial g_{ik}}{\partial x^j} + \frac{\partial g_{ij}}{\partial x^k}\right)\frac{dx^k}{ds}\frac{dx^j}{ds} \\ &= -\frac{1}{2}\left[\frac{\partial g_{ik}}{\partial x^j} + \frac{\partial g_{ij}}{\partial x^k} - \frac{\partial g_{kj}}{\partial x^i}\right]\frac{dx^k}{ds}\frac{dx^j}{ds} \end{aligned} \tag{2.54}$$

Changing the dummy index k to m, Equation (2.54) is:

$$g_{ik}\frac{d^2x^k}{ds^2} = -\frac{1}{2}\left[\frac{\partial g_{im}}{\partial x^j} + \frac{\partial g_{ij}}{\partial x^m} - \frac{\partial g_{mj}}{\partial x^i}\right]\frac{dx^m}{ds}\frac{dx^j}{ds} \tag{2.55}$$

The final geodesic equation is

$$\frac{d^2x^k}{ds^2} + \Gamma^k_{mj}\frac{dx^m}{ds}\frac{dx^j}{ds} = 0. \tag{2.56}$$

where Γ^k_{mj} are called Christoffel symbols. They are defined in terms of the metric tensor as follows:

$$\Gamma^k_{mj} = \frac{1}{2}g^{ik}\left[\frac{\partial g_{im}}{\partial x^j} + \frac{\partial g_{ij}}{\partial x^m} - \frac{\partial g_{mj}}{\partial x^i}\right]. \tag{2.57}$$

Here, g^{ik} is the inverse of the metric g_{ik} satisfying $g^{ik}g_{ki} = \delta^i_k$. Here, δ^i_k is the Kronecker delta which vanishes for $i \neq k$.

Chapter 3

Contribution: Summary of the Papers

3.1 Introduction

Outcomes of this research work is published in different conferences and journal. The relation between the papers and the method is demonstrated by the block diagram in Figure (3.1). In this figure, the letters A, B, C, D and E in block represent five different papers. The arrow lines show how they relate each other. The 'metric' blocks represent the Riemanian metrics of four color difference formulas ΔE^*_{ab}, ΔE^*_{uv}, the Remannaized (approximate form) ΔE_{00}, the OSA-UCS ΔE_E. For example, 'DE^*ab Metric' block means the Riemannian metric tensor of ΔE^*_{ab} color difference formula derived from the line element in the CIELAB color space. Similarly, how these metrics transformed in different color spaces by the Jacobian method are shown in other blocks connecting them by double arrow lines. Such a line also describes that the process is vice versa. Experimental data used in this research work is shown in red outlined blocks. Their use in different papers are shown by connecting the red lines. Comparison of computed ellipses from different metrics with experimentally observed ellipses is done in chromaticity diagram. Paper E focuses how these different metrics are used to study perceptual attributes hue and chroma. Variational method block represents computation of Euler-Lagrange equations associated with these metrics which give hue geodesics and chroma contours according to the Schrödinger's hypothesis [50]. This hypothesis is tested with the Munsell hue and chroma in the CIELAB color space.

Figure 3.1: Block diagram demonstrating the relation between the papers and the method - A pictorial overview of this research work.

3.2 Paper A: Evaluating Color Difference Formulae by Riemannian Metric

In this paper, line elements for the CIELAB (ΔE^*_{ab}) and the CIELUV (ΔE^*_{uv}) formulas [8] are derived to study their performance for measuring experimentally observed threshold color matching data sets. These data sets were developed by MacAdam [34] using single observer and Wyszecki and Fielder [69] using three observers. They are represented in terms of JND ellipses in the xy chromaticity diagram. A method to relate Riemannian metric tensor g_{ik} with the ellipse parameters, the principal axes and the angle formed by them are presented in details. The final form of equation is (this can also be found in [70]):

$$\begin{aligned} g_{11} &= \frac{1}{a^2}\cos^2\theta + \frac{1}{b^2}\sin^2\theta \\ g_{12} &= \cos\theta\sin\theta\,(\frac{1}{a^2} - \frac{1}{b^2}) \\ g_{22} &= \frac{1}{a^2}\sin^2\theta + \frac{1}{b^2}\cos^2\theta \end{aligned} \tag{3.1}$$

Here, a and b represent the semi major axis and the semi minor axis of an ellipse respectively and g_{ik} are the coefficients of the metric tensor. The equation for angle is:

$$\tan(2\theta) = \frac{2g_{12}}{(g_{11} - g_{22})} \tag{3.2}$$

Line elements for the CIELAB and the CIELUV color difference equations to measure the infinitesimal color difference at a color point in their respective color spaces are derived as follows:

Line element of the CIELAB color difference formula:

$$(dE^*_{ab})^2 = \begin{bmatrix} dL^* & da^* & db^* \end{bmatrix} \begin{bmatrix} 1 & 0 & 0 \\ 0 & 1 & 0 \\ 0 & 0 & 1 \end{bmatrix} \begin{bmatrix} dL^* \\ da^* \\ db^* \end{bmatrix}. \tag{3.3}$$

Line element for the CIELUV color difference formula:

$$(dE^*_{uv})^2 = \begin{bmatrix} dL^* & du^* & dv^* \end{bmatrix} \begin{bmatrix} 1 & 0 & 0 \\ 0 & 1 & 0 \\ 0 & 0 & 1 \end{bmatrix} \begin{bmatrix} dL^* \\ du^* \\ dv^* \end{bmatrix}. \tag{3.4}$$

Since the experimentally observed ellipses are represented in the CIE xyY space,

it is necessary to map or transfer the line elements of above two formulas from their respective color spaces to the same xyY color space. The Jacobian method is applied to transfer the g_{ik} metrics of above two formulas derived from line elements into the CIE xyY space. It takes following steps:

- CIELAB $\Leftrightarrow$ CIEXYZ $\Leftrightarrow$ CIExyY
- CIELUV $\Leftrightarrow$ CIEXYZ $\Leftrightarrow$ CIExyY

This method requires computation of partial derivatives between color vectors of two color spaces. For example, the g_{ik} metric transfered from the CIELAB to CIEXYZ space is expressed as:

$$\begin{bmatrix} dL^* \\ da^* \\ db^* \end{bmatrix} = \begin{bmatrix} \frac{\partial L^*}{\partial X} & \frac{\partial L^*}{\partial Y} & \frac{\partial L^*}{\partial Z} \\ \frac{\partial a^*}{\partial X} & \frac{\partial a^*}{\partial Y} & \frac{\partial a^*}{\partial Z} \\ \frac{\partial b^*}{\partial X} & \frac{\partial b^*}{\partial Y} & \frac{\partial b^*}{\partial Z} \end{bmatrix} \begin{bmatrix} dX \\ dY \\ dZ \end{bmatrix}. \tag{3.5}$$

In Equation (3.5) the partial derivatives of color vectors in matrix form is called the Jacobian matrix and it is also expressed as $\partial(L, a^*, b^*)/\partial(X, Y, Z)$. The final transformation of g_{ik} metric tensor from the CIELAB color space to the CIE xyY with two Jacobian matrices is:

$$(dE^*_{ab})^2 = \begin{bmatrix} dx dy dY \end{bmatrix} \frac{\partial(X,Y,Z)}{\partial(x,y,Y)}^T \frac{\partial(L,a^*,b^*)}{\partial(X,Y,Z)}^T I \frac{\partial(L,a^*,b^*)}{\partial(X,Y,Z)} \frac{\partial(X,Y,Z)}{\partial(x,y,Y)} \begin{bmatrix} dx \\ dy \\ dY \end{bmatrix} \tag{3.6}$$

Here, the whole transformation matrix is $\frac{\partial(X,Y,Z)}{\partial(x,y,Y)}^T \frac{\partial(L,a^*,b^*)}{\partial(X,Y,Z)}^T I \frac{\partial(L,a^*,b^*)}{\partial(X,Y,Z)} \frac{\partial(X,Y,Z)}{\partial(x,y,Y)}$ and it represents the metric tensor of the CIELAB color space in the CIE xyY color space. The coefficients of the first two columns and rows of the three dimensions metric tensor gives us the threshold ellipse in the chromaticity diagram. The similar method is applied to compute the threshold ellipse of the CIELUV formula.

Ellipse comparison method: A technique is developed to compare the line element derived ellipses of above two formulas with experimentally observed ellipses in the xy chromaticity diagram. In such a technique, the ratio of the union area and the intersection area of a pair of ellipses is calculated. Figure (3.2) shows two ellipses A and B. The ratio of the intersection area and the union area between them is expressed

Figure 3.2: A pair of ellipses having same center - illustration of a pair of ellipses comparison method.

as:

$$R = \frac{\text{Area}(A \bigcap B)}{\text{Area}(A \bigcup B)} \tag{3.7}$$

where R is a nonnegative value between $0 < R \leq 1$. Higher value of R means two ellipses are closely matched.

In this paper, a traditional approach to compare a pair of ellipses having same center is also presented [69]. Three parameters, the area of ellipse, the ratio of the principal axes and the angle between them are calculated. The difference in numerical values of these parameters between a pair of ellipses indicate how well they match.

Result: Figure (3.3) shows MacAdam's original and the computed ΔE^*_{ab} and ΔE^*_{uv} ellipses in the CIE xy chromaticity diagram. The color centers for these computed ellipses are according to the MacAdam's data. Ellipses are computed at $L^* = 70$, for the CIELAB and CIELUV color space formulas and to achieve this lightness value the Y component of the CIE xyY color space is approximated at 0.4 scale. First, the comparison between MacAdam's ellipses and the computed ellipses of above two formulas are done by the traditional approach [69] as stated above.

The comparative data of shape (the ratio of semi major (a) and semi minor (b) axes) and the orientation (angle) between MacAdam, the ΔE^*_{ab} and ΔE^*_{uv} ellipses show that there are disagreement with experimentally observed ellipses and computed ellipses of the CIELAB and CIELUV space formulas [46]. However, it can be seen that computed ellipses of two formulas have general trends of agreement comparing with area of MacAdam's ellipses. For example, the blue is the smallest, the green largest

(a) CIELAB Ellipses having same color centers as MacAdam.

(b) CIELUV Ellipses having same color centers as MacAdam.

Figure 3.3: MacAdam's original and the computed (ΔE^*_{ab}) and (ΔE^*_{uv}) ellipses in the CIE31 chromaticity diagram(enlarged 10 times).

and that red, blue and yellow are more elongated than others.

Similarly, comparing between computed ΔE^*_{ab} and ΔE^*_{uv} ellipses with respect to the shape, it is found that a/b ratio is significantly higher in most of the ΔE^*_{ab} ellipses than the ΔE^*_{uv} ellipses of same color centers. This result indicates that the ΔE^*_{uv} ellipses are more circular than the ΔE^*_{ab} ellipses.

The numerical values of R of the proposed technique stated above to compare the ΔE^*_{ab} and ΔE^*_{uv} ellipses with respect to MacAdam's ellipses are also calculated. This technique has specific advantage over the traditional method for comparing a pair of ellipses. For a pair of ellipses, it takes account of variations in the size, the shape and the orientation simultaneously. Therefore, this value is an indicator which tells us how well two ellipses match each other. The sign test (standard statistical test) of these ratio values R indicates that the ΔE^*_{uv} is performing better than the $\Delta E*_{ab}$ at a level of significance $p = 0.015$.

Figure (3.4) shows the ΔE^*_{ab} and the ΔE^*_{uv} ellipses having the same color centers as Wyszecki's three observers color-matching ellipses respectively. The comparative data of area, shape and orientation between three observers ellipses and computed ΔE^*_{ab} and ΔE^*_{uv} ellipses show a similar behavior as found for the MacAdam data. The sign test of the ratio R for this data set also indicates that the ΔE^*_{uv} is better than the ΔE^*_{ab} with $p = 0.0125$.

Conclusion: The presented method can compute threshold ellipses of the CIELAB and CIELUV space formulas in the chromaticity diagram and thus gives the opportunity to evaluate how well they match the experimentally observed visual color matching data. The comparison between the computed ΔE^*_{ab} and ΔE^*_{uv} ellipses with two different visual data sets [34, 69] suggest that neither formulas are good enough to predict the visual color matching. However, the ratio test method shows that the CIELUV space based formula performs better than the CIELAB space based formula to predict visual color difference for both of the data sets tested.

(a) CIELAB ellipses having same color centers as Wyszecki ellipses.

(b) CIELUV ellipses having same color centers as Wyszecki color-matching ellipses.

Figure 3.4: Wyszecki's three observers color-matching ellipses and computed the ΔE^*_{ab} and ΔE^*_{uv} ellipses in the CIE31 chromaticity diagram (enlarged 5 times).

Contribution in paper A:

In this paper, formulation of the line elements of ΔE^*_{ab} and ΔE^*_{uv} metrics in their respective color spaces are introduced. The Riemannian metrics of ΔE^*_{ab} and ΔE^*_{uv} are transformed into the CIE XYZ and the CIE xyY color spaces by the Jacobian method. Threshold ellipses are computed in the xy chromaticity diagram by this method. Mathematical derivations for this method is derived. A pair of ellipses comparison method is developed. Statistical sign test method is employed to find out the relationship between the predicted ellipses and experimentally observed ellipses.

3.3 Paper B: Riemannian Formulation of the CIEDE2000 Color Difference Formula

In this paper, Riemannian metric tensor of the CIE recommended latest color difference formula, the CIEDE2000 [32] is formulated by applying the line element theory. The CIEDE2000 is the improved version of the CIELAB space based formula with specific weighting functions known as lightness (S_L), chroma (S_C) and hue (S_H), parametric factors (k_L, k_C, k_H), and the rotation term R_T to correct chroma and hue differences in the blue region. This formula is based on the supra threshold data like BFD-P [31] and claimed as an excellent out performing formula, when measured against the aggregate data set. The main focus of this paper is to study the performance of this advanced formula for measuring small color differences in other color space as the formula does not have its specific or corresponding color space.

Line element of the CIEDE2000 color difference equation gives the Riemannian metric tensor g_{ik} in a non-Euclidean metric form. The Jacobian method is used to transform this metric tensor into the CIE 1964 xyY color space. The transformation steps are:

- CIELCH $\Leftrightarrow$ CIELAB $\Leftrightarrow$ CIEXYZ $\Leftrightarrow$ CIExyY

The purpose of such transformation is to compute the ellipses in that color space where experimentally observed BFD-P ellipses are represented. The computed ellipses of the CIEDE2000 formula and the original ellipses obtained from the BFD-P data set are compared by calculating the ratio of the area of the intersection and the area of the union as described in the paper A. MacAdam's ellipses are also compared with the computed CIEDE2000 ellipses in the CIE 1931 xy chromaticity diagram.

Result: Figure (3.5)shows the computed ellipses of the CIEDE2000 formula and BFD-P ellipses in the CIE1964 xy chromaticity diagram with same color centers at the constant lightness value ($L^* = 50$). It can be seen that both BFD-P and CIEDE2000 ellipses for the neutral and gray color centers are almost the same. However, in CIEDE2000, the orientation of ellipses in the blue region are rotated compared to the BFD-P ellipses of same region. On the other hand, in the red region too, the CIEDE2000 ellipses are rotated in opposite direction and stretched in length. For

Figure 3.5: BFD-P and Computed CIEDE2000 ellipses in the CIE64 Chromaticity diagram - Enlarged 1.5 times

comparing the similarity of a pair of ellipses, the ratio R as stated in paper A: has

maximum value .95 in the neutral color region and minimum value .25 around high chroma blue. Figure (3.6) shows the MacAdam's original ellipses and the CIEDE2000 ellipses in the CIE 1931 xy chromaticity diagram. This figure helps to visualize the difference between experimentally observed and computed ellipses in terms of size shape and orientation in a simple manner.

Figure 3.6: MacAdam and CIEDE2000 ellipses plotted in the CIE1931 chromaticity xy diagram - Enlarged 10 times.

Conclusion: Formulation of the CIEDE2000 formula into the Riemannian metric and application of the Jacobian method to transfer it into different color spaces as well as to compute ellipses from this metric are successfully accomplished. Comparing the computed ellipses with BFD-P ellipses, orientation problems are seen the CIEDE2000 ellipses in the blue region as well as in the red region. This indicates that further research for the improvement of the rotation term or the color difference metric, in general is necessary.

Contribution in paper B:

Formulation of the complex the CIEDE2000 formula in terms of the line element

is performed. Ellipses of this formula is computed in the xy chromaticity diagram to compare with experimentally observed BFD-P data as well as with the MacAdam data in the CIE 1964 chromaticity diagram. In this process, mathematical derivations of the Jacobian metrics in the CIE XYZ and xyY color spaces are done (See Appendix A for the detail derivations).

3.4 Paper C: Riemannian Formulation and Comparison of Color Difference Formulas

In this paper four color difference formulas the CIELAB (ΔE^*_{ab}), the CIELUV (ΔE^*_{uv}), the OSA-UCS (ΔE_E) and the infinitesimal approximation of the CIEDE2000 (ΔE_{00}) are taken to study by the line element theory. It is an extended version of paper A and paper B with another color difference formula the the OSA-UCS (ΔE_E). The purpose of this paper is to do a comparative study between computed ellipses of these four color difference metrics with respect to the supra-threshold BFD-P [31] ellipses in the CIE 1964 xy chromaticity diagram. In this paper, formulating Remiannian metric of ΔE_{00} (refer Equation 2.11) is improved than presented in the paper B. The Remiannian metric of the ΔE_{00} is formulated by using $L'C'h'$ coordinates instead of $L'C'H'$ due to the rule of the Riemannian geometry. Calculation of the Remiannian metric using $L'C'h'$ coordinates gives us an approximation of ΔE_{00} when we substitute $dH' = C'dh'$ as proposed by Völz [59] at infinitesimal color difference only. It is called here Riemannized ΔE_{00} which can not be integrated to build CIE defined ΔE_{00} due to the definition of $\Delta H'$. The detailed explanation is given in paper C. However, it is approximately equal to the original CIEDE2000 formula at infinitesimal color difference with a error rate less than 0.5% for $\Delta E_{00} \leq 1$.

For the ΔE_E of the OSA-UCS log-compressed color space the line element as given

in Equation (3.8) is written as:

$$(dE_E)^2 = \begin{bmatrix} dL_E & dG_E & dJ_E \end{bmatrix} \begin{bmatrix} 1 & 0 & 0 \\ 0 & 1 & 0 \\ 0 & 0 & 1 \end{bmatrix} \begin{bmatrix} dL_E \\ dG_E \\ dJ_E \end{bmatrix}. \tag{3.8}$$

The transformation of the Riemannian metric of this formula into the xyY color space is:

$$\begin{bmatrix} dL_{OSA} \\ dG \\ dJ \end{bmatrix} = \frac{\partial(L_{OSA}, G, J)}{\partial(x, y, Y)} \begin{bmatrix} dx \\ dy \\ dY \end{bmatrix} = \begin{bmatrix} \frac{\partial L_{OSA}}{\partial(x,y,Y)} \\ \frac{\partial(G,J)}{\partial(x,y,Y)} \end{bmatrix} \begin{bmatrix} dx \\ dy \\ dY \end{bmatrix}, \tag{3.9}$$

where $\partial(L_{OSA}, G, J)/\partial(x, y, Y)$ is a 3×3 Jacobian matrix that is further divided into the 1×3 and 2×3 Jacobian matrices $\partial L_{OSA}/\partial(x, y, Y)$ and $\partial(G, J)/\partial(x, y, Y)$, respectively. The detail computation of Jacobian metrics are found in paper C as well as in appendix I.

Result: The transformed 3×3 Riemmanian metrics of the CIELAB (ΔE^*_{ab}), the CIELUV (ΔE^*_{uv}), the OSA-UCS (ΔE_E) and the Riemannized CIEDE2000 (ΔE_{00}) give ellipsoid in the CIE xyY color space. If we define constant lightness, then partial derivatives of lightness functions of all Jacobians will be zero. This gives 2×2 metric tensors and ellipses are computed in the xy chromaticity diagram. Ellipses of above four formulas are computed at the constant lightness value ($L^* = 50$) and compared with the BFD-P ellipses. Similarity comparison between the BFD-P and ellipses derived from above four formulas is done by calculating R values as stated in the paper A. Figure (3.7) shows histogram of R values between BFD-P and ΔE^*_{ab}, ΔE^*_{uv}, Riemannized ΔE_{00} and ΔE_E ellipses. The maximum R values given by ΔE^*_{ab}, ΔE^*_{uv}, Riemannized ΔE_{00} and ΔE_E are .81, .87, .95, and .93 respectively. Similarly, the lowest R values of these four formulas are, .1, .14, .2 and .2 respectively. Ellipse pairs of all four color difference metrics having maximum R values are located around neutral color region

(a) CIELAB. (b) CIELUV.

(c) CIEDE00. (d) OSA-UCS ΔE_E .

Figure 3.7: Histogram of comparison values of ΔE^*_{ab}, ΔE^*_{uv}, Riemannized ΔE_{00} and OSA-UCS ΔE_E with respect to BFD-P ellipses. The values lie in the range $0 < x \leq 1$.

while matching pairs with lowest R are found around high chroma blue. The result indicates that the Riemannized ΔE_{00} and ΔE_E perform better than the ΔE^*_{ab} and the ΔE^*_{uv}.

Box plots are also used to study ellipse matching values (R) of these metrics (see figure 3.8). The Riemannized ΔE_{00} gives the highest median value while the CIELAB median value is the lowest. the performance ranking of these metrics are categorized as follows: Riemannized ΔE_{00} first, ΔE_E second, ΔE^*_{uv} third and ΔE^*_{ab} fourth. However, there is no big difference between ΔE_{00} and ΔE_E and between ΔE^*_{uv} and ΔE^*_{ab}.

The pairwise statistical sign test of R values shows that at 5 % confidence level,

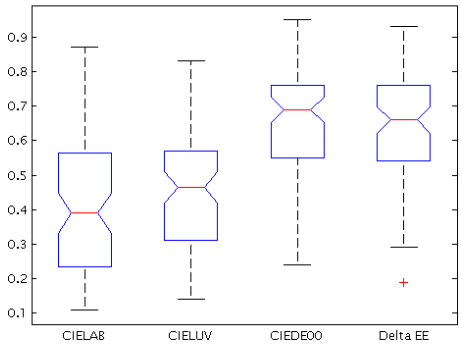

Figure 3.8: Box plots of ellipse matching values (R) of the ΔE^*_{ab}, ΔE^*_{uv}, Riemannized ΔE_{00} and OSA-UCS ΔE_E with respect to BFD-P ellipses - .

Riemannized ΔE_{00} and ΔE_E both performed significantly better than ΔE^*_{uv} and ΔE^*_{ab} metrics. Further, ΔE^*_{uv} performs better than ΔE^*_{ab} with $p = 0.0176$. There is no significant difference between ΔE_{00} and ΔE_E metrics.

The difference (ΔE) between the Riemannized ΔE_{00} and the original ΔE_{00} metrics for finite color differences by using test data of Gaurav Sharma et.al. [52] shows that the error is less than 0.5% for $\Delta E_{00} \leq 1$ and for $\Delta E_{00} \leq 2$, it is smaller than 1.2%. Therefore, the Riemannized ΔE_{00} is very close to the exact ΔE_{00} for the small colour differences. **Conclusion** Riemannized ΔE_{00} and OSA-UCS ΔE_E formulas measure the visual color differences significantly better than ΔE^*_{ab} and ΔE^*_{uv} formulas.

However, neither formulas are fully perfect for matching the visual color differences data. Among the CIELAB and CIELUV formulas, performance of the CIELUV is found slightly better than the CIELAB. Similarly, there is no significant difference between Euclidean ΔE_E and Riemannized CIEDE2000 formulas. It is interesting to note that the Euclidean ΔE_E formula is not inferior to the complex, non-Euclidean industry standard ΔE_{00} for measuring small color differences.

Contribution in paper C:

Formulation of the the OSA-UCS (ΔE_E) in terms of the line element is done. A

comparative study between four color difference metrics to predict experimentally observed BFD-P data in xy chromaticity diagram is done. The line element formulation of the CIEDE2000 is elaborated more precisely. Box plots are used to show the comparative study of their performance. Based on the result, features of color spaces are discussed.

3.5 Paper D: CIE Uniform Chromaticity Scale Diagram for Measuring Performance of OSA-UCS Delta EE and CIEDE00 Formulas

The CIELUV based u^*, v^* diagram is used to compare the non-Euclidean approximate form of ΔE_{00} and the Euclidean ΔE_E color difference formulas for measuring the visual data. At constant lightness,u^*, v^* diagram is identical in shape to the CIE recommended (CIE 15:2004) the uniform chromaticity scale (UCS) diagram. The motivation for this paper is to implement the idea of other researchers who suggested to use u^*, v^* diagram before drawing any conclusions about visual color differences [23, 39, 57]. The uniform chromaticity scale (UCS) diagram based on the CIELUV color space is developed by the projective transform of tristimulus (XYZ) values. The intention of such transformation is to get perceptual uniformity which means it is more suitable for measuring small color differences. It is also interesting to know how well these two advanced formulas predict visual color differences in an independent uniform color space like the CIELUV.

In this paper, equi-distance ellipses of the approximate form of ΔE_{00} and ΔE_E are computed in the u^*, v^* diagram. They are compared with the BFD-P ellipses. Here, the BFD-P ellipses are transformed into the CIELUV space from the xyY space where theses ellipses are observed. The comparison between the computed ellipses of each formula and BFD-P ellipses is done by calculating a matching ratio, $R \in (0, 1]$.

Result The ellipses of both formulas are similar in the neutral region with respect

to the BFD-P ellipses. In the blue region, ellipses of both formulas appear smaller in size than the observed ellipses and they are following close pattern to BFD-P in the green part but, rotated in the red region. Figure **??** shows box plot of the R values. We

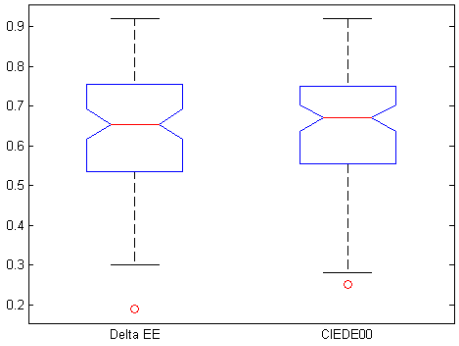

Figure 3.9: Box plots of ellipse matching values of the approximate form of ΔE_{00} and OSA-UCS ΔE_E with respect to BFD-P ellipses - Upper and lower quartiles show full range of matching data.

can see that both ΔE_{00} and the ΔE_E have similar median values with slight differences. Figure shows (3.10) cumulative distribution function (CDF) of two R values . This

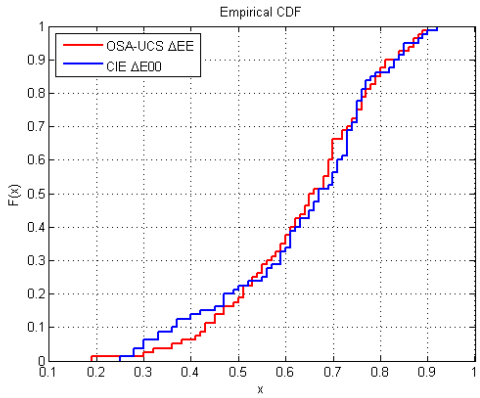

Figure 3.10: CDF plot of R values of the OSA-UCS ΔE_E and the approximate form of ΔE_{00} - .

function describes the distribution of R values by taking the sum of each value of R having finite mean and variance. The maximum difference between two curves is .1

and follow the pattern of normal distribution.

Conclusion: Simple Euclidean ΔE_E metric is not inferior to the complex non-Euclidean mathematical framework of ΔE_{00} for evaluating color differences in the u* v* chromaticity diagram of the CIELUV color space.

Contribution in paper D

The CIELUV color space based $u*v*$ chromaticity diagram is used to compare the performance of the approximate form of ΔE_{00} and the OSA-UCS ΔE_E for predicting the experimental data. To accomplish this task, the Jacobian metrics of these formulas are computed in the CIELUV color space. Similarly, the BFD-p data which is represented in the CIE xy diagram is also transformed in the $u*v*$ chromaticity diagram by the Jacobian method. Cumulative distribution function (CDF) plot is used to show the comparison values of these metrics.

3.6 Paper E: Geodesic Calculation of Color Difference Formulas and Comparison with the Munsell Color Order System

This paper mainly focuses study of perceptual attributes hue, chroma and lightness predicted by the four color difference formulas the CIELAB (ΔE^*_{ab}), the CIELUV (ΔE^*_{uv}), the OSA-UCS (ΔE_E) and the infinitesimal approximate form (Riemannized) of the CIEDE2000 (ΔE_{00}) in the CIELAB color space based on Schrödinger's hypothesis [50]. Riemannian metric tensors of these formulas can be used to compute the shortest curve between two points in a color space which is called a geodesic.

Schrödinger's explained the idea of deriving surfaces of constant brightness from line element. He also hypothesized that all colors along a geodesic curve originating from a point representing an achromatic stimulus on a surface of constant brightness share the same hue. He further hypothesized that contours of constant chroma can be

determined from these geodesics (henceforth called hue geodesics) by taking each point on a chroma contour as the terminus of a hue geodesic such that all the hue geodesics terminate on that chroma contour at the same geodesic distance. Explanation of this hypothesis is also found in Wyszecki and Stiles [70]

Schrödinger's hypothesis is tested by computing the hue geodesics and chroma contours of four color difference formulas, the ΔE^*_{ab} , the ΔE^*_{uv}, the infinitesimal approximate form of ΔE_{00} and the OSA-UCS based ΔE_E in the CIELAB color space, and comparing the results to the Munsell color order system. The mathematical construct to compute these hue geodesics and chroma contours using Riemannian metric tensors of each formula are explained in section 2.9. For such computation the Euler-Lagrange equations are necessary to solve by using numerical method like the Runge-Kutta [16].

Results: The hue geodesics and chroma contours of the ΔE^*_{ab} , the ΔE^*_{uv}, the Riemannized ΔE_{00} and the ΔE_E are computed at $L = 30/50/70$, which correspond to the Munsell value 3, 5 and 7 respectively. In the CIELAB color space, hue geodesics of these color difference formulas start from the origin of a^*, b^* to different directions. In a similar way, chroma contours start from the a^*, b^* origin. They are also evenly spaced along the hue geodesic distance. The hue geodesics and chroma contours form the geodesic grids of the above four color difference formulas. For example, Figure (3.11) shows the hue geodesics and chroma contours of these four formulas computed at $L = 50$

All these formulas derived hue geodesics and chroma contours do not match the Munsell chromas and hue circles. Comparatively, the approximate ΔE_{00} and the ΔE_E predicted hue geodesics and chroma contours are found slightly better than predicted ones by the ΔE^*_{ab} and the ΔE^*_{uv}. In the case of the approximate ΔE_{00}, chroma contours are elliptical in the central region of the CIELAB color space and their shapes also diverge from circular to notch on their path in the blue and violet regions. This happened due to the G parameter in the CIEDE2000 formula. Similarly, the shape of

(a) CIELAB geodesic grid.

(b) CIELUV geodesic grid.

(c) Riemannized CIEDE00 geodesic grid.

(d) OSA-UCS ΔE_E geodesic grid.

Figure 3.11: Computed geodesic grids of the ΔE^*_{ab}, the ΔE^*_{uv}, the Riemannized ΔE_{00} and the OSA-UCS ΔE_E in the CIELAB space and compared with the Munsell chromas and hues at the Munsell value 5.

ΔE_E and ΔE^*_{uv} predicted geodesic grid is similar.

Conclusion:

The latest color difference formulas like the OSA-UCS ΔE_E and the CIEDE2000 do not show better performance to predict hue geodesics and chroma contours than the conventional CIELAB and CIELUV color difference formulas. These findings also suggest that the distribution of hue geodesics and chroma contours of the above four color difference formulas are weak to predict perceptual color attributes of the Munsell system in all over the color space even though their quantitative color difference measures are comparatively good.

Contribution in paper E:

With the Riemannian metrics developed in paper C, Schrödinger's hypothesis is tested for the CIELAB (ΔE^*_{ab}), the CIELUV (ΔE^*_{uv}), the OSA-UCS (ΔE_E) and the infinitesimal approximate form (Riemannized) of the CIEDE2000 (ΔE_{00}). This is done by computing hue geodesics and chroma contours of these metrics in the CIELAB color space and compared with the Munsell system. The Jacobian metrics in the CIELAB space is derived. Distribution of their color stimuli are studied to show how well they predict perceptual color attributes.

3.7 Discussion

The development of many standard color difference formulas and color spaces suggest that quantitative measurement of color differences between two colors has progressed in the color science. All these color difference formulas attempt to decide whether two colors are visually equivalent or not. But, to predict visual difference between two colors is still challenging. There are mainly two reasons: first no existence of perfect uniform color space. Secondly, color difference formulas are optimized to predict certain experimental data and as a result, we can not say that such a color difference formula

can able to approximate other kind of experimental data. For a specific application, which color space or color difference formula should be used need mathematical analysis.

In color science, two colors can be discriminated locally at a point in a color space with an infinitesimal approximation. Such an approach to predict the discriminability between two colors is called the line element theory. In this theory, the metric g_{ik} is introduced to describe nonlinear distortions imposed by the color vision system in the color discrimination. This metric is based on the Riemannian space and it is also called Riemannian metric tensor. It gives the intrinsic properties about the color measured at a point in the color space. Specifically, the metric represents the chromaticity difference of any two colors measured along the geodesic of the surface. This line element theory has also limitations specially if we want to relate the value of g_{ik} to light adaptation (varying light conditions). However, considering the iso-luminance plane as hypothesized by Schrödinger [50], the line element theory and the g_{ik} metric provide an adequate characterization of the color discrimination data. Construction of ellipses using color discrimination data sets in an iso-luminance plane prove this fact. For example, starting from MacAdam [34], Brown [5], Wyszecki and Fielder [69], to recent BFD-Perceptibility(BFD-P) [31], RIT-DuPont [3], Witt [66]and others constructed ellipses from their data sets. The main concern in this research study is not primarily to discover better formulas for predicting the small color differences. It intends rather with testing hypothesis concerning the organization of perceptual (visual) color mechanisms as well as to study the relation between different color space and color difference formulas. Therefore, study of the various color difference metrics by the line element theory treating the color spaces as Riemannian spaces is useful as it represents a natural theory of color vision.

The first four papers presented here describe the implementation of line element theory for four color difference formulas, the ΔE^*_{ab}, the ΔE^*_{uv}, the approximate form of ΔE^*_{00} and the ΔE_E to evaluate their performance for measuring visual color differences.

This is done by a comparative study between computed ellipses of these four color difference metrics with respect to experimentally observed data sets. In this research study, MacAdam, Wyszecki and Fielder and BFD-P data sets are used. The first two are known as threshold data sets and the last one is supra-threshold data set. A pair of ellipses comparison method is developed (see section 3.1) to compare between computed ellipses of these formulas and experimentally observed ellipses from threshold and supra-threshold data sets. This method gives color matching R values which takes account of variations in the size, the shape and the orientation simultaneously for a pair of ellipses. The pairwise statistical sign test of R values is also done between all pairs of metrics.

The summary results of first four papers indicate that all these four formulas show poor performance to measure visual color difference data in the blue region. Even the latest ΔE^*_{00} which has many parameters to correct chroma and hue differences in the blue region does not show superior performance as expected in that region with respect to other three color difference formulas. In the green region, the performance of these formulas are seen better than in the blue region. Like wise, in the red region such performance lies in between than blue and green regions. Comparatively, among the four color difference formulas, the ΔE^*_{ab} shows the least performance to predict the visual color difference, the ΔE^*_{uv} is better than the ΔE^*_{ab} and the approximate form of ΔE^*_{00} and the ΔE_E tops the preceding two formulas. The statistical sign test of R values shows that there is no significant difference between the approximate form of ΔE^*_{00} and the ΔE_E. Here , the error between the approximate form of ΔE^*_{00} and the original form of ΔE^*_{00} is less than 0.5% for $\Delta E_{00} \leq 1$.

The overall analysis of above results also describes the characteristics of color spaces used by above color difference metrics responsible for better performance. For example, saturation is defined in ΔE^*_{uv} not in ΔE^*_{ab} [2]. In ΔE_E, the lightness L_{OSA} takes into account the Helmholtz-Kohlrausch and crispening effects [44]. Further, the OSA-UCS

system adopts a regular rhombohedral geometry which gives square grid with integer value of lightness [45]. This makes OSA-UCS space more uniform than CIELAB and CIELUV and suitable for small to medium color difference measurement. On the other hand, the non-Euclidean Riemannized ΔE_{00} have many parameters for computing color differences to predict visual color difference closely but, still it is lagging to reach its goal. However, this formula has its specific advantage to correct the non-linearity of the visual system. But, the quality of the formula depends on selecting parameters values as well as the color space on which it is based. It could be a discussion point further that without improving the color space, would it be a good idea to improve a color difference formula?

The last paper describes how the Riemannian metrics of these formula are used to test Schrödinger's hypothesis for predicting perceptual attributes hue, chroma and lightness with respect to the Munsell system. At a fixed value of lightness L^*, hue geodesics originating from the achromatic point and their corresponding chroma contours of the above four formulas in the CIELAB color space can be computed by solving the Euler-Lagrange equations in association with the Riemannian metrics of these color difference formulas. Hue geodesics and chroma contours predicted by above formulas can be compared with the Munsell chromas and hues circles at different Munsell values. For such comparison, the necessary condition is that the lightness value should correspond to the Munsell value. The result shows that computed hue geodesics and chroma contours of these formulas do not predict precisely the Munsell chromas and hue circles. In the blue and violet region, all formulas hue geodesics disagree highly than the Munsell chroma. The ΔE^*_{ab} hue geodesics are intersecting the Munsell chromas around yellow, green and blue areas and they are straight whereas the Munsell chromas are curved at high chroma. The ΔE^*_{uv} predicted hue geodesics are intersecting the Munsell chromas mostly in the third quadrant of the CIELAB space. They follow the curvature pattern of the of the Munsell chromas, and their directions in the red

and yellow regions of the CIELAB space are very close to the Munsell chromas.

In the case of approximate ΔE_{00}, sharply curved hue geodesics and change in circular shape of chroma contours are found in the blue region which show poor performance of this formula for predicting the Munsell chromas in that region. In the central region, chroma contours of this formula are also found elliptical instead to be circular. Calculating hue geodesics and chroma counters setting $G = 0$(G parameter defined in the ΔE_{00} formula) improves the elliptical nonlinearity except at the blue region. This finding suggests that correcting chroma in the blue region of the color space can have a diverse effect in the whole color space.

The ΔE_E predicted chroma contours are seen similar to the Munsell hue circles in the achromatic region of the CIELAB color space but, in other parts of the CIELAB color space they are not matching the Munsell hue circles. The shape of ΔE_E chroma contours are similar to the ones predicted by the CIELUV formula, but they appear to be more correct.

In general, the approximate ΔE_{00} and the ΔE_E do not show better performance for predicting the Munsell chroma and hue circles than the ones predicted by the conventional the ΔE^*_{ab} and the ΔE^*_{uv}.

Chapter 4

Conclusion and Perspective

The main purpose of this research work is to develop the line element model of different color difference formulas to study their performance for predicting visual color difference. Next, to compute hue geodesics and chroma contours of these formulas to test how well they predict perceptual color attributes. The concluding remarks of this research study are listed below:

- Formulation of the line element distance of the ΔE^*_{ab}, the ΔE^*_{uv}, the approximate (Riemannized) ΔE_{00} and the ΔE_E and deriving their Riemannian metric tensors by converting color coordinates into color vectors are accomplished. The Riemannized ΔE_{00} is found indistinguishable to the exact ΔE_{00} for the small color differences.

- Computation of the threshold ellipses of these four formulas in different color spaces is successfully done by applying the Jacobian method.

- A pair of ellipses comparison method is developed to compare the computed ellipses of the formulas with the experimentally observed standard data sets. This method gives a matching ratio R which takes account of variations in the size, the shape and the orientation for a pair of ellipses simultaneously.

- Comparison of the computed ellipses of the above four formulas with the experimentally observed different standard data sets shows that neither formulas are fully perfect for matching visual color difference data sets. However, Riemannized ΔE_{00} and the ΔE_E formulas measure the visual color differences better than the ΔE^*_{ab} and the ΔE^*_{uv} formulas at local level.

- The Euclidean ΔE_E formula is not inferior to the complex, non-Euclidean industry standard ΔE_{00} for measuring small color differences.

- Computation of hue geodesics and chroma contours of above color difference formulas are succeeded using their Riemannian metrics in the CIELAB color space to test Schrödinger's hypothesis with respect to the Munsell system.

- Comparisons of the geodesic grids (combined geometrical structure of hue geodesics and chroma contours) of these formulas with the Munsell chromas and hue circles at the Munsell values 3, 5 and 7 show that none of these four formulas can precisely fit the Munsell data.

- It is interesting to note that the latest color difference formulas like the OSA-UCS ΔE_E and the Riemannized ΔE_{00} do not show better performance to predict hue geodesics and chroma contours than the conventional CIELAB and CIELUV color difference formulas.

In this research work, the line element theory of Riemannian form for four color difference formulas as described above is tested to predict a variety of experimental color discrimination data sets (MacAdam, Wyszecki and BFD-P). The recent BFD-P data sets are based on printed color samples. To validate effectiveness of the line element theory, it should be tested with other kind of color discrimination data sets based rather than the printed color samples. One example could be color discrimination data sets based on self illuminating color samples.

Line elements basically concerns with the color vision mechanism and they are developed by vision researchers. Whereas color difference formulas and color spaces typically concern with printed color samples originated from the paint industry. These color spaces and color difference formulas are developed on basis of trial and error with the CIE XYZ system as underlying color description. The inadequacy of the CIE system is that it does not consider cone receptor primaries for the color discrimination. In the color vision research, color discrimination in the cone receptor level is important [64].

In addition, color order systems like the Munsell system are based on hue, chroma and value ordering principle. These systems are considered perceptually uniform and in many color discrimination context, they have proven to be useful. However, they do not have any theoretical base.

From these facts, the development of a color space model based on the line element theory that can be used for color and brightness discrimination could be the future work. In such a model, Schrödinger's hypothesis [50] as well the Vos and Walraven's zone fluctuation line element [65] concept can be integrated for more primitive investigations.

References

[1] CIE colorimétrie, resolutions 1-4. 9

[2] R. S. Berns. *Principles of Color Technology.* John Wiley and Sons, New York, 2000. 14, 23, 55

[3] R.S. Berns, D. H Alman, L. Reniff, G.D. Snyder, and M.R. Balonon-Rosen. Visual determination of suprathreshold color-difference tolerances using probit analysis. *Color Res. Appl.*, 16:297–316, 1991. 3, 8, 14, 54

[4] W. M. Boothby. *An Introduction to Differentiable Manifolds and Riemannian Geometry.* Academic Press, New York, 1955. 24

[5] W.R.J. Brown. Colour discrimination of twelve observers. *J. Optical Society of America*, 47:137–143, 1957. 3, 14, 54

[6] J. Chao, R. Lenz, D. Matsumoto, and T Nakamura. Riemann geometry for color characterization and mapping. In *In: Proc. CGIV , IS&T, Springfield*, 2008. 25

[7] K.D. Chickering. Optimization of the MacAdam modified 1965 friele color-difference formula. *J. Optical Society of America*, 57:537, 1967. 14

[8] CIE. Recommendations on uniform colour spaces, colour difference equations and psychometric color terms. Technical Report 15, CIE Central Bureau, Vienna, 1978. 3, 15, 17, 35

[9] CIE. Industrial colour difference evaluation, CIE publication number 116, CIE central bureau, Vienna, 1985. 18

[10] CIE. Parametric effects in color-difference evaluation. Technical report, CIE Central Bureau, Vienna, 1993. 19

[11] CIE. Industrial colour difference evaluation. Technical Report 116, CIE Central Bureau, Vienna, 1995. 3

[12] CIE. Improvement to industrial color–difference evaluation. Technical Report 142, CIE central bureau, Vienna, 2001. 3, 4, 19

[13] Nickerson D. OSA uniform color samples: a unique set. *Color Res. Appl.*, 6:7–33, 1981. 21

[14] Nickerson D. and Stultz K.F. Color tolerance specification. *J.Optical Society of America*, 34:550–570, 1944. 15

[15] D.B.Judd. Standard response function for protanopic and deuteranopic vision. *J.Optical Society of America*, 39:505, 1949. 9

[16] D.R.Pant and I.Farup. Geodesic calculation of color difference formulas and comparison with the munsell color order system. *Color Res. Appl. (accepted for publication)*, 2011. 51

[17] Adams EQ. X-Z planes in the 1931 I.C.I system of colorimetry. *J.Optical Society of America*, 32:168–173, 1942. 15

[18] C. E. Foss. Space lattice used to sample the color space of the committee on uniform color scales of the Optical Society of America. *J.Optical Society of America*, 68: 1616–1619, 1978. 20

[19] Manuel Melgosa Garcia Pedro A., Huertas Rafael and Cui Guihua. Measurement of the relationship between preceived and computed color differences. *J.Optical Society of America*, 24:1823–1829, 2007. 4

[20] J. Gay and R. Hirschler. Field trials for CIEDE2000: Correlation of visual and instrumental pass/fail decisions in industry. Technical Report ISBN 390190621, 25th, The CIE Session, San Diego, Jun. 2003. 3

[21] H.G. Grassmann. Zur theorie der farbenmischung. *Annalen der Physik*, 89:69–84, 1853. 7

[22] John Guild. The colorimetric properties of the spectrum. *Philosophical Transactions of the Royal Society of London*, 230:149–187, 1931. 8

[23] R. W.G. Hunt. The challenge of our unknown knowns. In *18th Color Imaging Conference*, pages 280–284. IS&T, November 2010. 48

[24] D. Judd and G. Wyszecki. *Colour in business, science and Industry*. Wiley, New York, 1975. 23

[25] D.B. Judd. Ideal color space: Curvature of color space and its implications for industrial color tolerances. *Palette*, 29:21–28, 1968. 4, 25

[26] Witt K. CIE guidelines for coordinated future work on industrial colour-difference evaluation. *Color Res. Appl.*, 20:399–403, 1995. 14

[27] D.H Kim and J.H Nobbs. New weighting functions for the weighted CIELAB colour difference formula. In *Proceedings of AIC Colour*, pages 446–449, Kyoto, 1997. AIC. 3, 14

[28] Toko Kohei, Jinhui Chao, and Reiner Lenz. On curvature of color spaces and its implications. In *5th European Conference on Colour in Graphics, Imaging, and Vision, CGIV 2010*, June 2010. 9

[29] R. G. Kuehni. *Color Space and its Division*. John Wiley and Sons, New York, 2003. 4, 26

[30] R. G. Kuehni and Schwarz A. *A survey of Color Order Systems from Antiquity to the Present*. Oxford University Press, 2008. 7

[31] M. R. Luo and B. Rigg. Chromaticity-discrimination ellipses for surface colors. *Color Res. Appl.*, 11:25–42, 1986. 3, 8, 14, 41, 44, 54

[32] M.R Luo, G.H. Cui, and B. Rigg. The development of the CIE2000 colour difference formula. *Color Res. Appl.*, 26:340–350, 2001. 3, 19, 41

[33] D. L. MacAdam. Specification of small chromaticity differences. *Optical Society of America*, 33(4), 1942. 3

[34] D.L MacAdam. Visual sensitivities to color differences in daylight. *J. Optical Society of America*, 32:247–274, 1942. 1, 8, 13, 35, 39, 54

[35] D.L MacAdam. Uniform color scales. *J.Optical Society of America*, 64:1691–1702, 1974. 20

[36] MacDonald. *Colour Physics for Industry*. Society of Dyers and Colourists, 2 edition, 1997. 11

[37] J.C. Maxwell. On the theory of compound colours, and the relations of the colours of the spectrum. *Proceedings of the Royal Society*, 10:57–84, 1857. 7

[38] M. Melgosa, R. Huertas, and R. S. Berns. Performance of recent advanced color difference fromulae using the standardized residual sum of squares index. *J. Optical Society of America*, 25(7):pp. 1828–1834, July 2008. 3

[39] M.Mahy, L. Van Eycken, and A. Oosterlinck. Evaluation of uniform color spaces developed after the adoption of CIELAB and CIELUV. *Color research and application*, 19(2):105–121, April 1994. 48

[40] Albert H Munsell. A pigment color system and notation. *The American Journal of Psychology*, 23:236–244, 1912. 9, 23

[41] Sir ISAAC NEWTON. *Opticks*. William Innys, London, 1730. 7

[42] C. Oleari. Color opponencies in the system of the uniform color scales of the Optical Society of America. *J. Optical Society of America*, 21:677–682, 2004. 21

[43] C. Oleari. Hypotheses for chromatic opponency functions and their performance on classical psychophysical data. *Color Res. Appl.*, 30:31–41, 2005. 21

[44] C. Oleari, M. Melgosa, and R. Huertas. Euclidean colour difference formula for small-medium colour differences in log-compressed OSA-UCS space. *J. Optical Society of America*, 26(1):121–134, 2009. 3, 21, 55

[45] Claudio Oleari. Uniform color space for 10 degree visual field and OSA uniform color scales. *J. Optical Society of America*, 10(7):pp. 1490–1498, July 1993. 56

[46] D. R. Pant and I. Farup. Evaluating color difference formulae by riemannian metric. In *Fifth European Conference on Colour in Graphics, Imaging (CGIV 2010)*, 2010. 37

[47] A. B. Poirson, B. A. Wandell, D.C. Varner, and D. H. Brainard. Surface characterizations of color thresholds. *J.Optical Society of America*, 7:783–789, 1990. 13

[48] H. L. Resnikoff and Houston. Differential geometry and color perception. *Journal of Mathematical Biology, Springer-Vertag*, 1:97–131, 1974. 25

[49] G Riemann. Über die Hypothesen, welche der Geometrie zu Grunde liegen. *Abh Königl Ges Wiss Göttingen*, 12:133–152, 1868. 1, 7

[50] E Schrödinger. Grundlinien einer Theorie der Farbenmetrik im Tagessehen. *Annalen der Physik*, 4:397–426, 1920. 1, 8, 26, 27, 33, 50, 54, 61

[51] W. Schultze. The usefulness of colour difference formulas for fixing colour tolerances. In *AIC Proceedings*, pages 254–265, 1972. 4

[52] Gaurav Sharma, Wencheng Wu, and Edul N. Dalal. The CIEDE2000 color-difference formula: Implementation notes, supplementary test data, and mathematical observations. *Color Res. Appl.*, 30:21–30, 2004. 47

[53] L. Silberstein. Notes on W.S. Stiles paper entitled : A modified Helmholtz line-element in brightness-colour space. *J. Optical Society of America*, 37(4):pp. 292–295, 1947. 4

[54] NI. Speranskaya. Determination of spectral color coordinates for twenty-seven normal observers. Technical report, Optics Spectrosc, 1959. 9

[55] W. Stiles and JM Burch. Color matching investigation. Technical report, Optica Acta, 1958. 9

[56] W.S. Stiles. A modified Helmholtz line element in brightness-colour space. In *Proc. Phys. Soc. London*, pages 41–65, 1946. 1, 8, 27

[57] S. Takamura and N. Kobayashi. Practical extension to CIELUV color space to improve uniformity. In *IEEE, ICIP*, pages 393–396, 2002. 48

[58] P. Urban, M. R. Rosen, and R. S. Berns. Embedding non-euclidean color spaces into euclidean color spaces with minimal isometric disagreement. *Optical Society of America*, 27(6), 2007. 4

[59] H. G. Völz. Euclidization of the first quadrant of the CIEDE2000 color difference system for the calculation of large color differences. *Color Res. Appl.*, 31:5–12, 2006. 44

[60] H. von Helmholtz. Das psychophysische Gesetz auf die Farbunterschiede trichro-

matischer Auge anzuwenden. *Psychol. Physiol. Sinnesorgane*, 3:1–20, 1892. 1, 7, 25, 26

[61] J. J. Vos. Colorimetric and photometric properties of a 2 degree fundamental observer. *Color Res. Appl.*, 3:125–128, 1978. 9

[62] JJ Vos. Line elements and physiological models of color vision. *Color Res. Appl.*, 4:208–216, 1979. 28

[63] JJ Vos. From lower to higher colour metrics: a historical account. *Clinical and Experimental Optometry*, 89(6):348–360, November 2006. 1, 2

[64] JJ. Vos and PL Walraven. On the derivation of the foveal receptor primaries. *J. Vision Research*, 11:799–818, 1971. 61

[65] JJ Vos and PL Walraven. An analytical description of the line element in the zone fluctuation model of color vision. *J. Vision Research*, 12:1345–1365, 1972. 1, 8, 27, 61

[66] K. Witt. Geometric relations between scales of small colour differences. *Color Res. Appl.*, 24:78–92, 1999. 3, 8, 14, 54

[67] R. F. Witzel, R. W. Burnham, and J. W. Onley. Threshold and suprathreshold perceptual color differences. *J. Optical Society of America*, 63:615–625, 1973. 14

[68] William David Wright. A re-determination of the trichromatic coefficients of the spectral colours. *Transactions of the Optical Society*, 30:141–164, 1928. 8

[69] G. Wyszecki and G. H. Fielder. New color-matching ellipses. *J. Optical Society of America*, 61(9):1135–1152, 1971. 3, 14, 35, 37, 39, 54

[70] G. Wyszecki and W.S. Stiles. *Color Science: Concepts and Methods, Quantitative Data and Formula*. John Wiley and Sons, New York, second edition, 2000. 4, 13, 14, 23, 27, 35, 51

[71] T. Young. The bakerian lecture: on the theory of light and colours. *Philosophical Transactions of the Royal Society of London*, 92:12–48, 1802. 7

Part II

Attached Papers

5

Paper A

Evaluating Color Difference Formulae by Riemannian Metric

Dibakar Raj Pant and Ivar Farup

Published in

Fifth European Conference on Colour in Graphics, Imaging, Joensuu, Finland.

CGIV 2010, Pages 497-503.

Evaluating Color Difference Formulae by Riemannian Metric

Dibakar Raj Pant [1,2]***, Ivar Farup*** [1]
1) The Norwegian Color Research Laboratory, Gjøvik University College, Norway
2) The Laboratoire Hubert Curien, The University Jean Monnet, Saint Etienne, France

Abstract

For precision color matching, visual sensitivity to small color difference is an essential factor. Small color differences can be measured by the just noticeable difference (JND) ellipses. The points on the ellipse represent colours that are just noticably different from the colour of the centre point. Mathematically, such an ellipse can be described by a positive definite quadratic differential form, which is also known as the Riemannian metric. In this paper, we propose a method which makes use of the Riemannian metric and Jacobian transformations to transform JND ellipses between different colour spaces. As an example, we compute the JND ellipses of the CIELAB and CIELUV color difference formulae in the xy chromaticity diagram. We also propose a measure for comparing the similarity of a pair of ellipses and use that measure to compare the CIELAB and CIELUV ellipses to two previously established experimental sets of ellipses. The proposed measure takes into account the size, shape and orientation. The technique works by calculating the ratio of the area of the intersection and the area of the union of a pair of ellipses. The method developed can in principle be applied for comparing the performance of any color difference formula and experimentally obtained sets of colour discrimination ellipses.

Introduction

Color spaces and color difference metrics have been active fields of research for many decades and it is still going on. Among the many aspects, one important objective is to reduce the gap between the visual perception of the color difference and the mathematical model describing it. Since the establishment of The International Commission on Illumination (CIE), many colour difference formulae have been developed to measure the visual color difference, but no single formula can be considered a perfect one for all applications due to, among other things, the curvilinear nature of the color space as pointed out by many previous researchers [2, 3, 4]. In the CIELAB and CIELUV systems, the color space is considered as a flat space and the color difference in such a space is simply the Euclidean distance between points. In a Euclidean space, the distance between points are straight lines and the advantage of such a space is simplicity for calculating the color difference in practice. The disadvantage of such a space is that color difference calculation or color distance does not agree sufficiently with the perceptually observed color difference. For this reason, colour difference calculations using the CIELAB and CIELUV formulae between standards and their matches have been a disputed issue with respect to the visual perception of the color difference [8, 10, 11]. Hence, it is highly desirable to know how well the CIELAB and CIELUV colour difference formulae map the visual perception of the color difference.

For precision color matching, visual sensitivity to small color difference is the essential factor. The first systematic studies of visual color matching precision in the different parts of the tristimulus space were done by MacAdam[1], MacAdam and Brown[4], but also by other researchers such as Wyszecki and Fielder [6], Guild and Wright [9]. MacAdam pointed out that small color difference can be measured by the just noticeable differences (JND) through the discrimination ellipse which ultimately manifests an observer's precision of matching the chromaticity of the test color [1, 2]. These findings suggest that the colour space is Riemannian where the small distance between two points is described by a positive definite quadratic differential form, also known as the Riemannian metric. From this positive definite metric, the discrimination ellipse is uniquely determined and vice versa. Hence, considering the color space as a Riemannian space the difference between two colors are described by the line element which describe the colour perception properties of an observer from the measured discrimination thresholds [2, 7, 14, 18].

Many current color science researchers suggest that the color matching ellipses and the Riemannian metric still hold significant role in the color perception or visual color difference and can be applied in many practical cases where it is required to discriminate small or medium color differences[11, 13, 14, 15, 16]. In these contexts, it is useful to study the performance of the CIELAB and CIELUV color difference formulae based on small color distances. In other words, MacAdam's approach to compute the just noticeable difference (JND) or the discrimination ellipse on the chromaticity diagram would be the reliable evaluating tool to study the performance of different colour difference formulae.

In this paper, the authors present a method of local linear transform of the CIELAB and CIELUV colour difference metrics into the chromaticity diagram using the principle of the Riemannian metric and Jacobian transformations. This is then used to visualize the color differences predicted by the ΔE_{ab} and ΔE_{uv} colour difference metrics. In other words, the above mentioned formulae from their respective color spaces are transformed into the xyY space by the Riemaninan metric. Then, the corresponding JND or the color matching ellipses are plotted into the chromaticity diagram. The principal axes (semi major axis and semi minor axis) of the ellipse are calculated from the coefficients of the metric tensor, g_{ik}. The ellipse corresponds to the chroma and hue differences and can be considered as a tool for representing an observer's ability to determine perceptual color difference.

To test our method, We have used the visual colour matching experimental data done by MacAdam [1] and Wyszecki and Fielder [6]. MacAdam's data set was prepared by the experiment performed by a single observer. Wyszecki and Fielder's data set was prepared by the color matching matching experiments done by three observers having extensive experience in visual colorimetry. In this paper, we have used average of three sets color matching data. Both these data sets are based on the xyY colour space. The CIELAB and CIELUV ellipses are computed using these data sets. Then, computed CIELAB and CIELUV ellipses are compared with ellipses obtained from the experimental data by two approaches. The first approach is to compare each

pair of computed and observed ellipses by the size, the shape and the orientation respectively. The second approach is to calculate a single value comparison index of each set of ellipse by calculating the ratio of the intersection area to the union area of the ellipses. The obtained results shows that this is a useful method for comparing the performance of different color difference formulae.

Riemannian Metric and the Ellipse Equation

In a Riemannian space, there exists a positive definite symmetric metric tensor called the Riemannian Metric. In general, the metric tensor g_{ik} is a function that tells us how to compute the infinitesimal distance between any two points in a given space. So, considering the 2D color space as the Riemannian space, an ellipse whose length is equal to the arc length of a curve between two points is expressed by a differential quadratic form:

$$ds^2 = g_{11} \cdot dx^2 + 2 \cdot g_{12} \cdot dx \cdot dy + g_{22} \cdot dy^2 \tag{1}$$

The matrix form of Equation (1) is

$$ds^2 = \begin{bmatrix} dx & dy \end{bmatrix} \cdot \begin{bmatrix} g_{11} & g_{12} \\ g_{21} & g_{22} \end{bmatrix} \cdot \begin{bmatrix} dx \\ dy \end{bmatrix} \tag{2}$$

where, ds is the distance between two points, dx is the difference of x coordinates, dy is the difference of y coordinates and g_{11}, g_{12} and g_{22} are the coefficients of the metric tensor g_{ik}. Here, the coefficient g_{12} is equal to the the coefficient g_{21}. Mathematically, it is written as :

$$g_{ik} = \begin{bmatrix} g_{11} & g_{12} \\ g_{21} & g_{22} \end{bmatrix} \tag{3}$$

The metric g_{ik} gives intrinsic properties of the color of a geometric surface. Alternatively, it represents the chromaticity difference of any two colors measured along the geodesic of the surface [2]. The coefficients of g_{ik} also determine an ellipse in terms of its parameters a, b and θ defined as the semi major axis, the semi minor axis and the angle of inclination in a geometric plane respectively and vice versa. To determine the value of the the coefficients g_{ik} in terms of the parameters of an ellipse, let us consider the standard equation of an ellipse having center at origin in a geometric plane in the matrix form as follows:

$$1 = \begin{bmatrix} x & y \end{bmatrix} \cdot \begin{bmatrix} \frac{1}{a^2} & 0 \\ 0 & \frac{1}{b^2} \end{bmatrix} \cdot \begin{bmatrix} x \\ y \end{bmatrix} = X^T \cdot D \cdot X \tag{4}$$

where X is a 2×1 vector and equals to $[xy]^T$, the 2×2 diagonal matrix $D = Diag(\frac{1}{a^2}, \frac{1}{b^2})$ and the superscript T denotes the transpose operation. The ellipse can be rotated in different orientation by a 2×2 rotation matrix R expressed as :

$$R = \begin{bmatrix} \cos\theta & -\sin\theta \\ \sin\theta & \cos\theta \end{bmatrix} \tag{5}$$

The general transformation is $Y = RX$ with inverse $X = R^T Y$. Substituting this into Equation (4), we have :

$$Y^T \cdot R \cdot D \cdot R^T \cdot Y = 1 \tag{6}$$

where, Y equals $[x^{'} y^{'}]^T$, new axes after the rotation. Similarly, the transformation matrix M_t equals $R \cdot D \cdot R^T$. In the expanded form, Equation (6)is

$$1 = \begin{bmatrix} x^{'} & y^{'} \end{bmatrix} \begin{bmatrix} \frac{1}{a^2}\cos^2\theta + \frac{1}{b^2}\sin^2\theta & \cos\theta\sin\theta\,(\frac{1}{a^2} - \frac{1}{b^2}) \\ \cos\theta\sin\theta\,(\frac{1}{a^2} - \frac{1}{b^2}) & \frac{1}{a^2}\sin^2\theta + \frac{1}{b^2}\cos^2\theta \end{bmatrix} \begin{bmatrix} x^{'} \\ y^{'} \end{bmatrix} \tag{7}$$

If we consider the value of ds in Equation (1) is constant and compare with it Equation(7), the coefficients of g_{ik} can be related to the parameters of an ellipse as follows:

$$\begin{aligned} g_{11} &= \frac{1}{a^2}\cos^2\theta + \frac{1}{b^2}\sin^2\theta \\ g_{12} &= \cos\theta\sin\theta\,(\frac{1}{a^2} - \frac{1}{b^2}) \\ g_{22} &= \frac{1}{a^2}\sin^2\theta + \frac{1}{b^2}\cos^2\theta \end{aligned} \tag{8}$$

The angle formed by the major axis with the positive x-axis is given by

$$\tan(2\theta) = \frac{2g_{12}}{(g_{11} - g_{22})} \tag{9}$$

The value of θ is $\leq 90^\circ$ when $g_{12} \leq 0$ otherwise θ is $\geq 90^\circ$. Similarly, the inverse of Equation(7) is written as:

$$\begin{aligned} \frac{1}{a^2} &= g_{22} + g_{12}\cot\theta \\ \frac{1}{b^2} &= g_{11} - g_{12}\cot\theta \end{aligned} \tag{10}$$

Alternatively, the semi major axis (a) and the semi minor axis (b) of an ellipse can also be determined by the eigenvector and eigenvalue of the metric g_{ik}. If λ_1 and λ_2 are eigenvalues of the metric g_{ik}, the semi major axis (a) and the semi minor axis (b) are equal to $\frac{1}{\sqrt{\lambda_1}}$ and $\frac{1}{\sqrt{\lambda_2}}$ respectively. [16]

Color Space Transformation

In order to compare the CIELAB and CIELUV colour difference formulae to the visual perception of the color difference, we compute the JND threshold ellipses of the CIELAB and CIELUV color difference formulae. Since the experimentally observed ellipses are based on the xyY space, it is necessary to map color vectors of the CIELAB and CIELUV colour spaces to the xyY space by a Jacobean transformation. The mapping is done in two steps: first mapping of colour vectors of the CIELAB and the CIELUV spaces into the XYZ tristimulus space and then to the xyY space.

CIELAB is defined as given below:

$$\begin{aligned} L^* &= 116\left(\frac{Y}{Y_r}\right)^{\frac{1}{3}} - 16 \\ a^* &= 500\left[\left(\frac{X}{X_r}\right)^{\frac{1}{3}} - \left(\frac{Y}{Y_r}\right)^{\frac{1}{3}}\right] \\ b^* &= 200\left[\left(\frac{Y}{Y_r}\right)^{\frac{1}{3}} - \left(\frac{Z}{Z_r}\right)^{\frac{1}{3}}\right] \end{aligned} \tag{11}$$

where L^*, a^* and b^* corresponds to the Lightness, the redness-greenness and the yellowness-blueness scales in the CIELAB color space. Similarly, X, Y, Z and X_r, Y_r, Z_r are the tristimulas values of the color vectors and reference white respectively. The color difference in the CIELAB colour space is

$$\Delta E^*_{ab} = \sqrt{(\Delta L^*)^2 + (\Delta a^*)^2 + (\Delta b^*)^2} \tag{12}$$

If we Take line element distance to measure the color difference at a point in the color space, the Equation (12) becomes differential. In terms of the metric form, we can write

$$(dE^*_{ab})^2 = \begin{bmatrix} dL^* & da^* & db^* \end{bmatrix} \begin{bmatrix} 1 & 0 & 0 \\ 0 & 1 & 0 \\ 0 & 0 & 1 \end{bmatrix} \begin{bmatrix} dL^* \\ da^* \\ db^* \end{bmatrix} \tag{13}$$

Now, to transfer or map color vectors L^*, a^*, b^* into X, Y, Z tristimulas color space, we use the Jacobean transformation where the variables of the two color spaces are related by the continuous partial derivatives. By the chain rule, we have

$$\begin{bmatrix} dL^* \\ da^* \\ db^* \end{bmatrix} = \begin{bmatrix} \frac{\partial L}{\partial X} & \frac{\partial L}{\partial Y} & \frac{\partial L}{\partial Z} \\ \frac{\partial a}{\partial X} & \frac{\partial a}{\partial Y} & \frac{\partial a}{\partial Z} \\ \frac{\partial b}{\partial X} & \frac{\partial b}{\partial Y} & \frac{\partial b}{\partial Z} \end{bmatrix} \begin{bmatrix} dX \\ dY \\ dZ \end{bmatrix} \tag{14}$$

Again, from the equation 13 and 14, we have

$$(dE^*_{ab})^2 = \begin{bmatrix} dX dY dZ \end{bmatrix} \frac{\partial (L,a^*,b^*)}{\partial (X,Y,Z)}^T I \frac{\partial (L,a^*,b^*)}{\partial (X,Y,Z)} \begin{bmatrix} dX \\ dY \\ dZ \end{bmatrix} \tag{15}$$

where I is a 3 by 3 identity matrix and $\frac{\partial (L,a^*,b^*)}{\partial (X,Y,Z)}$ is a Jacobian matrix,

$$\begin{bmatrix} \frac{\partial L}{\partial X} & \frac{\partial L}{\partial Y} & \frac{\partial L}{\partial Z} \\ \frac{\partial a}{\partial X} & \frac{\partial a}{\partial Y} & \frac{\partial a}{\partial Z} \\ \frac{\partial b}{\partial X} & \frac{\partial b}{\partial Y} & \frac{\partial b}{\partial Z} \end{bmatrix} = \begin{bmatrix} 0 & \frac{116}{3} Y^{\frac{-2}{3}} & 0 \\ \frac{500}{3} X^{\frac{-2}{3}} & \frac{-500}{3} Y^{\frac{-2}{3}} & 0 \\ 0 & \frac{200}{3} Y^{\frac{-2}{3}} & \frac{-200}{3} Z^{\frac{-2}{3}} \end{bmatrix} \tag{16}$$

Again, the relationship between X, Y and Z tristimulus colour vectors and x, y and Y colour vectors are

$$\begin{aligned} X &= \frac{xY}{y} \\ Y &= Y \\ Z &= \frac{(1-x-y)Y}{y} \end{aligned} \tag{17}$$

Similarly, transformation from X, Y, Z tristimulus colour space into x, y, Y colour space is done by another Jacobian matrix $\frac{\partial (X,Y,Z)}{\partial (x,y,Y)}$ and expressed as :

$$\begin{bmatrix} dX \\ dY \\ dZ \end{bmatrix} = \begin{bmatrix} \frac{\partial X}{\partial x} & \frac{\partial X}{\partial y} & \frac{\partial X}{\partial Y} \\ \frac{\partial Y}{\partial x} & \frac{\partial Y}{\partial y} & \frac{\partial Y}{\partial Y} \\ \frac{\partial Z}{\partial x} & \frac{\partial Z}{\partial y} & \frac{\partial Z}{\partial Y} \end{bmatrix} \begin{bmatrix} dx \\ dy \\ dY \end{bmatrix} \tag{18}$$

where, $\frac{\partial (X,Y,Z)}{\partial (x,y,Y)}$ are

$$\begin{bmatrix} \frac{\partial X}{\partial x} & \frac{\partial X}{\partial y} & \frac{\partial X}{\partial Y} \\ \frac{\partial Y}{\partial x} & \frac{\partial Y}{\partial y} & \frac{\partial Y}{\partial Y} \\ \frac{\partial Z}{\partial x} & \frac{\partial Z}{\partial y} & \frac{\partial Z}{\partial Y} \end{bmatrix} = \begin{bmatrix} \frac{Y}{y} & \frac{-xY}{y^2} & \frac{x}{y} \\ 0 & 0 & 1 \\ \frac{-Y}{y} & \frac{(x-1)Y}{y^2} & \frac{1-x-y}{y} \end{bmatrix} \tag{19}$$

Finally, the transformation from of L^*, a^*, b^* into x, y, Y with two Jacobian matrices is

$$(dE^*_{ab})^2 = \begin{bmatrix} dx dy dY \end{bmatrix} \frac{\partial (X,Y,Z)}{\partial (x,y,Y)}^T \frac{\partial (L,a^*,b^*)}{\partial (X,Y,Z)}^T I \frac{\partial (L,a^*,b^*)}{\partial (X,Y,Z)} \frac{\partial (X,Y,Z)}{\partial (x,y,Y)} \begin{bmatrix} dx \\ dy \\ dY \end{bmatrix} \tag{20}$$

Here, the whole transformation matrix is $\frac{\partial (X,Y,Z)}{\partial (x,y,Y)}^T \frac{\partial (L,a^*,b^*)}{\partial (X,Y,Z)}^T I \frac{\partial (L,a^*,b^*)}{\partial (X,Y,Z)} \frac{\partial (X,Y,Z)}{\partial (x,y,Y)}$ and represents the metric tensor of three dimensional color space. The coefficients of the first two columns and rows of the 3D metric tensor gives us the JND threshold ellipse in the chromaticity diagram.

By the same approach as described in Equations (12–20), we can map the CIELUV colour space into xyY colour space

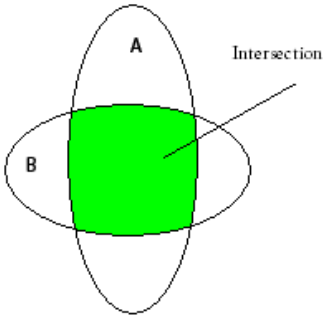

Figure 1: Illustration of the union and the intersection area of two ellipses.

with the following standard formulae:

$$\begin{aligned} L^* &= 116 \left(\frac{Y}{Y_r} \right)^{\frac{1}{3}} - 16 \\ u^* &= 13L \left[\left(\frac{4X}{X+15Y+3Z} \right) - \left(\frac{4X_r}{X_r+15Y_r+3Z_r} \right) \right] \\ v^* &= 13L \left[\left(\frac{9Y}{X+15Y+3Z} \right) - \left(\frac{9Y_r}{X_r+15Y_r+3Z_r} \right) \right] \end{aligned} \tag{21}$$

Method of Comparison

Using the principles of union intersection and ratio testing, we present the method to compare two ellipses with respect to their shape and orientation. Figure (1) shows two ellipses A and B. The shaded area is the intersection area between them and the total area of A and B is known as the union area. From the statistical point of view, the acceptance region is the intersection area and the rejection region is the union area. The ratio of these intersection and union area gives us a nonnegative value less than or equal to one. Large value of the ratio gives strong evidence that the two ellipses are closely matched.

Result and Discussion

We have applied our method on visual experimental data sets known as Macadam and three observer. Let us begin from MacAdam's data. In Figure(2), the subfigure (2(a)) shows MacAdam's color matching ellipses in the CIE chromaticity diagram according to his visual experiment data. The next two subfigures (2(b)) and (2(c)) are the computed CIELAB and CIELUV color matching ellipses obtained by the Jacobian transformation of the Riemenian metric as described in the section two. The color centers for these computed ellipses, at which color matches are according to the MacAdam's data. To do comparison with experimentally obtained MacAdam's ellipses, ellipses are computed in xyY color space where the Y component (brightness) is in the range [0.01.0] and plotted in the xy chromaticity diagram. Here, ellipses are computed at $L^* = 70$, and to achieve this lightness value the Y component is approximated at 0.4 scale. However, in our method the Y component of xyY can be scaled at any value in the range between 0.0 to 1.0 which allows to compare visual color difference at any lighting conditions. Table 1 gives the calculated area (size), the ratio of semi major (a) and semi minor (b) axes (shape) and the orientation in angle of MacAdam, the CIELAB and CIELUV ellipses. Comparing with area of MacAdam's ellipses, it can be seen that the CIELAB and CIELUV ellipses have general trends of agreement among different set of ellipses. For example, the blue is the smallest, the green largest and that red, blue and yellow are more elongated

Table 1: Calculated Area (Size), Ratio of major (a) and minor (b) axes (Shape) and Angle of orientation of MacAdam's and computed CIELAB and CIELUV ellipses.

Area of Ellipses $\times log10$			Ratio of major(a) and minor(b) axes			Orientation in Angle(Degree)		
MacAdam	CIELAB	CIELUV	MacAdam	CIELAB	CIELUV	MacAdam	CIELAB	CIELUV
-4.03	-3.96	-3.97	2.43	5.18	1.81	62.5	12.75	11.36
-3.42	-3.42	-3.45	4.00	3.12	1.54	77	23.17	16.95
-3.41	-3.38	-3.42	5.00	3.63	1.68	55.5	18.64	23.11
-2.16	-2.3	-2.24	4.17	2.10	1.83	105	85.74	89.08
-2.53	-2.61	-2.56	2.35	2.70	1.50	112.5	78.42	89.89
-2.38	-2.44	-2.4	2.52	1.76	1.61	100	75.1	80.45
-2.50	-2.53	-2.51	2.50	1.62	1.51	92	60.92	69.52
-2.64	-2.72	-2.7	2.00	2.31	1.21	110	67.53	78.84
-2.72	-2.68	-2.74	2.67	1.68	1.47	70	34	61.81
-2.78	-2.72	-2.76	3.67	1.09	1.83	104	44.53	22.22
-3.20	-3.11	-3.24	2.21	2.20	1.23	72	40.43	40.75
-3.06	-3.02	-3.16	3.44	2.12	1.31	58	39	50.77
-3.19	-3.01	-3.06	2.56	1.84	1.50	65.5	34.14	53.39
-2.72	-2.67	-2.92	2.38	1.40	1.76	51	5.16	49.13
-2.85	-2.76	-2.94	2.29	1.25	2.05	20	3.55	43.21
-2.97	-2.84	-3.03	2.00	1.43	2.30	28.5	18.74	41.2
-3.00	-2.80	-3.19	2.64	1.86	2.13	29.5	14.82	35.15
-3.04	-2.92	-3.40	2.00	2.50	2.44	13	4.32	36.38
-2.97	-2.96	-3.30	2.00	1.75	2.78	60	30.11	43.98
-3.19	-3.02	-3.18	2.56	2.04	1.64	47	22.01	37.65
-3.10	-3.09	-3.33	2.50	2.47	1.87	34.5	16.27	33.26
-3.08	-3.00	-3.49	2.95	3.07	2.20	57.5	30	36.56
-3.38	-3.21	-3.32	4.36	2.38	1.48	54	20.54	29.24
-3.26	-3.26	-3.31	4.83	3.18	1.70	86.74	86.69	94.83
-2.97	-3.04	-3.07	3.79	3.74	1.99	40	15.93	29.39

than others.

In Table 1, the comparative data of shape (the ratio of semi major (a) and semi minor (b) axes) and the orientation between MacAdam, the CIELAB and CIELUV formulae show that there are some disagreement with experimentally observed ellipses and computed ellipses using the Riemenian metric. We can see in Table 1 that CIELAB ellipses have higher values of a/b ratio than the CIELUV ellipses. Thus, they are more closer in shape than the CIELUV ellipses with respect to the observed MacAdam's ellipses but neither ellipses fully comply with the original ones. Similarly, with regard to the orientation, most of the ellipses are inclined downwards compared to the MacAdam ellipses. The computed ellipses are more circular than the MacAdam ellipses.

Similarly, comparing between computed CIELAB and CIELUV ellipses with respect to the shape, it is found (Table 1) that a/b ratio is significantly higher in most of the CIELAB ellipses than the CIELUV ellipses of same color centers. This result indicates that the CIELUV ellipses are more circular than the CIELAB ellipses.

We also computed the ratio of the area of intersection and the area of union between MacAdam's ellipses and the CIELAB and CIELUV ellipses. Such ratio gives the correlation between computed and original ellipses in terms of size, shape and orientation which is a more informative way for inter comparing the different sets of ellipses by a single value or number. For example, if the computed ellipse and the observed ellipse are same in terms of size, shape and orientation, the ratio of the area of intersection and the area of union is 1. This assures the full compatibility between a pair of ellipses in terms of size, shape and orientation. Table 2 gives the numerical values of such comparison of the CIELAB and CIELUV formulae with respect to MacAdam. We have also done sign test for these ratio values of the CIELAB and CIELUV ellipses. The results actually shows that the CIELUV is performing better than the CIELAB at a level of significanc $p = 0.015$.

Our second data set is the three observers color-matching ellipses data. Here, the ellipse parameters are taken as the average of three sets of color-matching ellipses made by three observers. Figure (3(a)) shows the three observers color-matching ellipses in the chromaticity diagram. Similarly, Figures (3(b)) and (3(c)) gives computed ellipses of the CIELAB and the CIELUV having the same color centers of three observers color-matching ellipses respectively. Like for the MacAdam's ellipses, the ellipses are plotted at constant lightness , and we can see the similarity between experimentally observed and computed ellipses from our method described above. Table 3 shows comparative data of area, shape and orientation between three observer ellipses and computed CIELAB and CIELUV ellipses. The result shows a similar behaviour as for the MacAdam data. The last table 4 gives the single value comparison index for each set of ellipses by comparing the ratio of the area of intersection and the area of union. In our second data set too, the sign test of the ratio of the area of intersection and the area of union shows that the CIELUV is better than the CIELAB with $p = 0.0125$.

Conclusion

We have developed a method to compare the behaviour of colour difference metrics to experimentally observed JND ellipses. The method uses Jacobean to transform the Riemannian metric tensor to the same colour space as the experimental data.

The presented method can compute JND ellipses of the CIELAB and CIELUV formulae in the chromaticity diagram and thus gives the opportunity to evaluate how well they match the visual colour difference obtained in experiments.

Such a pairs of ellipses are compared in terms of size, shape and orientation to see the compatibility between computed and observed ellipses. In our method, JND ellipses of CIE color difference formulae can be plotted at any value of lightness (L^*) in the CIE xy diagram. This feature allows to compare the visual colour difference in order to achieve the best possible match.

A pair of ellipses can be compared by using the ratio of the area of intersection and the area of union. This gives the single value index which represents three parameters of ellipse to compare in terms of shape, size and orientation respectively.

The comparison between the computed CIELAB and CIELUV ellipses with different visual data sets reveal out that

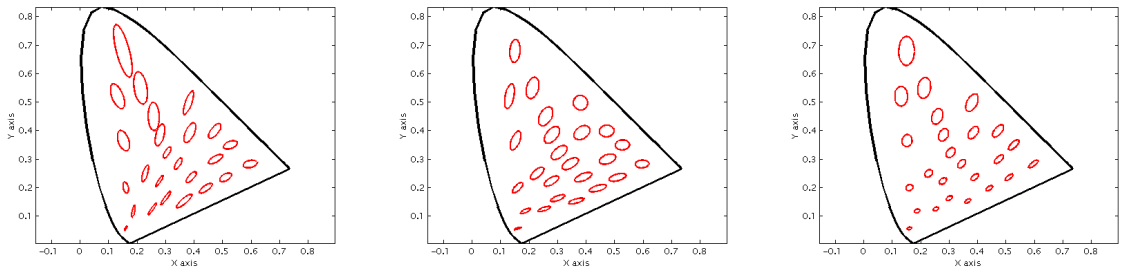

(a) MacAdam Ellipses. (b) CIELAB Ellipses having same color centers as MacAdam. (c) CIELUV Ellipses having same color centers as MacAdam.

Figure 2: MacAdam's original and Computed CIELAB and CIELUV ellipses in the CIE31 Chromaticity diagram(Enlarged 10 times)

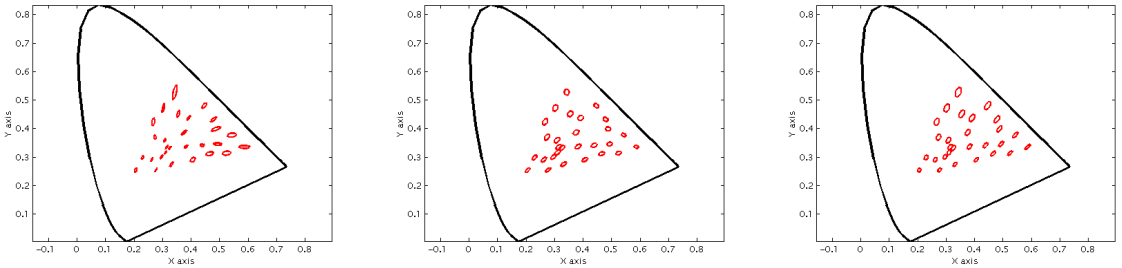

(a) Wyszecki Color-matching Ellipses (mean of three sets of data). (b) CIELAB Ellipses having same color centers as Wyszecki Color-matching Ellipses. (c) CIELUV Ellipses having same color centers as Wyszecki Color-matching Ellipses.

Figure 3: Wyszecki Color-matching ellipses and Computed the CIELAB and CIELUV ellipses in the CIE31 Chromaticity diagram (Enlarged 5 times)

Table 3: Calculated Area(size), Ratio of major(a) and minor(b) axes(Shape) and Angle of orientation of 3 observers and computed CIELAB and CIELUV ellipses.

Area of Ellipses $\times log10$			Ratio of major(a) and minor(b) axes			Angle of orientation (Degree)		
3 observers	CIELAB	CIELUV	3 observers	CIELAB	CIELUV	3 observers	CIELAB	CIELUV
-4.348	-4.922	-4.948	2.95	1.34	2.08	35	61.1	51.2
-4.557	-4.781	-4.907	2.72	1.18	1.8	48	30.6	56.7
-4.227	-4.903	-5.156	3.57	1.49	2.16	179	11.2	44.2
-4.706	-4.801	-5.049	1.74	1.69	1.52	63	41.9	55.2
-4.278	-4.921	-4.837	2.14	1.49	1.99	50	50.6	56.3
-4.532	-4.855	-5.144	1.63	1.61	1.94	5	21.6	46.1
-4.649	-4.834	-5.132	2.47	1.7	1.74	34	29.1	48.2
-4.697	-4.919	-5.165	1.6	1.98	1.29	59	46.5	51.6
-4.525	-4.925	-5.273	2.63	2.09	1.6	54	29.5	43.3
-4.935	-4.981	-5.304	3.7	2.16	1.44	65	33.4	41.6
-4.479	-5.028	-5.272	1.83	2.1	1.24	73	44.2	41.4
-4.056	-5.086	-5.223	3.57	1.53	2.61	179	71.9	40.2
-4.302	-4.751	-4.865	3	1.23	1.72	72	45.6	60.5
-4.833	-4.915	-5.198	3.25	1.98	1.38	70	40.3	48.2
-4.838	-4.858	-5.155	2.36	1.86	1.52	60	36.6	49.6
-4.852	-4.833	-5.12	2.29	1.78	1.56	50	36.3	50.8
-4.697	-4.886	-5.188	2.5	1.94	1.48	57	36.7	48.2
-4.787	-4.83	-5.109	3.08	1.78	1.53	59	38.2	51.8
-3.865	-4.765	-4.715	4.52	1.11	1.78	76	16	66.6
-4.313	-4.721	-4.807	4.78	1.37	1.62	77	59.1	66.6
-4.117	-4.904	-5.026	3.33	1.27	2.11	21	80.2	48.4
-4.01	-5.015	-5.099	2.27	1.46	2.35	8	66.8	44.5
-4.223	-4.744	-4.892	2.43	1.63	1.49	82	56.5	66.2
-4.416	-4.788	-5.012	3.05	1.45	1.73	36	33.7	53.4
-4.043	-4.954	-5.254	2.11	1.66	2.33	8	10	40.7
-4.492	-4.794	-5.011	1.64	1.73	1.44	103	48.7	59.6
-4.108	-4.9	-5.233	2.15	1.78	2.07	14	18.3	42.5
-4.251	-4.901	-5.264	1.46	1.99	1.86	40	23.6	42.7

Table 2: Ratio of area intersection and Union of Ellipses with respect to MacAdam Ellipses

CIELAB	CIELUV
0.29	0.47
0.25	0.33
0.28	0.35
0.34	0.5
0.48	0.65
0.57	0.6
0.58	0.54
0.49	0.55
0.59	0.6
0.41	0.61
0.4	0.52
0.44	0.47
0.35	0.66
0.59	0.62
0.55	0.81
0.68	0.63
0.64	0.64
0.69	0.44
0.83	0.47
0.4	0.68
0.52	0.59
0.59	0.39
0.32	0.46
0.31	0.38
0.39	0.24

Table 4: Ratio of area intersection and Union of Ellipses with respect to 3 observer ellipses

CIELAB	CIELUV
0.4	0.58
0.26	0.36
0.56	0.38
0.2	0.35
0.47	0.58
0.33	0.54
0.26	0.52
0.27	0.47
0.4	0.69
0.16	0.34
0.55	0.72
0.51	0.32
0.4	0.53
0.19	0.36
0.17	0.32
0.16	0.3
0.25	0.49
0.17	0.32
0.4	0.52
0.34	0.41
0.51	0.49
0.56	0.43
0.51	0.65
0.37	0.55
0.77	0.38
0.32	0.52
0.88	0.46
0.7	0.62

neither formulae is good enough for the perfect visual color matching. However, the ratio test method shows that CIELUV performs better than CIELAB to predict visual colour difference for both of the data sets tested. The general trend of color matching ellipses of CIE color difference formulae (CIELAB and CIELUV) are along the direction to experimentally obtained ellipses.

Finally, by our method we can transform any colour space to other colour space and vice versa, preserving the property of their original colour space and can be extended to our future work to study advanced colour difference formula like ΔE_{00}.

References

[1] David L. MacAdam, Specification of Small Chromaticity Differences, 1942 J. optical Society of America, Volume 33, Number 4

[2] L. Silberstein, Investigations on the Intrinsic Properties of the Color Domain J. optical Society of America, Volume 33, Number 1,1943

[3] Ludwik Silberstein Notes on W.S. Stiles paper Entitled " A Modified Helmholtz Line-Element in Brightness-Colour Space", J. optical Society of America, Volume 37, Number 4,1947

[4] Brown, W. R. and MacAdam, D. L. . Visual sensitivities to combined chromaticity and luminance differences. Journal of the Optical Society of America, 39, 808834,1949.

[5] D.B Judd, Ideal color space:curvature of color space and its implications for industrial color tolerances, Palette 29,25-31,1968

[6] Gunter Wyszecki& Fielder, New Color-Matching Ellipses, optical Society of America, Volume 61, Number 9, 1971

[7] Rolf G. Kuehni, Color Space and its Division, John Wiley and Sons,New york,2003

[8] Roy S. berns, Principle of Color Technology John Wiley and Sons,New york(2003)

[9] Wyszecki & Stiles, Color Science:Concepts and Methods, Quantirative Data and Formula" John Wiley and Sons,New york,(2000)

[10] CIE publication No.116, Industrial colour difference evaluation. CIE Central Bureau, Vienna, 1995.

[11] John H. Xin, Chuen Chuen Lam & M. Ronnier Luo, Investigation of Parametric Effects Using Mediumum Colour Difference Pairs J. COLOR research and application, Volume 26, Number 5,2001

[12] John Doe, Digital Imaging, J. Imaging. Sci. and Technol., 42, 112 (1998).

[13] Philipp Urban, Mitchell R. Rosen & Roy. S. Berns Embedding non-Euclidean Color Spaces into Euclidean Color Spaces with minimal isometric disagreement, J. optical Society of America, Volume 27, Number 6,2007

[14] Satoshi Ohsima,Rika Mochizuki,Jinhui Chao & Reiner Lenz Color Reproduction using Riemann Normal Coordinates Computational color Imaging, Volume 5646, pp140-149, Springerfield, Berlin / Heidelberg (2009)

[15] Rolf G. Kuehni, Threshold Color Differences Compared to Super-Threshold Color Differences J. COLOR research and application, Volume 25, Number 2,2000

[16] Chao, J., Lenz, R., Matsumoto, D.& Nakamura, T., Riemann geometry for color characterization and mapping. In: Proc. CGIV, pp. 277282. IS&T, Springfield (2008)

[17] George B. Thomas & Ross L. Finney, Calculus and Analytic Geometry, 7th edition Addision-Wesley publishing company, Massachusetts (1988).

[18] H. L. Resnikoff, Houston, Differential Geometry and Color Perception, Journal of Mathematical Biology 1, 97–131. Springer-Vertag 1974

[19] Hans G. VolZ Euclidization of the First Quadrantn of the CIEDE2000 Color Difference System for the calculation of Large Color differences. J. Color research and application , Volume 31

Author Biography

D*ibakar Raj Pant received his B.Sc.in Electrical and Electronics Engineering from Rajshai University of Technology, Bangladesh, and M.Sc. in Information Technology from the University of Joensuu, Finland (2006). He is currently pursuing a PhD in Color Difference metric under the supervision of Prof. A. Tremeau , University of Jean Monnet, Saint etinne, France and Ass. Prof. I. Farup, Gjovik University College. He is working in The Norwagian Color Research Laboratory, Gjovik, Norway, where his work is centered on Visual color differences, but he is also interested on color reproduction, color measurement, Image color difference and spectral imaging. During his Masters studies, He worked as a trainee researcher in the Color research Laboratory, the University of Joensuu.*

6

Paper B

Riemannian Formulation of the CIEDE2000 Color Difference Formula

Dibakar Raj Pant and Ivar Farup

Published in

Eighteenth Color Imaging Conference: Color Science and Engineering Systems, Technologies, and Applications San Antonio, Texas

Volume 18, pages 103-108

ISBN/ISSN: 978-0-89208-294-0 November, 2010.

Riemannian Formulation of the CIEDE2000 Color Difference Formula

Dibakar Raj Pant [1,2]***, Ivar Farup*** [1]
1)The Norwegian Color Research Laboratory, Faculty of Computer Science and Media Technology, Gjovik University College, Norway
2)The Laboratoire Hubert Curien, The University Jean Monnet, Saint Etienne, France

Abstract

The CIELAB based CIEDE2000 colour difference formula to measure small to medium colour differences is the latest standard formula of today which incorporates different corrections for the non uniformity of the CIELAB space. It also takes account of parametric factors. In this paper, we present a mathematical formulation of the CIEDE2000 by the line element to derive a Riemannian metric tensor in a color space. The coefficients of this metric give Just Noticeable Difference (JND) ellipsoids in three dimensions and ellipses in two dimensions. We also show how this metric can be transformed between various colour spaces by means of the Jacobian matrix. Finally, the CIEDE2000 JND ellipses are plotted into the xy chromaticity diagram and compared to the observed BFD-P colour matching ellipses by a comparing method described in Pant and Farup (CGIV2010).

Introduction

A color difference formula or a color difference metric, which measures the difference between two colors, is becoming a prime research topic in the modern colorimetry. The target is to find a good color difference formula, which can give a quantitative measure (ΔE) of the perceived color difference correctly. It is also the requirement of many color applied fields such as image analysis, color reproduction, color image restoration and so on.

MacAdam [2] described that small or medium color differences can be measured by the Just Noticeable Difference (JND) ellipses, which represent the human perception of threshold colour differences. Since then, many color difference formulae have been developed for measuring the color difference accurately. In 1976, the CIE recommended two color difference formulae, the CIELAB and CIELUV formulae, have become popular in colour industries, but, they fail to measure the visual perception of the color differences sufficiently, although, they are said to be uniform colour difference formulae [3],[4].

In 2001, the CIE recommended the CIEDE2000 formula based on the CIELAB to improve the correlation between measured and human observed color differences. In particular, the CIEDE2000 is the improved version of the CIELAB with specific weighting functions known as lightness (S_L), chroma (S_C) and hue (S_H), parametric factors (k_L, k_C, k_H), and the rotation term R_T to correct chroma and hue differences in the blue region. All these modifications are based on visual data obtained from four different experiments known as BFD-P [5], Leeds [6] RIT-DuPont [7] and Witt [8]. In other words, visual results from these four experiments were adjusted to a common scale by computing scaling factors for each data set and adopting the visual scale of BFD-P as a unit [9]. Luo et al. [10] have described in the detail about the CIEDE2000 formula as an excellent out performing formula, when measured against the aggregate data set, but still it has some issues related to its development [11]. Similarly, Sharma et al. [12] have shown mathematical discontinuity in the formula. Further, field test reports and performance studies on the CIEDE2000 have also not shown conclusively that the latest CIE formula performs better than previous existing formulae [13–15].

In such contexts, it would be useful from many aspects to study the CIEDE2000 color difference formula by the Riemannian approach. First, in this approach, we can map or transfer this formula into other color spaces preserving the subjective property of the formula. Second, the formula does not have its specific or corresponding color space, it is only the improved L, a^*, b^* color space formulated in terms of lightness (L), chroma (C) and hue (H). So, it is interesting to know how well this advanced formula measures small colour differences in other color spaces. Third, Riemannian space is curved and such space is considered suitable for small to medium color difference measurement because many researchers have described that small color difference calculation using the Euclidean distance does not agree sufficiently with the perceptual color difference due to the curvilinear nature of the color space [16–20].

In this paper, the authors present a method to formulate the CIEDE2000 color difference formula in terms of the Riemannian metric and this metric is used to compute the JND ellipses. Here, the authors take the line element to calculate the color differences dE. To calculate line element, the CIEDE2000 color difference equation should be converted into the differential form. This gives us the Riemannian metric in a non-Euclidean color space. Again, to obtain the Riemannian metric in a new color space, we also need to transform color vectors from one color space to another. This is accomplished by the Jacobian transformation. To illustrate our method, the authors transformed the CIEDE2000 formula into the xyY color space. And, the JND ellipses are plotted into the xy chromaticity diagram. The input data to compute the JND ellipses for our method is BFD-P data sets [5]. BFD-P data sets were assessed by about 20 observers using a ratio method, and the chromaticity discrimination ellipses were calculated and plotted in the xy chromaticity diagram for each set [21]. A comparison has also been done between the computed JND ellipses of the CIEDE2000 formula and the original ellipses obtained from the BFD-P data set. The detailed description, for comparing a pair of ellipses, by calculating the ratio of the area of intersection and the area of union can be found in Pant and Farup (CGIV,2010). This method gives a single comparison value which takes account

of variations in the size, the shape and the orientation simultaneously for a pair of ellipses. Therefore, this value is an indicator which tells us how well two ellipses match each other. Further, using MacAdam data, the authors also plot the JND ellipses of the formula in the xy chromaticity diagram to see simple visual comparison with the original data set. The authors see a good mathematical technique in this method to study the CIEDE2000 color difference formula.

Formulation of the CIEDE2000 Metric Tensor and Color Space Transformation

In this section, the authors will describe our method to compute metric tensor of the CIEDE2000 formula in the xyY space. Let us begin the process by defining the standard form of the formula [22].

$$\Delta E_{00} = \left[\left(\frac{\Delta L'}{k_L S_L} \right)^2 + \left(\frac{\Delta C'}{k_C S_C} \right)^2 + \left(\frac{\Delta H'}{k_H S_H} \right)^2 + R_T \left(\frac{\Delta C'}{k_C S_C} \right) \cdot \left(\frac{\Delta H'}{k_H S_H} \right) \right]^{0.5} \quad (1)$$

In Equation (1), R_T is the rotation function and expressed as $R_T = -\sin(2\Delta\theta) R_c$

where $\Delta\theta = 30 \cdot exp - \left(\frac{\bar{h}' - 275}{25} \right)^2$ and $R_c = 2\sqrt{\frac{\bar{C}'^7}{\bar{C}'^7 + 25^7}}$

Similarly, the weighting functions are defined as:

$S_L = 1 + \frac{0.015(\bar{L}' - 50)^2}{\sqrt{20 + (\bar{L}' - 50)^2}}$

$S_C = 1 + 0.045\bar{C}'$ and $S_H = 1 + 0.015\bar{C}'T$ with

$T = 1 - 0.17\cos(\bar{h}' - 30^o) + 0.24\cos(2\bar{h}' + .32\cos(3\bar{h}' + 6^o) - 0.2\cos(4\bar{h}' - 63^o)$

Here, we define for a pair of color samples $\bar{L}' = \frac{L_1^* + L_2^*}{2}$

$\bar{C}' = \frac{C_1' + C_2'}{2}$ and $\bar{h}' = \frac{h_1' + h_2'}{2}$ and $\Delta H = 2\sqrt{C_1' C_2'} \sin \frac{\Delta h'}{2}$

The other symbols used in the formula are also defined in the following way:

$L' = L^*,\ a' = a^*(1 + G),\ b' = b^*$ and $C' = \sqrt{a'^2 + b'^2}$ with

$h' = \arctan \frac{b'}{a'}$ and $G = \frac{1}{2}\left(1 - \sqrt{\frac{C_{ab}^{*7}}{C_{ab}^{*7} + 25^7}}\right)$

where L^*, a^* and b^* corresponds to the Lightness, the redness-greenness and the yellowness-blueness scales and C^* chroma in the CIELAB color space. Likewise, h' is the hue angle for a pair of samples. To formulate Riemannian Metric, the authors take only L', C' and h' values rather than their arithmetic mean values $\bar{L}', \bar{C}'$ and $\bar{h}'$ because in the Riemannian or non-Euclidean color space, infinitesimal distance is taken to measure colour differences. So, Equation (1) becomes a differential form as follows:

$$(dE_{00}^*)^2 = \begin{bmatrix} dL' & dC' & dH' \end{bmatrix} \begin{bmatrix} (k_L S_L)^{-2} & 0 & 0 \\ 0 & (k_C S_C)^{-2} & \frac{1}{2}(k_C S_C k_H S_H)^{-1} \\ 0 & \frac{1}{2}(k_C S_C k_H S_H)^{-1} & (k_H S_H)^{-2} \end{bmatrix} \begin{bmatrix} dL' \\ dC' \\ dH' \end{bmatrix} \quad (2)$$

In Equation (2), the matrix of coefficients of weighting functions, parametric factors, and the rotation term is the Riemannian metric of the formula in its original form. As said in the introduction section, the authors will show the process to transform it into the xyY space in terms of metric form. In general, the transformation process takes the following steps: First, from $L'C'H'$ to $L^*a^*b^*$ then to XYZ tristimulus color space and finally into the xyY color space.

So, at first, we need to transform differential color vectors dL, dC', dH' into dL^*, da^*, db^*. Since, they are different color vectors or functions at a given point in a color space, we can only relate them by applying the Jacobian method. In this method, we compute all partial derivatives of vector functions L', C', and H' with respect to L^*, a^*, and b^*. This gives us a 3×3 matrix of continuous partial derivatives, which is known as a Jacobian matrix.

In the equation form, we write:

$$\begin{bmatrix} dL' \\ dC' \\ dH' \end{bmatrix} = \begin{bmatrix} \frac{\partial L'}{\partial L^*} & \frac{\partial L'}{\partial a^*} & \frac{\partial L'}{\partial b^*} \\ \frac{\partial C'}{\partial L^*} & \frac{\partial C'}{\partial a^*} & \frac{\partial C'}{\partial b^*} \\ \frac{\partial H'}{\partial L^*} & \frac{\partial H'}{\partial a^*} & \frac{\partial H'}{\partial b^*} \end{bmatrix} \begin{bmatrix} dL^* \\ da^* \\ db^* \end{bmatrix} \quad (3)$$

where, the matrix of partial derivatives in Equation (3) can also be denoted by $\frac{\partial(L', C', H')}{\partial(L^*, a^*, b^*)}$. Now, the Equation (2) becomes as follows:

$$(dE_{00}^*)^2 = \begin{bmatrix} dL^* & da^* & db^* \end{bmatrix} \frac{\partial(L', C', H')}{\partial(L^*, a^*, b^*)}^T \begin{bmatrix} (k_L S_L)^{-2} & 0 & 0 \\ 0 & (k_C S_C)^{-2} & \frac{1}{2}(k_C S_C k_H S_H)^{-1} \\ 0 & \frac{1}{2}(k_C S_C k_H S_H)^{-1} & (k_H S_H)^{-2} \end{bmatrix} \frac{\partial(L', C', H')}{\partial(L^*, a^*, b^*)} \begin{bmatrix} dL^* \\ da^* \\ db^* \end{bmatrix} \quad (4)$$

The calculation of $\frac{\partial(L', C', H')}{\partial(L^*, a^*, b^*)}$ appears as

$$\begin{bmatrix} 1 & 0 & 0 \\ 0 & \frac{\partial C'}{\partial a^*} & \frac{\partial C'}{\partial b^*} \\ 0 & \frac{\partial H'}{\partial a^*} & \frac{\partial H'}{\partial b^*} \end{bmatrix} \quad (5)$$

where

$dH' = C'dh'$ because $\lim\ \Delta H \to 0 \sin\frac{\Delta h'}{2} \approx \frac{\Delta h'}{2} \Rightarrow dH' = 2C'dh/2'$

$$\begin{aligned}
\frac{\partial C'}{\partial a^*} &= \frac{a'}{C'}\left[(1+G) + \frac{a^{*2}}{C^*}\left(-\frac{175\times 25^6}{4}\frac{C^{*5/2}}{(C^{*7}+25^7)^{3/2}}\right)\right] \\
\frac{\partial C'}{\partial b^*} &= \frac{b'}{C'} + \frac{a'}{C'}\left[\frac{a^*b^*}{C^*}\left(-\frac{175\times 25^6}{4}\frac{C^*5/2}{(C^{*7}+25^7)^{3/2}}\right)\right] \\
\frac{\partial H'}{\partial a^*} &= C'\frac{\partial h'}{\partial a^*} - \frac{b'}{C'}\left[1+G+\frac{a^{*2}}{C^*}\left(-\frac{175\times 25^6}{4}\frac{(C^*)^{5/2}}{((C^*)^7+25^7)^{3/2}}\right)\right] \\
\frac{\partial H'}{\partial b^*} &= C'\frac{\partial h'}{\partial b^*} = \frac{a'}{C'}
\end{aligned} \tag{6a}$$

In a similar way, $\frac{\partial(L,a^*,b^*)}{\partial(X,Y,Z)}$ Jacobian matrix map color vectors L^*, a^*, b^* into X, Y, Z tristimulus color space and by another Jacobian matrix $\frac{\partial(X,Y,Z)}{\partial(x,y,Y)}$, we can relate X, Y and Z tristimulus and x, y and Y color vectors. The detailed derivations of these Jacobians can be found in Pant and Farup (CGIV,2010). Finally, the mapping of the CIEDE2000 formula into the xyY color space in terms of the metric tensor is

$$\begin{aligned}
(dE_{00})^2 = \begin{bmatrix} dx & dy & dY \end{bmatrix} & \frac{\partial(X,Y,Z)}{\partial(x,y,Y)}^T \frac{\partial(L,a^*,b^*)}{\partial(X,Y,Z)}^T \frac{\partial(L',C',H')}{\partial(L^*,a^*,b^*)}^T \\
& \begin{bmatrix} (k_L S_L)^{-2} & 0 & 0 \\ 0 & (k_C S_C)^{-2} & \frac{1}{2}(k_C S_C k_H S_H)^{-1} \\ 0 & \frac{1}{2}(k_C S_C k_H S_H)^{-1} & (k_H S_H)^{-2} \end{bmatrix} \\
& \frac{\partial(L',C',H')}{\partial(L^*,a^*,b^*)} \frac{\partial(L,a^*,b^*)}{\partial(X,Y,Z)} \frac{\partial(X,Y,Z)}{\partial(x,y,Y)} \begin{bmatrix} dx \\ dy \\ dY \end{bmatrix}
\end{aligned} \tag{7}$$

Multiplying all the Jacobian matrices, their transposes and the matrix of original form (matrix of correction terms) together, we will get a 3×3 matrix in the xyY color space.

This matrix is known as the Riemannian metric tensor (g_{ik}) of the CIEDE2000 formula in the xyY color space, which gives JND ellipsoids in three dimensions and ellipses in two dimensions. The principal axes of ellipses can be calculated from eigenvectors and eigenvalues of the metric g_{ik}. So, if λ_1 and λ_2 are eigenvalues of the g_{ik}, the axis (a) and the axis (b) equal to $\frac{1}{\sqrt{\lambda_1}}$ and $\frac{1}{\sqrt{\lambda_2}}$ respectively.

Result and Discussion

In this section, the authors will discuss on the behavior of computed ellipses of the formula in the xyY color space with respect to the BFD-P ellipses.

One severe problem is found at the gray axis where the Jacobian (Equation 5) is not defined. It can be easily seen by inserting $a*$ and $b* = 0$ in Equations (6. In fact, the limit does not exist, since it depends on the path. Thus, a Riemannian metric does not exist at the gray axis. However, JND ellipses can be computed by the metric defined in Equation (7) for the rest of the colour space.

Here, all the calculated or computed ellipses of the CIEDE2000 formula and BFD-P ellipses have same color centers. Again, to draw the computed ellipses into the xy chromaticity diagram, the authors have taken the constant lightness value ($L^* = 50$) and this value equals to the lightness value which was taken to draw original BFD-P ellipses. The variables (k_L, k_C and k_H) are set to 1 for calculating ellipses. Now, at first, the authors describe qualitative analysis between computed and original ellipses. Figures 2(a) and 2(b) show BFD-P and computed CIEDE2000 ellipses drawn in the CIE64 chromaticity diagram respectively. It can be seen that ellipses for the neutral and gray color centers are almost the same in both figures. Similarly, in both BFD-P and CIEDE2000, the ellipses for blue, green-blue, green-yellow, yellow and red centers tend to point along lines of constant dominant wavelength. However, in CIEDE2000, the orientation of ellipses in the blue region are rotated compared to the BFD-P ellipses of same region. On the other hand, in the red region too, the CIEDE2000 ellipses are rotated in opposite direction and stretched in length. In terms of size, the CIEDE2000 ellipses in blue and green-blue are slightly smaller than the BFD-P ellipses in the corresponding region, where as they are slightly larger as well as more circular in shape in the yellow region.

Our next analysis between CIEDE2000 and BFD-P is based on our method for comparing the similarity of a pair of ellipses as said in the introduction section. The value obtained by this method lies in the range of $0 < x \leq 1$. Hence, a comparison value of 1 between a pair of ellipses ensures the full compatibility between them in terms of size, shape and orientation. According to this method, the authors have got maximum matching value of .96 between a pair of CIEDE2000 and BFD-P ellipses. This pair appears in the neutral color region. Similarly, the minimum value has come .29 around high chroma blue. The matching values of all ellipse pairs can be seen in the histogram 1 as well as from the Table 1.

Similarly, Figures 3(c) and 3(b) show the MacAdam's original ellipses and the CIEDE2000 ellipses taking his original color centers in the 1931 xy chromaticity diagram. Ellipses are plotted at constant lightness level at $L^* = 50$. These figures also help to visualize the difference between original and computed ellipses in terms of size shape and orientation in a simple manner and the general trend of difference is also similar to the BFD-P and the CIEDE2000 ellipses as described above.

Conclusion

The first objective of this paper is to formulate the CIEDE2000 formula into the Riemannian metric and apply the Jacobian method to transfer it into different color spaces as well as to compute JND ellipses from this metric. This is successfully accomplished, except at the gray axis. Second objective is to study the behavior of the formula in the xyY color space with respect to the experimentally observed data. This is also done by drawing JND ellipses of the formula and experimentally observed BFD-P ellipses into the xy chromaticity diagram and comparing them by our comparison technique described above.

On the basis of our findings as discussed above, the authors can say that the CIEDE2000 significantly measures the visual color differences. However, it is seen orientation problem in the CIEDE2000 ellipses compared to BFD-P ellipses in the blue region as well as in the red region. This indicates that further research for the improvement of the rotation term or the colour difference metrics, in general is necessary. Our method has also shown that the formula measures small color difference well in

Table 1: Comparison values of CIEDE2000 and BFD-P Ellipses pairs . A comparison value of 1 between a pair of ellipses ensures the full compatibility between them in terms of size, shape and orientation.

Ellipse pair number	1	2	3	4	5	6	7	8	9	10	11	12
Value	0.96	0.93	0.9	0.88	0.88	0.88	0.86	0.85	0.85	0.83	0.82	0.81
Ellipse pair number	13	14	15	16	17	18	19	20	21	22	23	24
Value	0.79	0.79	0.78	0.77	0.77	0.77	0.76	0.75	0.75	0.75	0.75	0.75
Ellipse pair number	25	26	27	28	29	30	31	32	33	34	35	36
Value	0.75	0.75	0.75	0.74	0.74	0.73	0.73	0.72	0.72	0.72	0.71	0.71
Ellipse pair number	37	38	39	40	41	42	43	44	45	46	47	48
Value	0.71	0.71	0.7	0.7	0.69	0.69	0.69	0.69	0.68	0.68	0.68	0.68
Ellipse pair number	49	50	51	52	53	54	55	56	57	58	59	60
Value	0.66	0.66	0.65	0.65	0.64	0.62	0.6	0.58	0.58	0.57	0.54	0.53
Ellipse pair number	61	62	63	64	65	66	67	68	69	70	71	72
Value	0.53	0.53	0.52	0.52	0.51	0.5	0.49	0.48	0.47	0.46	0.46	0.44
Ellipse pair number	73	74	75	76	77	78	79	80				
Value	0.4	0.38	0.37	0.34	0.34	0.33	0.33	0.29				

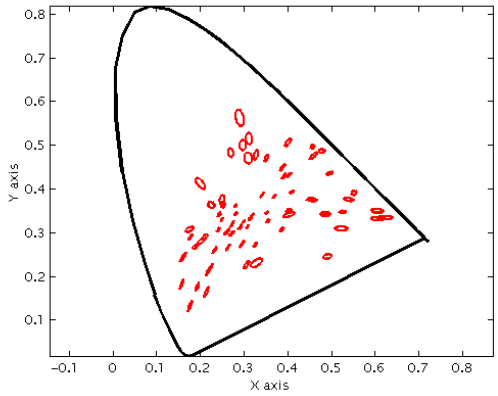

(a) BFD-P Ellipses.

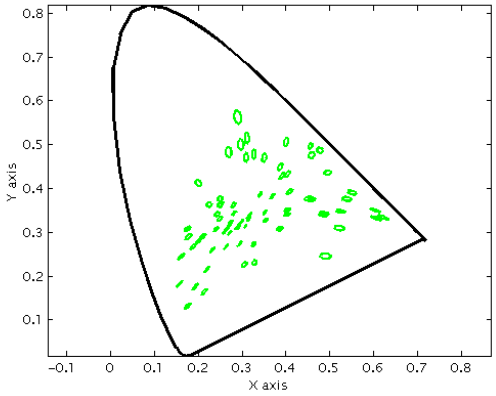

(b) CIEDE2000 Ellipses having same color centers as BFD-P.

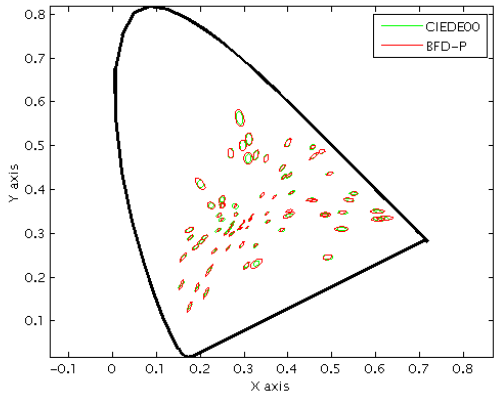

(c) BFD-P and CIEDE2000 Ellipses plotted on the same xy diagram

.

Figure 2: BFD-P Ellipses and Computed CIEDE2000 Ellipses in the CIE64 Chromaticity diagram(Enlarged 1.5 times)

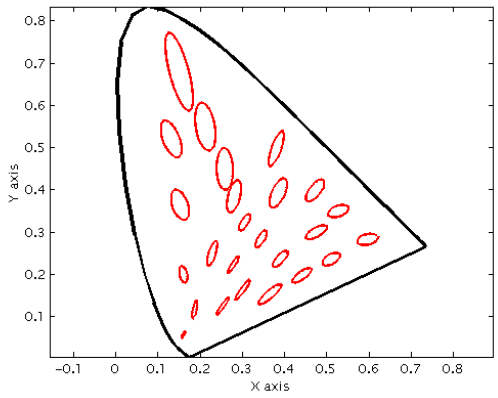

(a) MacAdam Ellipses.

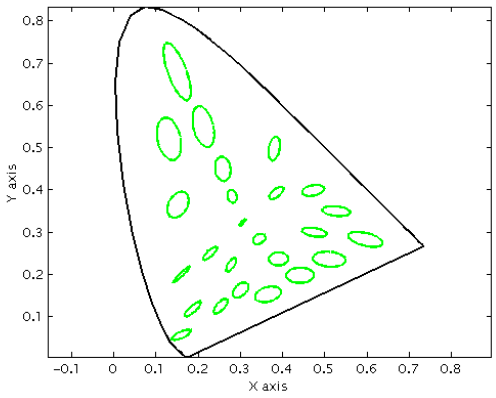

(b) CIEDE2000 Ellipses having same color centers as MacAdam.

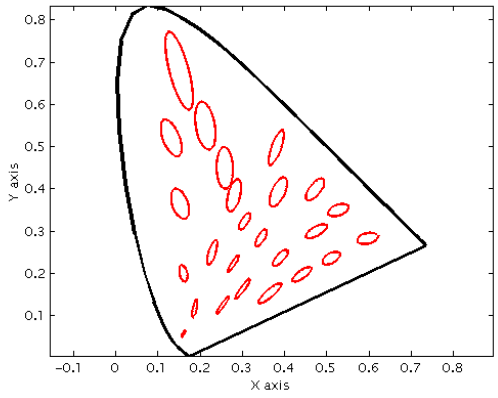

(c) MacAdam and CIEDE2000 Ellipses plotted on the same xy diagram.

Figure 3: MacAdam's original and Computed CIEDE2000 ellipses in the CIE31 Chromaticity diagram(Enlarged 10 times)

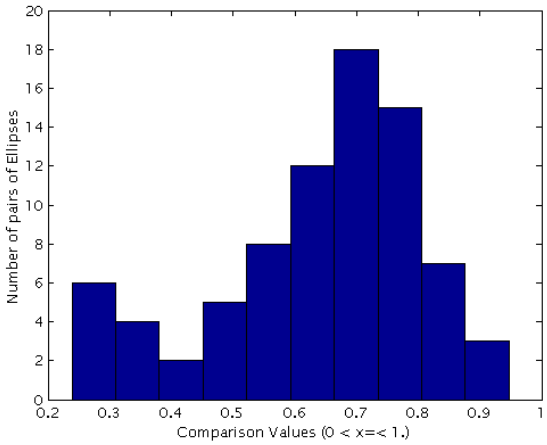

Figure 1: Histogram of comparison values between CIEDE2000 and BFD-P Ellipses. The values lie in the range $0 < x \leq 1$. Higher comparison value indicates better matching between a pair of ellipses.

the non-Euclidean space.

The authors hope that the formula presented here will be useful for the color research and applications.

References

[1] D. R. Pant and I. Farup. Evaluating color difference formulae by Riemannian metric. In *5th European Conference on Colour in Graphics, Imaging, and Vision, CGIV 2010*, page 497, Joensuu, Finland, June 2010.

[2] D.L MacAdam. Visual sensitivities to color differences in daylight. *J. Optical Society of America*, 32:247–274, 1942.

[3] CIE. Industrial colour difference evaluation, CIE publication number 116, CIE central bureau, Vienna, 1995.

[4] A. R. Robertson. Historical development of CIE recommended color difference equations. *Color Res. Appl.*, 15 (3):167–170, 1989.

[5] M. R Luo and B. Rigg. Chromaticity-discrimination ellipses for surface colours. *Color Res. Appl.*, 11:25–42, 1986.

[6] D.H Kim and J.H Nobbs. New weighting functions for the weighted CIELAB colour difference formula. In *Proceedings of AIC Colour*, pages 446–449, Kyoto, 1997. AIC.

[7] R.S. Berns, D. H Alman, L. Reniff, G.D. Snyder, and M.R. Balonon-Rosen. Visual determination of suprathreshold color-difference tolerances using probit analysis. *Color Res. Appl.*, 16:297–316, 1991.

[8] K. Witt. Geometric relations between scales of small colour differences. *Color Res. Appl.*, 24:78–92, 1999.

[9] M. Melgosa and R. Huertas. Relative significance of the terms in the CIEDE2000 and CIE94 color difference formulas. *Optical Society of America*, 21(12), July 2004.

[10] M.R Luo, G.H. Cui, and B. Rigg. The development of the CIE2000 colour difference formula. *Color Res. Appl.*, 26: 340–350, 2001.

[11] M. Melgosa, R. Huertas, and R. S. Berns. Performance of recent advanced color difference fromulae using the standardized residual sum of squares index. *J. Optical Society of America*, 25(7):pp. 1828–1834, July 2008.

[12] Gaurav Sharma, Wencheng Wu, and Edul N. Dalal. The CIEDE2000 color-difference formula: Implementation notes, supplementary test data, and mathematical observations. *Color Res. Appl.*, 30:21–30, 2004.

[13] J. Gay and R. Hirschler. Field trials for CIEDE2000: Correlation of visual and instrumental pass/fail decisions in industry. Technical Report ISBN 390190621, 25th, The CIE Session, San Diego, Jun. 2003.

[14] K. Noor, D. Hinks, A. Laidlaw, and R. Harold. Comparison of the performance of CIEDE2000 and DECMC. In *Color Measurement and Test Methods Committee (AATCC) International Conference and Exhibition*, pages 140–147, 2003.

[15] J.R. Aspland and P. Shanbhag. Comparison of color difference equations for textiles CMC(2:1) and CIEDE2000. In *AATCC Review*, volume 4, pages 26–30, 2004.

[16] R. G. Kuehni. *Color Space and its Division*. John Wiley and Sons, New York, 2003.

[17] W. Schultze. The usefulness of colour difference formulas for fixing colour tolerances. In *AIC Proceedings*, pages 254–265, 1972.

[18] D.B. Judd. Ideal color space: Curvature of color space and its implications for industrial color tolerances. *Palette*, 29: 21–28, 1968.

[19] W. R. Brown and D.L. MacAdam. Visual sensitivities to combined chromaticity and luminance differences. *J. Optical Society of America*, 39:808–834, 1949.

[20] L. Silberstein. Notes on W.S. Stiles paper entitled : A modified Helmholtz line-element in brightness-colour space. *J. Optical Society of America*, 37(4):pp. 292–295, 1947.

[21] C. Alder, K. P. Chaing, T. F. Chong, E. Coates, A A. Khalili, and B. Rigg. Uniform chromaticity scales – new experimental data. *Society of Dyers and Colurist, UK*, 98:14–20, 1982.

[22] CIE. Improvement to industrial color–difference evaluation. Technical Report 142, CIE central bureau, Vienna, 2001.

7

Paper C

Riemannian formulation and comparison of color difference formulas

Dibakar Raj Pant and Ivar Farup

Published in J. Color Research and Application

Article first published online: 13 SEP 2011

DOI: 10.1002/col.20710

Riemannian Formulation and Comparison of Color Difference Formulas

Dibakar Raj Pant[1,2] and Ivar Farup[1]

[1]The Norwegian Color Research Laboratory,
Gjøvik University College, Norway
[2]The Laboratoire Hubert Curien,
University Jean Monnet, Saint Etienne, France

Abstract

Study of various color difference formulas by the Riemannian approach is useful. By this approach, it is possible to evaluate the performance of various color difference fourmlas having different color spaces for measuring visual color difference. In this paper, the authors present mathematical formulations of CIELAB (ΔE^*_{ab}), CIELUV (ΔE^*_{uv}), OSA-UCS (ΔE_E) and infinitesimal approximation of CIEDE2000 (ΔE_{00}) as Riemannian metric tensors in a color space. It is shown how such metrics are transformed in other color spaces by means of Jacobian matrics. The coefficients of such metrics give equi-distance ellipsoids in three dimensions and ellipses in two dimensions. A method is also proposed for comparing the similarity between a pair of ellipses. The technique works by calculating the ratio of the area of intersection and the area of union of a pair of ellipses. The performance of these four color difference formulas is evaluated by comparing computed ellipses with experimentally observed ellipses in the xy chromaticity diagram. The result shows that there is no significant difference between the Riemannized ΔE_{00} and the ΔE_E at small colour difference, but they are both notably better than ΔE^*_{ab} and ΔE^*_{uv}.

Introduction

Color difference metrics are in general derived from two kinds of experimental data. The first kind is threshold data obtained from color matching experiments and they are described by just noticeable difference (JND) ellipses. The second kind is visual colour difference data and it gives supra-threshold colour difference ellipses [1]. For example, Friele-MacAdam-Chickering (FMC) colour difference metric [2] is based on first kind of data where as the CIELAB [3] is based on second kind data.

MacAdam [4] was the first to describe just noticeable difference (JND) ellipses. Later, more elaborated data sets were established by Brown [5], Wyszecki and Fielder [6]. Examples of supra-threshold colour difference based data are BFD-Perceptibility(BFD-P) [7], RIT-DuPont [8], Witt [9]and others. The former two data sets were also included in the BFD-P data sets and fitted in the CIE xy chromaticity diagram [7].

Riemann [10] was the first to propose that colors, as well as the other objects of sense, could be described by non-Euclidean geometry. Later, Helmholtz [11] derived the first line element for a color space. Similarly, Schrödinger [12] and Stiles [13] also elaborated more on Helmholtz's line element with modifications. The latest and most advanced contribution along this line, is the zone-fluctuation line element of Vos and Walraven [14]. A thorough review of color metrics following the line element can be found in [15–17].

On the other side, color and imaging industries have a continuous demand for a practical standard for measuring perceptual color differences accurately. So, at present, many color difference metrics are in existence. Among these, the CIELAB and the CIELUV [3] are popular and the most established ones in industries. Theses formulas are defined by Euclidean metrics in their own color spaces that are obtained by non-linear transformations of the tristimulus values. The CIEDE2000 [18] is a revised and improved formula based on the CIELAB color space, resulting in a non-Euclidean metric. Another important example is the recent Euclidean color difference metric, ΔE_E proposed by Oleari [19] based on the OSA-UCS color space. However, all the formulas mentioned above have some demerits to measure the visual perception of the color differences sufficiently [20–24]. Further, it has also been noticed by many other color researchers that the small color difference calculation using the Euclidean distance does not agree sufficiently with the perceptual color difference due to the curvilinear nature of the color space [22, 25–29].

Studying the various color difference metrics by treating the color spaces as Riemannian spaces proves useful. In such a representation, one can map or transfer a color metric between many color spaces. Basically, in a curved space the shortest length or the distance between any two points is called a geodesic. In the Riemannian geometry, distances are defined in the similar way. Therefore, small color differences can be represented by an infinitesimal distance at a given point in a color space. This distance is given by a positive definite quadratic differential form, also known as the Riemannian metric. In this sense, the Riemannian metric provides a powerful mathematical tool to formulate metric tensors of different color difference formulas.These metric tensors allow us to compute equi-distance ellipses which can be analyzed and compared with experimentally observed ellipses in a common color space.

In this paper, the authors formulate the CIELAB, the CIELUV, and the OSA-UCS based ΔE_E color difference formulas in terms of Riemannian metric. Similarly, Riemannian approximation of the CIEDE2000 is also presented. The CIEDE2000 approximation is hereafter referred to as the Riemannized ΔE_{00}. This is done by taking the line element to calculate infinitesimal color differences dE. In this process, color difference equations are converted into the differential form. Again, to obtain the Riemannian metric in a new color space, we need to transform color vectors from one color space to another. This is accomplished by the Jacobian transformation. To illustrate the method, the authors transformed the four color difference formulas mentioned above into the xyY color space. The equi-distance ellipses of each formula are plotted in the xy chromaticity diagram for constant luminance. The input data to compute the ellipses for our method is the BFD-P data sets [7]. The BFD-P data sets were assessed by about 20 observers using a ratio method, and the chromaticity discrimination ellipses were calculated and plotted in the xy chromaticity diagram for each set [30]. A comparison has also been done between the computed equi-distance

ellipses of each formula and the original ellipses obtained from the BFD-P data set. A method for comparing a pair of ellipses by calculating the ratio of the area of intersection and the area of union was proposed by the authors [31]. This method gives a single comparison value which takes account of variations in the size, the shape and the orientation simultaneously for a pair of ellipses. Therefore, this value is an indicator which tells us how well two ellipses match each other. A comparative analysis has also discussed between computed equi-distance ellipses of different color difference formulas.

Method

Ellipse Equation

In the Riemannian space, a positive definite symmetric metric tensor g_{ik} is a function which is used to compute the infinitesimal distance between any two points. So, the arc length of a curve between two points is expressed by a differential quadratic form as given below :

$$ds^2 = g_{11}dx^2 + 2g_{12}dxdy + g_{22}dy^2. \tag{1}$$

The matrix form of Equation (1) is

$$ds^2 = \begin{bmatrix} dx & dy \end{bmatrix} \begin{bmatrix} g_{11} & g_{12} \\ g_{12} & g_{22} \end{bmatrix} \begin{bmatrix} dx \\ dy \end{bmatrix}, \tag{2}$$

and

$$g_{ik} = \begin{bmatrix} g_{11} & g_{12} \\ g_{21} & g_{22} \end{bmatrix} \tag{3}$$

where ds is the distance between two points, dx is the difference of x coordinates, dy is the difference of y coordinates and g_{11}, g_{12} and g_{22} are the coefficients of the metric tensor g_{ik}. Here, the coefficient g_{12} is equal to the coefficient g_{21} due to symmetry.

In a two dimensional color space, the metric g_{ik} gives the intrinsic properties about the color measured at a surface point. Specifically, the metric represents the chromaticity difference of any two colors measured along the geodesic of the surface.In general, it gives equi-distant contours. However, to calculate small colour differences considering infinitesimal distance ds, the coefficients of g_{ik} also determine an ellipse in terms of its parameters and vice versa. The parameters are the semimajor axis, a, the semiminor axis, b, and the angle of inclination in a geometric plane, θ, respectively. In equation form, the coefficients of g_{ik} in terms of the ellipse parameter are expressed as [31]:

$$\begin{aligned} g_{11} &= \frac{1}{a^2}\cos^2\theta + \frac{1}{b^2}\sin^2\theta, \\ g_{12} &= \cos\theta\sin\theta\,(\frac{1}{a^2} - \frac{1}{b^2}), \\ g_{22} &= \frac{1}{a^2}\sin^2\theta + \frac{1}{b^2}\cos^2\theta. \end{aligned} \tag{4}$$

The angle formed by the major axis with the positive x-axis is given by

$$\tan(2\theta) = \frac{2g_{12}}{(g_{11} - g_{22})}. \tag{5}$$

Here $\theta \leq 90^\circ$ when $g_{12} \leq 0$, and otherwise $\theta \geq 90^\circ$. Similarly, the inverse of Equations (4–5) are

$$\begin{aligned} \frac{1}{a^2} &= g_{22} + g_{12}\cot\theta, \\ \frac{1}{b^2} &= g_{11} - g_{12}\cot\theta. \end{aligned} \tag{6}$$

Alternatively, the semi major axis, a, and the semi minor axis, b, of an ellipse can also be determined by the eigenvector and eigenvalue of the metric g_{ik}. If λ_1 and λ_2 are eigenvalues of the metric g_{ik}, the semimajor axis, a, and the semiminor axis, b, equal to $1/\sqrt{\lambda_1}$ and $1/\sqrt{\lambda_2}$ respectively. Like wise, θ is the angle between the first eigenvector and the first axis [32].

Transformation of coordinates

In Equation (1), the quantity ds^2 is called the first fundamental form which gives the metric properties of a surface. Now, suppose that x and y are related to another pair of coordinates u and v. Then, these new coordinates will also have new metric tensor g'_{ik}. As analogy to Equation (3), it is written as:

$$g'_{ik} = \begin{bmatrix} g'_{11} & g'_{12} \\ g'_{21} & g'_{22} \end{bmatrix}. \tag{7}$$

Now, the new metric tensor g'_{ik} is related to g_{ik} via the matrix equation as follows:

$$\begin{bmatrix} g'_{11} & g'_{12} \\ g'_{21} & g'_{22} \end{bmatrix} = \begin{bmatrix} \frac{\partial x}{\partial u} & \frac{\partial x}{\partial v} \\ \frac{\partial y}{\partial u} & \frac{\partial y}{\partial v} \end{bmatrix}^T \begin{bmatrix} g_{11} & g_{12} \\ g_{21} & g_{22} \end{bmatrix} \begin{bmatrix} \frac{\partial x}{\partial u} & \frac{\partial x}{\partial v} \\ \frac{\partial y}{\partial u} & \frac{\partial y}{\partial v} \end{bmatrix}, \tag{8}$$

where the superscript T denotes the matrix transpose and the matrix

$$J = \frac{\partial(x,y)}{\partial(u,v)} = \begin{bmatrix} \frac{\partial x}{\partial u} & \frac{\partial x}{\partial v} \\ \frac{\partial y}{\partial u} & \frac{\partial y}{\partial v} \end{bmatrix} \tag{9}$$

is the Jacobian matrix for the coordinate transformation, or, simply, the Jacobian.

Ellipse comparison

Using the principles of union–intersection and ratio testing, the authors present the method to compare two ellipses with respect to their size, shape and orientation. Figure 1(a) shows two ellipses A and B. The common area is the intersection area between them and the total area of A and B is known as the union area. From the statistical point of view, the acceptance region is the intersection area and the rejection region is the union area. The ratio of these intersection and union area gives us a non-negative value which lies in the range of $0 < x \leq 1$. So, the matching ratio is expressed as:

$$R = \frac{\text{Area}(A \bigcap B)}{\text{Area}(A \bigcup B)} \tag{10}$$

High value of R gives strong evidence that the two ellipses are closely matched and vice versa. For example, a highly matched ellipse pair with R equal to .92 and a poorly matched ellipse pair with R equal to .21 are shown in Figure 1(b) and Figure 1(c) respectively. Hence, a match ratio of 1 between a pair of ellipses ensures full matching between them in terms of size, shape and orientation.

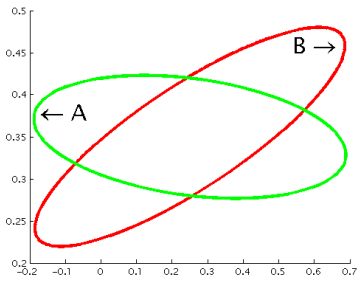

(a) The union and the intersection area of two ellipses.

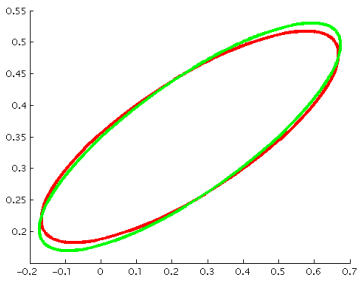

(b) Highly matched ellipse pair with R .92.

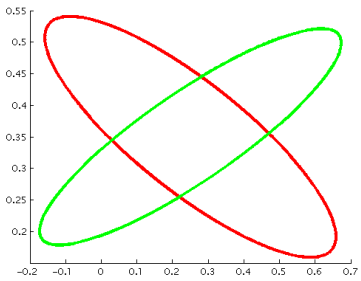

(c) Poorly matched ellipse pair with R .21.

Figure 1: Illustration of the method to compare two ellipses with respect to their size, shape and orientation.

The Color Difference Metrics

In this section, the authors show how to derive the Riemannian forms of the four color difference metrics chosen for the study. Only the outline of the derivations are given. For the detailed expressions of the coefficients of the Jacobian matrices, see the appendix.

The ΔE^*_{ab} Metric

The color difference in the CIELAB color space is defined as the Euclidean distance,

$$\Delta E^*_{ab} = \sqrt{(\Delta L^*)^2 + (\Delta a^*)^2 + (\Delta b^*)^2}\,. \tag{11}$$

The CIELAB color space defined for moderate to high lightness is given as

$$\begin{aligned} L^* &= 116\left(\frac{Y}{Y_r}\right)^{\frac{1}{3}} - 16, \\ a^* &= 500\left[\left(\frac{X}{X_r}\right)^{\frac{1}{3}} - \left(\frac{Y}{Y_r}\right)^{\frac{1}{3}}\right], \\ b^* &= 200\left[\left(\frac{Y}{Y_r}\right)^{\frac{1}{3}} - \left(\frac{Z}{Z_r}\right)^{\frac{1}{3}}\right], \end{aligned} \tag{12}$$

where L^*, a^* and b^* corresponds to the Lightness, the redness-greenness and the yellowness-blueness scales in the CIELAB color space. Similarly, X, Y, Z and X_r, Y_r, Z_r are the tristimulus values of the color stimuli and white reference respectively.

The relationship between X, Y and Z tristimulus coordinates and x, y and Y color coordinates are

$$\begin{aligned} X &= \frac{xY}{y}\,, \\ Y &= Y, \\ Z &= \frac{(1-x-y)Y}{y}\,. \end{aligned} \tag{13}$$

If we take the line element distance to measure the infinitesimal color difference at a point in the color space, Equation (11) becomes differential. In terms of the differential quadratic form, we can write

$$(dE^*_{ab})^2 = \begin{bmatrix} dL^* & da^* & db^* \end{bmatrix} \begin{bmatrix} dL^* \\ da^* \\ db^* \end{bmatrix}. \tag{14}$$

Now, to transfer or map differential color vectors dL^*, da^*, db^* into dX, dY, dZ tristimulus color space, it is necessary to apply the Jacobian transformation where the variables of two color spaces are related by continuous partial derivatives. Hence, it is expressed as:

$$\begin{bmatrix} dL^* \\ da^* \\ db^* \end{bmatrix} = \begin{bmatrix} \frac{\partial L}{\partial X} & \frac{\partial L}{\partial Y} & \frac{\partial L}{\partial Z} \\ \frac{\partial a}{\partial X} & \frac{\partial a}{\partial Y} & \frac{\partial a}{\partial Z} \\ \frac{\partial b}{\partial X} & \frac{\partial b}{\partial Y} & \frac{\partial b}{\partial Z} \end{bmatrix} \begin{bmatrix} dX \\ dY \\ dZ \end{bmatrix}. \tag{15}$$

Again, from Equations (14) and (15), we have

$$(dE^*_{ab})^2 = \begin{bmatrix} dX dY dZ \end{bmatrix} \frac{\partial(L,a^*,b^*)}{\partial(X,Y,Z)}^T \frac{\partial(L,a^*,b^*)}{\partial(X,Y,Z)} \begin{bmatrix} dX \\ dY \\ dZ \end{bmatrix}, \tag{16}$$

where $\partial(L,a^*,b^*)/\partial(X,Y,Z)$ is the Jacobian matrix in Equation (15).

Similarly, transformation from X, Y, Z tristimulus color space into x, y, Y color space is done by another Jacobian matrix $\partial(X,Y,Z)/\partial(x,y,Y)$ and expressed as :

$$\begin{bmatrix} dX \\ dY \\ dZ \end{bmatrix} = \begin{bmatrix} \frac{\partial X}{\partial x} & \frac{\partial X}{\partial y} & \frac{\partial X}{\partial Y} \\ \frac{\partial Y}{\partial x} & \frac{\partial Y}{\partial y} & \frac{\partial Y}{\partial Y} \\ \frac{\partial Z}{\partial x} & \frac{\partial Z}{\partial y} & \frac{\partial Z}{\partial Y} \end{bmatrix} \begin{bmatrix} dx \\ dy \\ dY \end{bmatrix}. \tag{17}$$

Finally, the L^*, a^*, b^* metric is transformed into x, y, Y as follows:

$$(dE^*_{ab})^2 = \begin{bmatrix} dx & dy & dY \end{bmatrix} \frac{\partial(X,Y,Z)}{\partial(x,y,Y)}^T \frac{\partial(L,a^*,b^*)}{\partial(X,Y,Z)}^T \frac{\partial(L,a^*,b^*)}{\partial(X,Y,Z)} \frac{\partial(X,Y,Z)}{\partial(x,y,Y)} \begin{bmatrix} dx \\ dy \\ dY \end{bmatrix}. \tag{18}$$

Thus, the Riemannian metric tensor corresponding to ΔE^*_{ab} in the xyY space is

$$g_{\Delta E^*_{ab}} = \frac{\partial(X,Y,Z)}{\partial(x,y,Y)}^T \frac{\partial(L,a^*,b^*)}{\partial(X,Y,Z)}^T \frac{\partial(L,a^*,b^*)}{\partial(X,Y,Z)} \frac{\partial(X,Y,Z)}{\partial(x,y,Y)}. \tag{19}$$

The ΔE^*_{uv} Metric

The color difference in the CIELUV color space is defined as the Euclidean distance,

$$\Delta E^*_{uv} = \sqrt{(\Delta L^*)^2 + (\Delta u^*)^2 + (\Delta v^*)^2}\,. \tag{20}$$

The CIELUV color space is defined as

$$\begin{aligned} L^* &= 116 \left(\frac{Y}{Y_r}\right)^{\frac{1}{3}} - 16, \\ u^* &= 13L \left[\left(\frac{4X}{X + 15Y + 3Z} \right) - \left(\frac{4X_r}{X_r + 15Y_r + 3Z_r} \right) \right], \\ v^* &= 13L \left[\left(\frac{9Y}{X + 15Y + 3Z} \right) - \left(\frac{9Y_r}{X_r + 15Y_r + 3Z_r} \right) \right]. \end{aligned} \tag{21}$$

In complete analogy with the case for ΔE^*_{ab}, the Riemannian metric tensor corresponding to ΔE^*_{uv} in the xyY space is

$$g_{\Delta E^*_{uv}} = \frac{\partial(X,Y,Z)}{\partial(x,y,Y)}^T \frac{\partial(L,u^*,v^*)}{\partial(X,Y,Z)}^T I \frac{\partial(L,u^*,v^*)}{\partial(X,Y,Z)} \frac{\partial(X,Y,Z)}{\partial(x,y,Y)}. \tag{22}$$

The Riemannized ΔE_{00} Metric

The CIEDE2000 formula derived from the CIELAB color space is defined as a non-Euclidean metric in a space as follows :

$$\Delta E_{00} = \left[\left(\frac{\Delta L'}{k_L S_L} \right)^2 + \left(\frac{\Delta C'}{k_C S_C} \right)^2 + \left(\frac{\Delta H'}{k_H S_H} \right)^2 + R_T \left(\frac{\Delta C'}{k_C S_C} \right) \left(\frac{\Delta H'}{k_H S_H} \right) \right]^{0.5} . \tag{23}$$

The rotation function, R_T, is defined as:

$$R_T = -\sin(2\Delta\theta) R_c, \tag{24}$$

$$\text{where } \Delta\theta = 30 \cdot \exp\left[-\left(\frac{\bar{h}' - 275}{25} \right)^2 \right], \tag{25}$$

$$\text{and } R_c = 2\sqrt{\frac{\bar{C}'^7}{\bar{C}'^7 + 25^7}} . \tag{26}$$

The weighting functions are defined as:

$$S_L = 1 + \frac{0.015(\bar{L}' - 50)^2}{\sqrt{20 + (\bar{L}' - 50)^2}}, \tag{27}$$

$$S_C = 1 + 0.045\bar{C}', \tag{28}$$

$$S_H = 1 + 0.015\bar{C}'T, \tag{29}$$

$$\text{with } T = 1 - 0.17\cos(\bar{h}' - 30^o) + 0.24\cos(2\bar{h}') + .32\cos(3\bar{h}' + 6^o) - 0.2\cos(4\bar{h}' - 63^o). \tag{30}$$

Here, the lightness, the chroma and the hue are obtained taking the average of the pair of color samples for which the color difference is to be determined, $\bar{L}' = (L_1^{'} + L_2^{'})/2$, $\bar{C}' = (C_1' + C_2')/2$ and $\bar{h}' = (h_1' + h_2')/2$. Furhter, $\Delta H = 2\sqrt{C_1' C_2'}\sin(\Delta h'/2)$.

The color coordinates used in the formula are defined from the CIELAB coordinates in the following way:

$$L' = L^*, \tag{31}$$

$$a' = a^*(1 + G), \tag{32}$$

$$b' = b^*, \tag{33}$$

$$C' = \sqrt{a'^2 + b'^2}\,, \tag{34}$$

$$h' = \arctan\frac{b'}{a'}\,, \tag{35}$$

$$G = \frac{1}{2}\left(1 - \sqrt{\frac{C_{ab}^{*7}}{C_{ab}^{*7} + 25^7}} \right), \tag{36}$$

where L^*, a^* and b^* corresponds to the lightness, the redness-greenness and the yellowness-blueness scales and C^* chroma in the CIELAB color space. Likewise, $h^{'}$ is the hue angle for a pair of samples. The authors like to explain

some problems for formulating Remiannian metric of ΔE_{00}. In the ΔE_{00} formula as given in Equation (23), the coordinate H' does not exist since $\Delta H'$ is not the difference of any H'. As per the rules of Riemannian geometry, it is not possible to get the Remiannian metric of the formula from its original configuration. However, at infinitesimal colour difference, it is possible to use $L'C'h'$ coordinates instead of $L'C'H'$ because $C^{'}$ and $h^{'}$ are legitimate coordinates. Calculation of Remiannian metric using $L'C'h'$ coordinates gives us an approximation of ΔE_{00} when we substitute $dH' = C'dh'$ as proposed by Völz [33] at infinitesimal colour difference only. But, this Riemannized ΔE_{00} can not be integrated to build CIE defined ΔE_{00} due to the definition of $\Delta H'$. Defining the metric for infinitesimal colour differences, the discontinuity problems in the hue angle as noted by Sharma et.al. [34] is vanished. This is due to taking h' values instead of taking airthmetic mean $\bar{h'}$. However, there are very small discontinuities remaining in R_T, caused by the discontinuity of h' at $h' = 0$ and in the transformation from XYZ to $L^*a^*b^*$.

To calculate line element L', C' and h' values are taken. So, the Equation (23) in the approximate differential form is written as follows:

$$\begin{aligned}(dE_{00})^2 = &\begin{bmatrix} dL' & dC' & dh' \end{bmatrix} \\ &\times \begin{bmatrix} (k_L S_L)^{-2} & 0 & 0 \\ 0 & (k_C S_C)^{-2} & \frac{1}{2} C^{'} R_T (k_C S_C k_H S_H)^{-1} \\ 0 & \frac{1}{2} C^{'} R_T (k_C S_C k_H S_H)^{-1} & C^{'2} (k_H S_H)^{-2} \end{bmatrix} \\ &\times \begin{bmatrix} dL' \\ dC' \\ dh' \end{bmatrix}. \end{aligned} \tag{37}$$

In Equation (37), the matrix consisting of weighting functions, parametric factors, and rotation term is the Riemannian metric of the formula in its approximate form. This metric is positive definite since $R_T^2/4 < 1$, $\sin(2\Delta\theta) \in [-1, 1]$ and $|R_C| < 2$ (see Equations (24)–(26)). It can be transformed into xyY color space by the Jacobian method. The first step is to transform differential color vectors $[dL'\, dC'\, dh']$ into $[dL^{'}\, da^{'}\, db^{'}]$ by computing all partial derivatives of vector functions L', C', and h' with respect to $L^{'}$, $a^{'}$, and $b^{'}$. Then, the $L^{'}$, $a^{'}$, and $b^{'}$ differential vecors are again transformed into L^*, a^*, and b^* . Rest of the other process is analog to the CIELAB space. The resulting Riemannian metric tensor representing the CIEDE2000 color difference metric in the xyY space is

$$\begin{aligned} g_{\Delta E_{00}} = &\frac{\partial(X,Y,Z)}{\partial(x,y,Y)}^T \frac{\partial(L,a^*,b^*)}{\partial(X,Y,Z)}^T \frac{\partial(L',a',b')}{\partial(L,a^*,b^*)}^T \frac{\partial(L',C',h')}{\partial(L',a',b')}^T \\ &\times \begin{bmatrix} (k_L S_L)^{-2} & 0 & 0 \\ 0 & (k_C S_C)^{-2} & \frac{1}{2} C^{'} R_T (k_C S_C k_H S_H)^{-1} \\ 0 & \frac{1}{2} C^{'} R_T (k_C S_C k_H S_H)^{-1} & C^{'2} (k_H S_H)^{-2} \end{bmatrix} \\ &\times \frac{\partial(L',C',h')}{\partial(L',a',b')} \frac{\partial(L',a',b')}{\partial(L,a^*,b^*)} \frac{\partial(L,a^*,b^*)}{\partial(X,Y,Z)} \frac{\partial(X,Y,Z)}{\partial(x,y,Y)}. \end{aligned} \tag{38}$$

The ΔE_E Metric

The ΔE_E color difference formula is defined as the Euclidean metric in the log compressed OSA-UCS color space,

$$\Delta E_E = \sqrt{(\Delta L_E)^2 + (\Delta G_E)^2 + (\Delta J_E)^2}\,. \tag{39}$$

Here, L_E G_E and J_E are the coordinates in the log-compressed OSA-UCS space. The lightness is derived from the original OSA-UCS formula and their definitions are expressed as follows[35, 36]:

$$L_E = \left(\frac{1}{b_L}\right) \ln\left[1 + \frac{b_L}{a_L}(10 L_{OSA})\right], \tag{40}$$

$$C_E = \left(\frac{1}{b_c}\right) \ln\left[1 + \frac{b_c}{a_c}(10 C_{OSA})\right], \tag{41}$$

$$C_{OSA} = \sqrt{G^2 + J^2}, \tag{42}$$

$$h = \arctan(\frac{-J}{G}), \tag{43}$$

$$G_E = -C_E \cos(h), \tag{44}$$

$$J_E = C_E \sin(h), \tag{45}$$

with the following constants,

$$\begin{aligned} a_L &= 2.890, \\ b_L &= 0.015, \\ a_c &= 1.256, \\ b_c &= 0.050. \end{aligned} \tag{46}$$

Expressing G_E and J_E in terms of C_{OSA}, we have:

$$\begin{aligned} \cos h &= \frac{G}{\sqrt{G^2 + J^2}}\,, \\ \sin h &= \frac{J}{\sqrt{G^2 + J^2}}\,, \\ G_E &= -\frac{C_E G}{C_{OSA}}\,, \\ J_E &= \frac{C_E J}{C_{OSA}}\,. \end{aligned} \tag{47}$$

The OSA-UCS color space is in turn related to the CIEXYZ color space:

$$\begin{aligned} L_{OSA} &= \left(5.9[(Y_0^{1/3} - \frac{2}{3}) + 0.042(Y_0 - 30)^{1/3}] - 14.4\right)\frac{1}{\sqrt{2}}, \\ Y_0 &= Y\left(4.4934x^2 + 4.3034y^2 - 4.2760xy - 1.3744x - 2.5643y + 1.8103\right). \end{aligned} \tag{48}$$

The coordinates J and G, which correspond to the empirical j and g of the OSA-UCS are defined through a sequence of linear transformations and a logarithmic

compression as follows:

$$\begin{bmatrix} A \\ B \\ C \end{bmatrix} = \begin{bmatrix} 0.6597 & 0.4492 & -0.1089 \\ -0.3053 & 1.2126 & 0.0927 \\ -0.0374 & 0.4795 & 0.5579 \end{bmatrix} \begin{bmatrix} X \\ Y \\ Z \end{bmatrix}, \tag{49}$$

$$\begin{bmatrix} J \\ G \end{bmatrix} = \begin{bmatrix} S_J & 0 \\ 0 & S_G \end{bmatrix} \begin{bmatrix} -\sin\alpha & \cos\alpha \\ \sin\beta & -\cos\beta \end{bmatrix} \begin{bmatrix} \ln\left(\frac{A/B}{A_n/B_n}\right) \\ \ln\left(\frac{B/C}{B_n/C_n}\right) \end{bmatrix} \tag{50}$$

$$\begin{aligned} &= \begin{bmatrix} 2(0.5735L_{OSA} + 7.0892) & 0 \\ 0 & -2(0.764L_{OSA} + 9.2521) \end{bmatrix} \\ &\times \begin{bmatrix} 0.1792[\ln A - \ln(0.9366B)] + 0.9837[\ln B - \ln(0.9807C)] \\ 0.9482[\ln A - \ln(0.9366B)] - 0.3175[\ln B - \ln(0.9807C)] \end{bmatrix}. \end{aligned} \tag{51}$$

For calculating the line element at a given point, the log-compressed OSA-UCS formula given in Equation (39) is written as:

$$(dE_E)^2 = \begin{bmatrix} dL_E & dG_E & dJ_E \end{bmatrix} \begin{bmatrix} dL_E \\ dG_E \\ dJ_E \end{bmatrix}. \tag{52}$$

The differential color vectors can be transformed into the OSA-UCS color space by applying the Jacobian method as follows:

$$(dE_E)^2 = \begin{bmatrix} dL_{OSA} & dG & dJ \end{bmatrix} \frac{\partial(L_E, G_E, J_E)}{\partial(L_{OSA}, G, J)}^T \frac{\partial(L_E, G_E, J_E)}{\partial(L_{OSA}, G, J)} \begin{bmatrix} dL_{OSA} \\ dG \\ dJ \end{bmatrix}. \tag{53}$$

In the OSA-UCS space, the coordinates J and G are also related with the lightness function L_{OSA}. So, to transfer the differential color vectors $[dL_{OSA}\ dG\ dJ]$ into $[dx\, dy\, dY]$, it is required to split the differential lightness vector dL_{OSA} and the differential coordinates dG and dJ in two parts. At first, let us relate $[dL_{OSA}\, dG\, dJ]$ in terms of $[dx\, dy\, dY]$ as follows:

$$\begin{bmatrix} dL_{OSA} \\ dG \\ dJ \end{bmatrix} = \frac{\partial(L_{OSA}, G, J)}{\partial(x, y, Y)} \begin{bmatrix} dx \\ dy \\ dY \end{bmatrix} = \begin{bmatrix} \frac{\partial L_{OSA}}{\partial(x,y,Y)} \\ \frac{\partial(G,J)}{\partial(x,y,Y)} \end{bmatrix} \begin{bmatrix} dx \\ dy \\ dY \end{bmatrix}, \tag{54}$$

where $\partial(L_{OSA}, G, J)/\partial(x, y, Y)$ is a 3×3 Jacobian matrix that is further divided into the 1×3 and 2×3 Jacobian matrices $\partial L_{OSA}/\partial(x, y, Y)$ and $\partial(G, J)/\partial(x, y, Y)$, respectively. The first one is again separated as follows:

$$\frac{\partial L_{OSA}}{\partial(x, y, Y)} = \frac{\partial L_{OSA}}{\partial Y_0} \begin{bmatrix} \frac{\partial Y_0}{\partial x} & \frac{\partial Y_0}{\partial y} & \frac{\partial Y_0}{\partial Y} \end{bmatrix}. \tag{55}$$

Similarly, the second one is also separated in two parts since both G and J depends on x, y, Y not only through A, B, and C, but also through L_{OSA}. So, the Jacobian follows as:

$$\frac{\partial(G, J)}{\partial(x, y, Y)} = \frac{\partial(G, J)}{\partial(L_{OSA}, A, B, C)} \cdot \frac{\partial(L_{OSA}, A, B, C)}{\partial(x, y, Y)}. \tag{56}$$

Again, in Equation (56), the last Jacobian $\partial(L_{OSA}, A, B, C)/\partial(x, y, Y)$ is further split in two parts according to

$$\frac{\partial(L_{OSA}, A, B, C)}{\partial(x, y, Y)} = \begin{bmatrix} \frac{\partial L_{OSA}}{\partial(x,y,Y)} \\ \frac{\partial(A,B,C)}{\partial(x,y,Y)} \end{bmatrix}, \tag{57}$$

where

$$\frac{\partial(A, B, C)}{\partial(x, y, Y)} = \frac{\partial(A, B, C)}{\partial(X, Y, Z)} \frac{\partial(X, Y, Z)}{\partial(x, y, Y)}. \tag{58}$$

The first of these is simply the constant matrix given in Equation (49), and the last one is already familiar from the other metrics.

Results and Discussion

In this section, first, the authors discuss the behaviour of computed ellipses of the ΔE^*_{ab}, the ΔE^*_{uv}, the Riemannized ΔE_{00} and the ΔE_E in the xyY color space with respect to BFD-P ellipses individually. Secondly, a comparative study between computed ellipses of these four color difference metrics will be done.A detailed quantitative comparison is done by using BFD-P data sets.

Before doing comparative analysis, it is necessary to mention that equidistance ellipses computed by the metric defined in Equation (38) represents Riemannized ΔE_{00} ellipses for infinitesimal colour differences. In fact, the ΔE_{00} metric in its original form does not define the Riemannian space in the strict sense.

Similarly, the ellipses are computed with a constant Y=0.4 in xyY color space. If we define constant lightness, then partial derivatives of lightness functions of all Jacobians will be zero. This gives 2×2 metric tensors and ellipses are computed in the xy chromaticity diagram.

Figure 2 shows BFD-P ellipses in the CIE 1964 chromaticity diagram. Similarly, Figures 3(a), 3(b), 3(c) and 3(d) show the ellipses of ΔE^*_{ab}, ΔE^*_{uv}, Riemannized ΔE_{00} and ΔE_E metrics respectively, using BFD-P data. All these ellipses are computed at the constant lightness value ($L^* = 50$) and color centers are taken from BFD-P data. In the xyY color space, this lightness value corresponds to the luminance $Y = 0.4$. In the Riemannized ΔE_{00} case, parametric factors (k_L, k_C and k_H) are set to 1. Comparing with BFD-P ellipses, disagreements can be seen with respect to the size, shape and rotation in ellipses of ΔE^*_{ab}, ΔE^*_{uv}, Riemannized ΔE_{00} and ΔE_E formulas. ΔE^*_{ab} and ΔE^*_{uv} ellipses appear more circular than BFD-P ellipses, but Riemannized ΔE_{00} and ΔE_E ellipses follow closer to the original ellipses in the blue and green region. However, it could be said that all computed ellipses of these four color difference metrics follow the general pattern of agreement with BFD-P ellipses. For example, the blue is the smallest, the green largest and the red, blue and yellow are more elongated than others. But, it is also seen that Riemannized ΔE_{00} and ΔE_E ellipses represent experimentally obtained ellipses more reasonably than compared to ΔE^*_{ab} and ΔE^*_{uv} ellipses. For example, ellipses of ΔE_{ab}, and ΔE^*_{uv} around neutral and gray color centers are bigger in size, while in the same region Riemannized ΔE_{00} and ΔE_E ellipses look more similar to the BFD-P ellipses. This indicates better quality performance of these two color difference formulas over two popular ΔE^*_{ab} and ΔE^*_{uv} formulas. Similarly, ΔE_E ellipses

perform better in the blue region than Riemannized ΔE_{00} ellipses. The authors also computed the difference between the Riemannized ΔE_{00} and the original ΔE_{00} metrices for finite colour differences by using the CIEDE2000 total colour difference test data of Gaurav Sharma et.al. [34]. For $\Delta E_{00} \leq 1$, the error is less than 0.5% and for $\Delta E_{00} \leq 2$, it is smaller than 1.2%. However, It is seen that in the cases where $\Delta E_{00} > 2.5$, the error between two metrices steeply raise. But, for larger colour differences, geodesic line can be calculated from the metric tensor of the Riemannized ΔE_{00}. Basically, ΔE_{00} formula is developed to calculate small colour differences because the BFD-P data set upon which the ΔE_{00} formula developed is scaled for $\Delta E*_{ab} < 2$ [7].

As described in the Section 2.C, the analysis is done by our method for comparing the similarity of a pair of ellipses. In Figure 4, histogram of R values between BFD-P and ΔE^*_{ab}, ΔE^*_{uv}, Riemannized ΔE_{00} and ΔE_E ellipses are given in Figures 4(a), 4(b), 4(c), 4(d) respectively. According to this method, the maximum R values given by ΔE^*_{ab}, ΔE^*_{uv}, Riemannized ΔE_{00} and ΔE_E are .81, .87, .95, and .93 respectively. Similarly, the lowest R values of these four formulas are, .1, .14, .2 and .2 respectively. Ellipse pairs of all metrics having maximum R values are located around neutral color region while matching pairs with lowest R are found around high chroma blue. Table 1 shows number of matching ellipses of four metrics with R values greater than .75 and less than .75. The result indicates that the Riemannized ΔE_{00} and ΔE_E perform better than the ΔE^*_{ab} and the ΔE^*_{uv}.

The authors have also used box plots to display ellipse matching values of these metrics in Figure 5. In the plots, the median value is marked by the central horizontal lines. The notch indicate the confidence interval of the median, and the box is bounded by the upper and lower quartiles of the grouped data. We can see that the Riemannized ΔE_{00} gives the highest median value while the CIELAB formula median value is the lowest. By using this technique, full range of matching value data is also plotted for comparing these four metrics simultaneously. The range of data is shown by dashed line, and outliers and marked with a cross. According to this box plot, the performance ranking of these metrics come in the following order: Riemannized ΔE_{00} first, ΔE_E second, ΔE^*_{uv} third and ΔE^*_{ab} fourth. However, there is no big difference between ΔE_{00} and ΔE_E and between ΔE_{uv} and ΔE_{ab}. But, with respect to Riemannized ΔE_{00} and ΔE_E, the performance of ΔE^*_{uv} and ΔE^*_{ab} metrics for matching ellipses is seen weaker.

In order to compare how well the different metrics reproduce the BFD-P ellipses, the pairwise statistical sign test of R values is also done between all pairs of metrics. The test result shows that at 5 % confidence level, Riemannized ΔE_{00} and ΔE_E both performed significantly better than ΔE^*_{uv} and ΔE^*_{ab} metrics. Further, ΔE^*_{uv} performs better than ΔE^*_{ab} with $p = 0.0176$. There is no significant difference between ΔE_{00} and ΔE_E metrics.

On the basis of above results, it is good to point the features of color spaces used by these metrics responsible for better performance. For example, saturation is defined in ΔE^*_{uv} not in ΔE^*_{ab} [37]. In ΔE_E, the lightness L_{OSA} takes into account the Helmholtz-Kohlrausch and crispening effects [19]. Further, the OSA-UCS system adopts a regular rhombohedral geometry which gives square grid with integer value of lightness [38]. This makes OSA-UCS space more uniform than CIELAB and CIELUV and suitable for small to medium color difference measurement. On the other hand, the non-Euclidean Riemannized

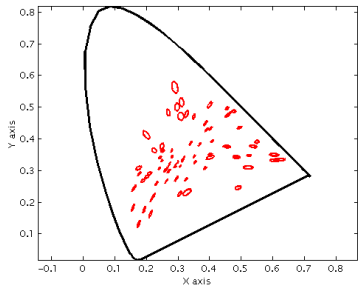

Figure 2: BFD-P ellipses in the CIE1964 chromaticity diagram (enlarged 1.5 times).

ΔE_{00} have many parameters for computing color differences. However, this formula has its specific advantage to correct the non-linearity of the visual system. But, the quality of the formula depends on selecting parameters values.

Table 1: Number of matching ellipses with matching values $\geq .75$ and $\leq .75$ of four color difference metrics. This matching is done with BFD-P ellipses.

	Number of Ellipse pairs with match ratio $\geq .75$	Number of Ellipse pairs with match ratio $\leq .75$
ΔE^*_{ab}	3	77
ΔE^*_{uv}	7	73
ΔE_{00}	57	23
ΔE_E	55	25

Conclusion

First, formulation of CIELAB, CIELUV, Riemannized CIEDE00 and OSA-UCS ΔE_E color difference formulas into the Riemannian metric is successfully accomplished. Secondly, The Riemannized ΔE_{00} is found indistinguishable to the exact ΔE_{00} for the small colour differences.

Thirdly, computation of equi-distance ellipses of these four formulas in the xyY color space is done by transferring Riemannian metrics of formulas into the xyY color space by the Jacobian method. Fourthly, a comparison between experimentally observed BFD-P and computed ellipses of these formulas is done in two ways: first descriptive and second by our developed comparison technique. On the basis of our findings as discussed above, the authors can say that Riemannized CIEDE2000 and OSA-UCS ΔE_E formulas measure the visual color differences significantly better than CIELAB and CIELUV formulas. However, neither formulas are fully perfect for matching visual color differences data. Among CIELAB and CIELUV formulas, performance of the CIELUV is found slightly better than the CIELAB. Similarly, there is no significant difference between Euclidean ΔE_E and Riemannized CIEDE2000 formulas. It is interesting to note that the Euclidean ΔE_E formula is not inferior to the complex, non-Euclidean industry standard ΔE_{00} for measuring small color differences.

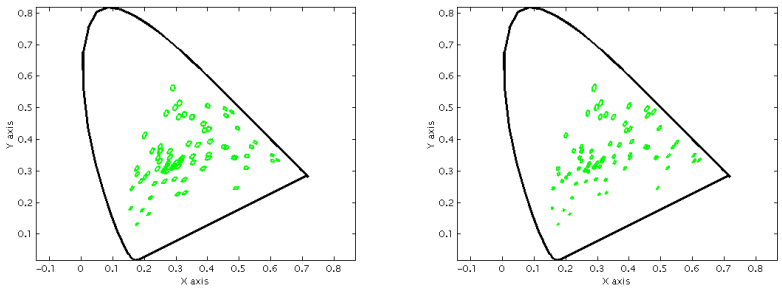

(a) CIELAB ellipses using BFD-P data.

(b) CIELUV ellipses using BFD-P data.

(c) CIEDE00 ellipses using BFD-P data.

(d) OSA-UCS ΔE_E ellipses using BFD-P data.

Figure 3: Computed CIELAB, CIELUV, Riemannized CIEDE00 and OSA-UCS ΔE_E ellipses in the CIE1964 chromaticity diagram (enlarged 1.5 times).

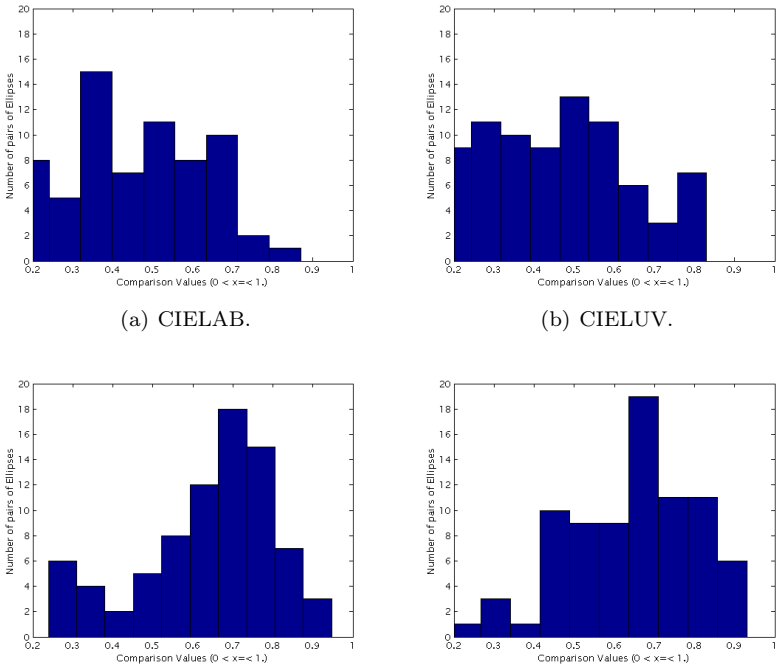

(a) CIELAB. (b) CIELUV.

(c) CIEDE00. (d) OSA-UCS ΔE_E .

Figure 4: Histogram of comparison values of CIELAB, CIELUV, Rie4annized CIEDE00 and OSA-UCS ΔE_E with respet to BFD-P Ellipses. The values lie in the range $0 < x \leq 1$. Higher comparison value indicates better matching between a pair of ellipses.

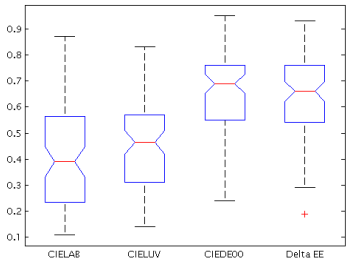

Figure 5: Box plots of ellipse matching values of CIELAB, CIELUV, Riemannized CIEDE00 and OSA-UCS ΔE_E with respect to BFD-P ellipses.

Acknowledgments

The authors would like to give special thanks of gratitude to Dr. Michael Brill for his insightful comments and discussions based upon preliminary results of this research [39]. Similarly, the authors are greatful to the anonymous reviewer for giving us valuable comments and suggestions.

References

[1] R. G. Kuehni, "Threshold color differences compared to super-threshold color differences," Color Res. Appl. **25**, 226–229 (2000).

[2] K. Chickering, "Optimization of the MacAdam modified 1965 friele color-difference formula," J. Optical Society of America **57**, 537 (1967).

[3] CIE, "Recommendations on uniform colour spaces, colour difference equations and psychometric color terms," Tech. Rep. 15, CIE Central Bureau, Vienna (1978).

[4] D. MacAdam, "Visual sensitivities to color differences in daylight," J. Optical Society of America **32**, 247–274 (1942).

[5] W. Brown, "Colour discrimination of twelve observers," J. Optical Society of America **47**, 137–143 (1957).

[6] G. Wyszecki and G. H. Fielder, "New color-matching ellipses," J. Optical Society of America **61**, 1135–1152 (1971).

[7] M. R. Luo and B. Rigg, "Chromaticity-discrimination ellipses for surface colours," Color Res. Appl. **11**, 25–42 (1986).

[8] R. Berns, D. H. Alman, L. Reniff, G. Snyder, and M. Balonon-Rosen, "Visual determination of suprathreshold color-difference tolerances using probit analysis," Color Res. Appl. **16**, 297–316 (1991).

[9] K. Witt, "Geometric relations between scales of small colour differences," Color Res. Appl. **24**, 78–92 (1999).

[10] G. Riemann, "Über die Hypothesen, welche der Geometrie zu Grunde liegen," Abh Königl Ges Wiss Göttingen **12**, 133–152 (1868).

[11] H. von Helmholtz, "Das psychophysische Gesetz auf die Farbunterschiede trichromatischer Auge anzuwenden," Psychol. Physiol. Sinnesorgane **3**, 1–20 (1892).

[12] E. Schrödinger, "Grundlinien einer Theorie der Farbenmetrik im Tagessehen," Annalen der Physik **4**, 397–426 (1920).

[13] W. Stiles, "A modified Helmholtz line element in brightness-colour space," in "Proc. Phys. Soc. London," (1946), pp. 41–65.

[14] J. Vos and P. Walraven, "An analytical description of the line element in the zone fluctuation model of color vision," J. Vision Research **12**, 1345–1365 (1972).

[15] J. Vos, "From lower to higher colour metrics: a historical account," Clinical and Experimental Optometry **89**, 348–360 (2006).

[16] J. Vos and P. Walraven, "Back to Helmholtz," Color Res. Appl. **16**, 355–359 (1991).

[17] G. Wyszecki and W. Stiles, *Color Science: Concepts and Methods, Quantitative Data and Formula* (John Wiley and Sons, New York, 2000), 2nd ed.

[18] M. Luo, G. Cui, and B. Rigg, "The development of the CIE2000 colour difference formula," Color Res. Appl. **26**, 340–350 (2001).

[19] C. Oleari, M. Melgosa, and R. Huertas, "Euclidean colour difference formula for small-medium colour differences in log-compressed OSA-UCS space," J. Optical Society of America **26**, 121–134 (2009).

[20] CIE, "Industrial colour difference evaluation," Tech. Rep. 116, CIE Central Bureau, Vienna (1995).

[21] D. Kim and J. Nobbs, "New weighting functions for the weighted CIELAB colour difference formula," in "Proceedings of AIC Colour," (AIC, Kyoto, 1997), pp. 446–449.

[22] CIE, "Improvement to industrial color–difference evaluation," Tech. Rep. 142, CIE central bureau, Vienna (2001).

[23] J. Gay and R. Hirschler, "Field trials for CIEDE2000: Correlation of visual and instrumental pass/fail decisions in industry." Tech. Rep. ISBN 390190621, 25th, The CIE Session, San Diego (2003).

[24] M. Melgosa, R. Huertas, and R. S. Berns, "Performance of recent advanced color difference fromulae using the standardized residual sum of squares index," J. Optical Society of America **25**, pp. 1828–1834 (2008).

[25] P. Urban, M. R. Rosen, and R. S. Berns, "Embedding non-euclidean color spaces into euclidean color spaces with minimal isometric disagreement," Optical Society of America **27** (2007).

[26] R. G. Kuehni, *Color Space and its Division* (John Wiley and Sons, New York, 2003).

[27] W. Schultze, "The usefulness of colour difference formulas for fixing colour tolerances," in "AIC Proceedings," (1972), pp. 254–265.

[28] D. Judd, "Ideal color space: Curvature of color space and its implications for industrial color tolerances," Palette **29**, 21–28 (1968).

[29] L. Silberstein, "Notes on W.S. Stiles paper entitled : A modified Helmholtz line-element in brightness-colour space," J. Optical Society of America **37**, pp. 292–295 (1947).

[30] C. Alder, K. P. Chaing, T. F. Chong, E. Coates, A. A. Khalili, and B. Rigg, "Uniform chromaticity scales – new experimental data," Society of Dyers and Colurist, UK **98**, 14–20 (1982).

[31] D. R. Pant and I. Farup, "Evaluating color difference formulae by Riemannian metric," in "5th European Conference on Colour in Graphics, Imaging, and Vision, CGIV 2010," (Joensuu, Finland, 2010), p. 497.

[32] G. B. Thomas and R. L. Finney, *Calculus and Analytic Geometry* (Addision-Wesley, Massachusetts, 1988).

[33] H. G. Völz, "Euclidization of the first quadrant of the CIEDE2000 color difference system for the calculation of large color differences," Color Res. Appl. **31**, 5–12 (2006).

[34] G. Sharma, W. Wu, and E. N. Dalal, "The CIEDE2000 color-difference formula: Implementation notes, supplementary test data, and mathematical observations," Color Res. Appl. **30**, 21–30 (2004).

[35] C. Oleari, "Color opponencies in the system of the uniform color scales of the Optical Society of America," J. Optical Society of America **21**, 677–682 (2004).

[36] C. Oleari, "Hypotheses for chromatic opponency functions and their performance on classical psychophysical data," Color Res. Appl. **30**, 31–41 (2005).

[37] R. S. Berns, *Principles of Color Technology* (John Wiley and Sons, New York, 2000).

[38] C. Oleari, "Uniform color space for 10 degree visual field and OSA uniform color scales," J. Optical Society of America **10**, pp. 1490–1498 (1993).

[39] D.R.Pant and I. Farup, "Riemannian formulation of the CIEDE2000 color difference formula," in "18th Color and Imaging Conference," (IS&T, 2010), pp. 103–108.

Appendix: Detailed expressions for the Jacobians

From x, y, Y to X, Y, Z

$$\frac{\partial(X,Y,Z)}{\partial(x,y,Y)} = \begin{bmatrix} \frac{\partial X}{\partial x} & \frac{\partial X}{\partial y} & \frac{\partial X}{\partial Y} \\ \frac{\partial Y}{\partial x} & \frac{\partial Y}{\partial y} & \frac{\partial Y}{\partial Y} \\ \frac{\partial Z}{\partial x} & \frac{\partial Z}{\partial y} & \frac{\partial Z}{\partial Y} \end{bmatrix} = \begin{bmatrix} \frac{Y}{y} & \frac{-xY}{y^2} & \frac{x}{y} \\ 0 & 0 & 1 \\ \frac{-Y}{y} & \frac{(x-1)Y}{y^2} & \frac{1-x-y}{y} \end{bmatrix} \tag{59}$$

From X, Y, Z to L^*, a^*, b^*

$$\begin{aligned} \frac{\partial(L,a,b)}{\partial(X,Y,Z)} &= \begin{bmatrix} \frac{\partial L}{\partial X} & \frac{\partial L}{\partial Y} & \frac{\partial L}{\partial Z} \\ \frac{\partial a}{\partial X} & \frac{\partial a}{\partial Y} & \frac{\partial a}{\partial Z} \\ \frac{\partial b}{\partial X} & \frac{\partial b}{\partial Y} & \frac{\partial b}{\partial Z} \end{bmatrix} \\ &= \begin{bmatrix} 0 & \frac{116}{3}(\frac{1}{Y_r})^{\frac{1}{3}} Y^{\frac{-2}{3}} & 0 \\ \frac{500}{3}(\frac{1}{X_r})^{\frac{1}{3}} X^{\frac{-2}{3}} & \frac{-500}{3}(\frac{1}{Y_r})^{\frac{1}{3}} Y^{\frac{-2}{3}} & 0 \\ 0 & \frac{200}{3}(\frac{1}{Y_r})^{\frac{1}{3}} Y^{\frac{-2}{3}} & \frac{-200}{3}(\frac{1}{Z_r})^{\frac{1}{3}} Z^{\frac{-2}{3}} \end{bmatrix} \end{aligned} \tag{60}$$

From X, Y, Z to L^*, u^*, v^*

$$\frac{\partial(L^*,u^*,v^*)}{\partial(X,Y,Z)} = \begin{bmatrix} \frac{\partial L^*}{\partial X} & \frac{\partial L^*}{\partial Y} & \frac{\partial L^*}{\partial Z} \\ \frac{\partial u^*}{\partial X} & \frac{\partial u^*}{\partial Y} & \frac{\partial u^*}{\partial Z} \\ \frac{\partial v^*}{\partial X} & \frac{\partial v^*}{\partial Y} & \frac{\partial v^*}{\partial Z} \end{bmatrix}, \tag{61}$$

where the calculations of all partial derivatives are as follows:

$$\frac{\partial L^*}{\partial X} = 0, \tag{62a}$$

$$\frac{\partial L^*}{\partial Y} = \frac{116}{3}(\frac{1}{Y_r})^{\frac{1}{3}} Y^{(-2/3)}, \tag{62b}$$

$$\frac{\partial L}{\partial Z} = 0, \tag{62c}$$

$$\frac{\partial u^*}{\partial X} = 13\left(116\left(\frac{Y}{Y_r}\right)^{(1/3)} - 16\right)\left[\frac{60Y+12Z}{(X+15Y+3Z)^2}\right], \tag{62d}$$

$$\begin{aligned}\frac{\partial u^*}{\partial Y} = {} & 13 \times \left(116\left(\frac{Y}{Y_r}\right)^{(1/3)} - 16\right)\left[\frac{-60\mathrm{X}}{(X+15Y+3Z)^2}\right] \\ & + \left[\frac{4X}{(X+15Y+3Z)}\right]\left(\frac{13\times 116(\frac{1}{Y_r})^{\frac{1}{3}} Y^{(-2/3)}}{3}\right) \\ & - \left(\frac{4X_r}{X_r+15Y_r+3Z_r}\right)\left(\frac{13\times 116(\frac{1}{\mathrm{Y_r}})^{\frac{1}{3}} \mathrm{Y}^{(-2/3)}}{3}\right),\end{aligned} \tag{62e}$$

$$\frac{\partial u^*}{\partial Z} = 13\left(116\left(\frac{Y}{Y_r}\right)^{(1/3)} - 16\right)\left[\frac{-12X}{(X+15Y+3Z)^2}\right], \tag{62f}$$

$$\frac{\partial v^*}{\partial X} = 13\left(116\left(\frac{Y}{Y_r}\right)^{(1/3)} - 16\right)\left[\frac{-9\mathrm{Y}}{(X+15Y+3Z)^2}\right], \tag{62g}$$

$$\begin{aligned}\frac{\partial v^*}{\partial Y} = {} & 13\left(116\left(\frac{Y}{Y_r}\right)^{(1/3)} - 16\right)\left[\frac{9\mathrm{X}+27\mathrm{Z}}{(X+15Y+3Z)^2}\right] \\ & + \left[\frac{9\mathrm{Y}}{(X+15Y+3Z)}\right]\left(\frac{13\times 116(\frac{1}{Y_r})^{\frac{1}{3}} Y^{(-2/3)}}{3}\right) \\ & - \left(\frac{9Y_r}{X_r+15Y_r+3Z_r}\right)\left(\frac{13\times 116(\frac{1}{\mathrm{Y_r}})^{\frac{1}{3}} \mathrm{Y}^{(-2/3)}}{3}\right),\end{aligned} \tag{62h}$$

$$\frac{\partial v^*}{\partial Z} = 13\left(116\left(\frac{Y}{Y_r}\right)^{(1/3)} - 16\right)\left[\frac{-27\mathrm{Y}}{(X+15Y+3Z)^2}\right]. \tag{62i}$$

From $L^{'}$, $a^{'}$, $b^{'}$ to L', C', h'

The Jacobian for this transformation is

$$\frac{\partial(L',C',h')}{\partial(L',a',b')} = \begin{bmatrix} \frac{\partial L'}{\partial L'} & \frac{\partial L'}{\partial a'} & \frac{\partial L'}{\partial b'} \\ \frac{\partial C'}{\partial L'} & \frac{\partial C'}{\partial a'} & \frac{\partial C'}{\partial b'} \\ \frac{\partial h'}{\partial L'} & \frac{\partial h'}{\partial a'} & \frac{\partial h'}{\partial b'} \end{bmatrix} = \begin{bmatrix} 1 & 0 & 0 \\ 0 & \frac{\partial C'}{\partial a'} & \frac{\partial C'}{\partial b'} \\ 0 & \frac{\partial h'}{\partial a'} & \frac{\partial h'}{\partial b'} \end{bmatrix}. \tag{63}$$

where the partial derivatives are as follows:

$$\frac{\partial C^{'}}{\partial a^{'}} = \frac{a^{'}}{\sqrt{a'^2 + b'^2}} = \frac{a^{'}}{C'} \tag{64a}$$

$$\frac{\partial C^{'}}{\partial b^{'}} = \frac{b^{'}}{\sqrt{a'^2 + b'^2}} = \frac{b'}{C'} \tag{64b}$$

$$\frac{\partial h^{'}}{\partial a^{'}} = \frac{-b'}{C'^2} \tag{64c}$$

$$\frac{\partial h'}{\partial b^{'}} = \frac{a^{'}}{C'^2}\,. \tag{64d}$$

From L^*, a^*, b^* to L', a', b'

The Jacobian for this transformation is

$$\frac{\partial(L', a', b')}{\partial(L^*, a^*, b^*)} = \begin{bmatrix} \frac{\partial L'}{\partial L^*} & \frac{\partial L'}{\partial a^*} & \frac{\partial L'}{\partial b^*} \\ \frac{\partial a'}{\partial L^*} & \frac{\partial a'}{\partial a^*} & \frac{\partial a'}{\partial b^*} \\ \frac{\partial b'}{\partial L^*} & \frac{\partial b'}{\partial a^*} & \frac{\partial b'}{\partial b^*} \end{bmatrix} = \begin{bmatrix} 1 & 0 & 0 \\ 0 & \frac{\partial a'}{\partial a^*} & \frac{\partial a'}{\partial b^*} \\ 0 & \frac{\partial b'}{\partial a^*} & \frac{\partial b'}{\partial b^*} \end{bmatrix}. \tag{65}$$

$$\frac{\partial a^{'}}{\partial a^*} = \left[(1+G) + \frac{a^{*2}}{C^*}\left(-\frac{1}{4}\frac{7\times 25^7 C^{*5/2}}{(C^{*7}+25^7)^{3/2}}\right)\right], \tag{66a}$$

$$\frac{\partial a^{'}}{\partial b^*} = \frac{a^* b^*}{C^*}\left(-\frac{1}{4}\frac{7\times 25^7 C^{*5/2}}{(C^{*7}+25^7)^{3/2}}\right), \tag{66b}$$

$$\frac{\partial b^{'}}{\partial a^*} = 0 \tag{66c}$$

$$\frac{\partial b'}{\partial b^*} = 1\,. \tag{66d}$$

From L_{OSA}, G, J to L_E, G_E, J_E

$$\frac{\partial(L_E, G_E, J_E)}{\partial(L_{OSA}, G, J)} = \begin{bmatrix} \frac{\partial L_E}{\partial L_{OSA}} & \frac{\partial L_E}{\partial G} & \frac{\partial L_E}{\partial J} \\ \frac{\partial G_E}{\partial L_{OSA}} & \frac{\partial G_E}{\partial G} & \frac{\partial G_E}{\partial J} \\ \frac{\partial J_E}{\partial L_{OSA}} & \frac{\partial J_E}{\partial G} & \frac{\partial J_E}{\partial J} \end{bmatrix}, \tag{67}$$

where the calculation of all partial derivatives are as follows:

$$\frac{\partial L_E}{\partial L_{OSA}} = \frac{10}{a_L + 10 b_L L_{OSA}}, \tag{68a}$$

$$\frac{\partial L_E}{\partial G} = 0, \tag{68b}$$

$$\frac{\partial L_E}{\partial J} = 0, \tag{68c}$$

$$\frac{\partial G_E}{\partial L_{OSA}} = 0, \tag{68d}$$

$$\frac{\partial G_E}{\partial G} = -\left(\frac{C_E}{C_{OSA}} + G \left[\frac{C_{OSA}(10/a_c + 10 b_c C_{OSA}) - C_E}{C_{OSA}^2} \right] \frac{G}{C_{OSA}} \right), \tag{68e}$$

$$\frac{\partial G_E}{\partial J} = -G \left[\frac{C_{OSA}(10/a_c + 10 b_c C_{OSA}) - C_E}{C_{OSA}^2} \right] \frac{J}{C_{OSA}}, \tag{68f}$$

$$\frac{\partial J_E}{\partial L_{OSA}} = 0, \tag{68g}$$

$$\frac{\partial J_E}{\partial G} = -J \left[\frac{C_{OSA}(10/a_c + 10 b_c C_{OSA}) - C_E}{C_{OSA}^2} \right] \frac{G}{C_{OSA}}, \tag{68h}$$

$$\frac{\partial J_E}{\partial J} = -\left(\frac{C_E}{C_{OSA}} + J \left[\frac{C_{OSA}(10/a_c + 10 b_c C_{OSA}) - C_E}{C_{OSA}^2} \right] \frac{J}{C_{OSA}} \right). \tag{68i}$$

From x, y, Y to L_{OSA}

$$\frac{\partial L_{OSA}}{\partial (x, y, Y)} = \frac{\partial L_{OSA}}{\partial Y_0} \begin{bmatrix} \frac{\partial Y_0}{\partial x} & \frac{\partial Y_0}{\partial y} & \frac{\partial Y_0}{\partial Y} \end{bmatrix}, \tag{69}$$

where

$$\frac{\partial L_{OSA}}{\partial Y_0} = 5.9 \left[\frac{1}{3} Y_0^{-2/3} + 0.042 \cdot \frac{1}{3} (Y_0 - 30)^{-2/3} \right] \frac{1}{\sqrt{2}}, \tag{70a}$$

$$\frac{\partial Y_0}{\partial x} = Y(4.4934 \cdot 2x - 4.2760 y - 1.3744), \tag{70b}$$

$$\frac{\partial Y_0}{\partial y} = Y(4.3034 \cdot 2y - 4.2760 x - 2.5643), \tag{70c}$$

$$\frac{\partial Y_0}{\partial Y} = 4.4934 x^2 + 4.3034 y^2 - 4.2760 xy - 1.3744 x - 2.5643 y + 1.8103. \tag{70d}$$

From L_{OSA}, A, B, C to G, J

$$\frac{\partial (G, J)}{\partial (L_{OSA}, A, B, C)} = \begin{bmatrix} \frac{\partial G}{\partial L_{OSA}} & \frac{\partial G}{\partial A} & \frac{\partial G}{\partial B} & \frac{\partial G}{\partial C} \\ \frac{\partial J}{\partial L_{OSA}} & \frac{\partial J}{\partial A} & \frac{\partial J}{\partial B} & \frac{\partial J}{\partial C} \end{bmatrix}, \tag{71}$$

where

$$\frac{\partial G}{\partial L_{OSA}} = T_G \frac{\partial S_G}{\partial L_{OSA}} = T_G \cdot -2 \times 0.764, \tag{72a}$$

$$\frac{\partial J}{\partial L_{OSA}} = T_J \frac{\partial S_J}{\partial L_{OSA}} = T_J \cdot 2 \times 0.57354, \tag{72b}$$

$$\frac{\partial G}{\partial A} = S_G \frac{0.9482}{A}\,, \tag{72c}$$

$$\frac{\partial G}{\partial B} = S_G \frac{-0.9482 - 0.3175}{B}\,, \tag{72d}$$

$$\frac{\partial G}{\partial C} = S_G \frac{0.3175}{C}\,, \tag{72e}$$

$$\frac{\partial J}{\partial A} = S_J \frac{0.1792}{A}\,, \tag{72f}$$

$$\frac{\partial J}{\partial B} = S_J \frac{-0.1792 + 0.9837}{B}\,, \tag{72g}$$

$$\frac{\partial J}{\partial C} = S_J \frac{-0.9837}{C}\,, \tag{72h}$$

where the shorthands

$$T_G = 0.9482[\ln A - \ln(0.9366B)] - 0.3175[\ln B - \ln(0.9807C)], \tag{73a}$$

$$T_J = 0.1792[\ln A - \ln(0.9366B)] + 0.9837[\ln B - \ln(0.9807C)], \tag{73b}$$

have been introduced.

8

Paper D

CIE Uniform Chromaticity Scale Diagram for Measuring Performance of OSA-UCS Delta EE and CIEDE00 formulas

Dibakar Raj Pant and Ivar Farup

Published in

2nd European Workshop on Visual Information Processing (EUVIP)

Paris, France, 5-7 July 2011

IEEE Catalog Number: CFP1006K-CDR ISBN: 978-1-4244-7287-1

CIE UNIFORM CHROMATICITY SCALE DIAGRAM FOR MEASURING PERFORMANCE OF OSA-UCS △EE AND CIEDE00 FORMULAS

Dibakar Raj Pant

Gjøvik University College
The Norwegian Color Research Laboratory
Gjøvik, Norway
and
University Jean Monnet
The Laboratoire Hubert Curien
Saint Etienne, France

Ivar Farup

Gjøvik University College
The Norwegian Color Research Laboratory
Gjøvik, Norway

ABSTRACT

The CIE recommended uniform chromaticity scale (UCS) diagram based on the CIELUV is used to evaluate the non-Euclidean approximate form of CIEDE2000 and the Euclidean ΔE_E colour difference formulas for measuring the visual data. Experimentally observed visual colour difference data in terms of supra threshold ellipses are plotted in the CIELUV u^*, v^* diagram. Similarly, equi-distance ellipses of two formulas are computed and plotted in the same diagram. Performance of these formulas are evaluated by calculating the matching ratio between observed and computed ellipse pairs. Various statistical tests are done for these ratio values. It is found that there is no significant difference between the complex non-Euclidean approximate form of ΔE_{00} and the simple Euclidean ΔE_E.

Index Terms— CIEDE2000, OSA-UCS ΔE_E, ellipses, visual colour difference

1. INTRODUCTION

Among the many colour difference formulas so far developed, the CIEDE2000 [1] and ΔE_E proposed by Oleari [2] based on the OSA-UCS color space are considered more robust and latest. The first one is an improved formula based on the CIELAB color space, resulting in a non-Euclidean metric. The second is the recent Euclidean color difference metric defined in OSA-UCS space with interger values of lightness L in a regular rhombohedron planes [2]. These two color difference formulas are established with different criteria. It is interesting to know how the two color difference formulas perform for measuring the visual data.

The visual data is the experimental color discrimination data derived from visual color difference experiments. They are described by supra threshold ellipses. In general, these data represent the sum of a number of threshold differences along a particular path between two colors called line element [3]. MacAdam [4] was the first to study about discrimination data and from this data he constructed just noticeable difference (JND) ellipses. Later, similar data sets were derived by Brown [5], Wyszecki and Fielder [6]. Similarly, more advanced data sets such as BFD-Perceptibility(BFD-P) [7] were developed based on supra threshold color differences. Bigg and Luo established BFD-P as a standard data set for surface colors represented in the xyY colour space [7]. On the other hand, if we treat a color space as a Riemannian space [8], the ellipses of the approximate form of CIEDE2000 [1] and ΔE_E can be computed in any other colour space, as shown by Pant et. al. [9]. These computed ellipses can be compared with experimentally obtained ellipses. However, comparing ellipses in xy chromaticity scale diagram have limitations due to the large deviation from uniform spacing [10–12].

To compare visual differences, a uniform color space is very important because in such a space a unit change in hue, chroma and lightness are equal. In practice, realization of these scales are difficult. As a result, many uniform color spaces are proposed such as CIELUV [13], ATD [14] OSA 90 [15] and so on. The CIE recommended CIELUV based uniform chromaticity scale (UCS) diagram is developed by projective transform of the CIE tristimulus (XYZ) values. Because of this, the CIELUV chromaticity u^*, v^* follows the property of linearity. Further, the aim of CIELUV space is to map MacAdam's JND ellipses as close to circles, it is more suitable for measuring small colour differences. Since these formulas are optimized to predict visual color differences in their specific colour spaces, it is also desirable to know how well they perform to accomplish such tasks in an independent uniform colour space like CIELUV. In the literature, many other researchers also suggest to use u^*, v^* diagram before drawing any conclusions about visual differences [16–18].

In this paper, the authors compute equi-distance ellipses

of the CIEDE2000 and ΔE_E in the u^*, v^* diagram. The CIEDE2000 is treated here as the Riemannian approximation considering L, C, h coordinates instead of the formula defined L, C, H. The detailed explanation about this can be found in the authors previous article [19]. They are compared with the experimental BFD-P data which is also plotted in the CIELUV chromaticity u^*, v^* diagram. We take an infinitesimal distance to compute the ellipses of approximate CIEDE2000 and ΔE_E formulas. In this process, color difference equations are converted into the differential form. This gives metric tensors (g_{ik}) of above mentioned two formulas. Ellipse parameters, major axes and angle of rotation can be determined by this metric tensor and vice versa. The Jacobian transformation method is used to transform computed metric from one colour space to another. For example, The BFD-P data is plotted in the xy chromaticity diagram. These ellipses give g_{ik} metrics in the xyY space. To obtain ellipses in the u^*, v^* diagram, this metric should be transformed into the CIELUV space through XYZ space. A similar technique is applied to plot the computed ellipses of above formulas in u^*, v^* diagram.

In this paper, a comparison is done between the computed ellipses of each formula and the ellipses obtained from the BFD-P data set in the u^*, v^* chromaticity diagram. The comparison method is shown by Pant et. al. [20]. This method gives a matching ratio, $R \in (0, 1]$, which takes account of variations in the size, the shape and the orientation simultaneously for a pair of ellipses. Statistical tests are also performed between R values of two formulas. Box plot and cumulative distribution function (CDF) of two R values are also plotted. Such plots illustrate the performance of two formulas for measuring visual differences.

2. COLOUR SPACES AND FORMULATION OF ELLIPSE

2.1. Ellipse Formulation

In a Riemannian model of colour space, the infinitesimal distance between any two points is expressed by a differential quadratic form. If we consider the xy chromaticity diagram, such distance is expressed as:

$$ds^2 = g_{11}dx^2 + 2g_{12}dxdy + g_{22}dy^2 \tag{1}$$

where ds is the infinitesimal distance between two points, dx is the difference of x coordinates, dy is the difference of y coordinates and g_{11}, g_{12} and g_{22} are the coefficients of the metric tensor g_{ik}. The ellipse parameters in terms of the coefficents of g_{ik} are expressed as [12]:

$$\begin{aligned} g_{11} &= \frac{1}{a^2}\cos^2\theta + \frac{1}{b^2}\sin^2\theta, \\ g_{12} &= \cos\theta\sin\theta\,(\frac{1}{a^2} - \frac{1}{b^2}), \\ g_{22} &= \frac{1}{a^2}\sin^2\theta + \frac{1}{b^2}\cos^2\theta. \end{aligned} \tag{2}$$

The angle formed by the major axis with the positive x-axis is given by

$$\tan(2\theta) = \frac{2g_{12}}{(g_{11} - g_{22})}. \tag{3}$$

Here $\theta \leq 90^\circ$ when $g_{12} \leq 0$, and otherwise $\theta \geq 90^\circ$. The ellipse parameters can also be derived from the g_{ik} metric tensor by solving the above equations for a, b and θ.

2.2. CIELUV space

The CIELUV in terms of CIE(X,Y,Z) is defined as:

$$\begin{aligned} L^* &= 116\left(\frac{Y}{Y_r}\right)^{\frac{1}{3}} - 16 \\ u^* &= 13L^*\left[\left(\frac{4X}{X+15Y+3Z}\right) - \left(\frac{4X_r}{X_r+15Y_r+3Z_r}\right)\right] \\ v^* &= 13L^*\left[\left(\frac{9Y}{X+15Y+3Z}\right) - \left(\frac{9Y_r}{X_r+15Y_r+3Z_r}\right)\right] \end{aligned} \tag{4}$$

The plot of u^* and v^* values gives us UCS diagram in the CIELUV colour space. Now, to plot xyY space based BFD-P data in u^*v^* diagram, it is necsessary to transform the data from the xyY space to the CIELUV space. This is done by applying Jacobian transformation where the variables of two color spaces are related by continuous partial derivatives. This process takes following steps: First, compute the g_{ik} metric of the data according to Equation (2). Secondly, transform this metric into the XYZ color space and then to the CIELUV space. Thirdly, compute ellipse parameter from the transformed matric tensor and plot it in u^*v^* diagram. In equation form, we write:

$$g_{\Delta E^*_{uv}} = \frac{\partial(X,Y,Z)}{\partial(L,u^*,v^*)}^T \frac{\partial(x,y,Y)}{\partial(X,Y,Z)}^T g_{ik} \frac{\partial(x,y,Y)}{\partial(X,Y,Z)} \frac{\partial(X,Y,Z)}{\partial(L,u^*,v^*)}. \tag{5}$$

where $\partial(x,y,Y)/\partial(X,Y,Z)$ and $\partial(X,Y,Z)/\partial(L,u^*,v^*)$ are the Jacobian metrics. They are expressed as:

$$\begin{bmatrix} dx \\ dy \\ dY \end{bmatrix} = \begin{bmatrix} \frac{\partial x}{\partial X} & \frac{\partial x}{\partial Y} & \frac{\partial x}{\partial Z} \\ \frac{\partial y}{\partial X} & \frac{\partial y}{\partial Y} & \frac{\partial y}{\partial Z} \\ \frac{\partial Y}{\partial X} & \frac{\partial Y}{\partial Y} & \frac{\partial Y}{\partial Z} \end{bmatrix} \begin{bmatrix} dX \\ dY \\ dZ \end{bmatrix} \tag{6}$$

$$\begin{bmatrix} dX \\ dY \\ dZ \end{bmatrix} = \begin{bmatrix} \frac{\partial X}{\partial L^*} & \frac{\partial X}{\partial u^*} & \frac{\partial X}{\partial v^*} \\ \frac{\partial Y}{\partial L^*} & \frac{\partial Y}{\partial u^*} & \frac{\partial Y}{\partial v^*} \\ \frac{\partial Z}{\partial L^*} & \frac{\partial Z}{\partial u^*} & \frac{\partial Z}{\partial v^*} \end{bmatrix} \begin{bmatrix} dL^* \\ du^* \\ dv^* \end{bmatrix} \tag{7}$$

2.3. CIEDE2000 space

The CIEDE2000 formula based on CIELAB space is expressed as a non-Euclidean metric as follows :

$$\begin{aligned} \Delta E_{00} = \Bigg[&\left(\frac{\Delta L'}{k_L S_L}\right)^2 + \left(\frac{\Delta C'}{k_C S_C}\right)^2 + \left(\frac{\Delta H'}{k_H S_H}\right)^2 \\ &+ R_T\left(\frac{\Delta C'}{k_C S_C}\right)\left(\frac{\Delta H'}{k_H S_H}\right)\Bigg]^{0.5} \end{aligned} \tag{8}$$

where, lightness (S_L), chroma (S_C) and hue (S_H) are specific weighting functions. Similarly, (k_L, k_C, k_H), and R_T describe parametric factors for experimental condition and the rotation term respectively. The color coordinates used in the formula are defined from the CIELAB coordinates in the following way:

$$L' = L^*, a' = a^*(1+G), b' = b^*, \tag{9}$$

$$C' = \sqrt{a'^2 + b'^2}, h' = \arctan\frac{b'}{a'} \tag{10}$$

$$G = \frac{1}{2}\left(1 - \sqrt{\frac{C_{ab}^{*7}}{C_{ab}^{*7} + 25^7}}\right), \tag{11}$$

For formulating Remiannian metric of ΔE_{00}, we need to to use $L'C'h'$ coordinates instead of $L'C'H'$ because the coordinate H' does not exist. The metric using $L'C'h'$ coordinates gives us an approximation of ΔE_{00}. Considering $dH' = C'dh'$ [21], the approximate CIEDE2000 color difference metric tensor in the CIELUV space is

$$g_{\Delta E_{00}} = \frac{\partial(X,Y,Z)}{\partial(L^*,u^*,v*)}^T \frac{\partial(L,a^*,b^*)}{\partial(X,Y,Z)}^T \frac{\partial(L',C',h')}{\partial(L,a^*,b^*)}^T \times \begin{bmatrix} (k_L S_L)^{-2} & 0 & 0 \\ 0 & (k_C S_C)^{-2} & \frac{1}{2}C' R_T (k_C S_C k_H S_H)^{-1} \\ 0 & \frac{1}{2}C' R_T (k_C S_C k_H S_H)^{-1} & C'^2 (k_H S_H)^{-2} \end{bmatrix} \times \frac{\partial(L',C',h')}{\partial(L,a^*,b^*)} \frac{\partial(L,a^*,b^*)}{\partial(X,Y,Z)} \frac{\partial(X,Y,Z)}{\partial(L,u^*,v^*)} \tag{12}$$

where, $\partial(L',C',h')/\partial(L,a^*,b^*)$, $\partial(L,a^*,b^*)/\partial(X,Y,Z)$ are the Jacobian metrices. The derivations of these metrices can be found in the paper Pant and Farup [9].

2.4. OSA-UCS based ΔE_E space

The ΔE_E color difference formula based in the log compressed OSA-UCS color space are derived from the original OSA-UCS formula. Their definitions are expressed as follows:

$$L_E = \left(\frac{1}{b_L}\right)\ln\left[1 + \frac{b_L}{a_L}(10 L_{OSA})\right], \tag{13}$$

$$C_E = \left(\frac{1}{b_c}\right)\ln\left[1 + \frac{b_c}{a_c}(10 C_{OSA})\right], \tag{14}$$

$$C_{OSA} = \sqrt{G^2 + J^2}, h = \arctan(\frac{-J}{G}), \tag{15}$$

$$G_E = -C_E\cos(h), J_E = C_E\sin(h) \tag{16}$$

Expressing G_E and J_E in terms of C_{OSA}, we have:

$$G_E = -\frac{C_E G}{C_{OSA}}, J_E = \frac{C_E J}{C_{OSA}} \tag{17}$$

The OSA-UCS color space is also related to the CIEXYZ color space. The details can be found in the paper of Huertas et al. [22]. For calculating the line element at a given point, the log-compressed OSA-UCS formula is written as:

$$(dE_E)^2 = \begin{bmatrix} dL_E & dG_E & dJ_E \end{bmatrix} \begin{bmatrix} 1 & 0 & 0 \\ 0 & 1 & 0 \\ 0 & 0 & 1 \end{bmatrix} \begin{bmatrix} dL_E \\ dG_E \\ dJ_E \end{bmatrix}. \tag{18}$$

Then, in the similar way as mentioned for the CIEDE00, it is transformed to OSA-UCS color space and finally into the CIELUV space. From the transformed metric tensor, we compute JND ellipses in u^*, v^* chromaticity diagram. The computation of ΔE_E metric tensor is published in the previous article [19].

2.5. Ellipse pair matching ratio

The matching ratio to compare a pair of ellipses A and B is expressed as:

$$R = \frac{\text{Area}(A \bigcap B)}{\text{Area}(A \bigcup B)} \tag{19}$$

High value of R gives strong evidence that the two ellipses are closely matched and vice versa.

3. RESULTS

The ellipses of BFD-P, the ΔE_E and the ΔE_{00} in the uniform u^*, v^* chromaticity diagram are shown in Figures 1(a), 1(b), and 1(c) respectively. All the ellipses are computed at constant lightness value ($L^* = 50$). The colour centers for the computed ellipses are taken from the BFD-P data. Around the neutral region the computed and BFD-P ellipses look similar. In the blue region, ellipses of both formulas appear smaller in size than the observed ellipses. Similarly, in comparison to BFD-P, ΔE_{00} ellipses are rotated more in blue and red regions than the ΔE_E. So, the ΔE_E performs better for measuring experimental data in these region. Likewise, ellipses of both formulas are following close pattern to BFD-P in the green part.

Figures 2(a) and 2(b) are the histograms of R values of the ΔE_{00} and the ΔE_E with respect to BFD-P ellipses. The maximum R value of both formulas is approximately .92 where as the lowest value for the ΔE_{00} and the ΔE_E is .25 and .2 respectively. Ellipse pairs having maximum R values are located around neutral colour region. Similarly, in the ΔE_{00} case lowest R are found around blue and red regions while for the ΔE_E it is located in blue-violet region.

Figure 3(a) shows box plot of the R values. In such plots, the median value is marked by the central horizontal lines. The notch indicate the confidence interval of the median, and the box is bounded by the upper and lower quartiles of the grouped data. We can see that both ΔE_{00} and the ΔE_E have similar median values with slight differences. The authors also plotted cumulative distribution function (CDF) of two R values. This function describes the distribution of R values

by taking the sum of each value of R having finte mean and variance. The distribution curves of two sets of R is shown in figure 3(b). They follow the similar continous normal distribution and the maximum difference between two curves is .1. Similarly, the pairwise statistical sign test of R values shows that there is no significant difference between ΔE_{00} and ΔE_E formulas.

4. CONCLUSION

In this paper, the UCS diagram based on CIELUV colour space is used to evaluate two colour difference formulas ΔE_{00} and ΔE_E for measuring the visual data. On the basis of our analysis, the authors can say that statistically, there is no significant difference between the Euclidean ΔE_E and the non-Euclidean CIEDE2000 formulas compared to the BFD-P data set. However, the performance of the CIEDE2000 is found weaker in blue and red region compared to the ΔE_E. It is interesting to note that simple Euclidean ΔE_E metric is not inferior to the complex non-Euclidean mathematical framework of ΔE_{00} for evaluating color differences.

References

[1] M.R Luo, G.H. Cui, and B. Rigg, "The development of the CIE2000 colour difference formula," *Color Res. Appl.*, vol. 26, pp. 340–350, 2001.

[2] C. Oleari, M. Melgosa, and R. Huertas, "Euclidean colour difference formula for small-medium colour differences in log-compressed OSA-UCS space," *J. Optical Society of America*, vol. 26, no. 1, pp. 121–134, 2009.

[3] R. G. Kuehni, "Threshold color differences compared to super-threshold color differences," *Color Res. Appl.*, vol. 25, pp. 226–229, 2000.

[4] D.L MacAdam, "Visual sensitivities to color differences in daylight," *J. Optical Society of America*, vol. 32, pp. 247–274, 1942.

[5] W.R.J. Brown, "Colour discrimination of twelve observers," *J. Optical Society of America*, vol. 47, pp. 137–143, 1957.

[6] G. Wyszecki and G. H. Fielder, "New color-matching ellipses," *J. Optical Society of America*, vol. 61, no. 9, pp. 1135–1152, 1971.

[7] M. R Luo and B. Rigg, "Chromaticity-discrimination ellipses for surface colours," *Color Res. Appl.*, vol. 11, pp. 25–42, 1986.

[8] H. von Helmholtz, "Das psychophysische Gesetz auf die Farbunterschiede trichromatischer Auge anzuwenden," *Psychol. Physiol. Sinnesorgane*, vol. 3, pp. 1–20, 1892.

[9] D.R.Pant and I. Farup, "Riemannian formulation of the CIEDE2000 color difference formula," in *18th Color and Imaging Conference*. November 8-12 2010, pp. 103–108, IS&T.

[10] D. L. MacAdam, "Specification of small chromaticity differences," *Optical Society of America*, vol. 33, no. 4, 1942.

[11] W. R. Brown and D.L. MacAdam, "Visual sensitivities to combined chromaticity and luminance differences," *J. Optical Society of America*, vol. 39, pp. 808–834, 1949.

[12] G. Wyszecki and W.S. Stiles, *Color Science: Concepts and Methods, Quantitative Data and Formula*, John Wiley and Sons, New York, second edition, 2000.

[13] CIE, "Recommendations on uniform colour spaces, colour difference equations and psychometric color terms," Tech. Rep. 15, CIE Central Bureau, Vienna, 1978.

[14] S.L. Guth, R.W. Massof, and T. Benzschawel, "Vector model for normal and dichromatic color vision," *J. Optical Society of America*, vol. 70, pp. 197–212, 1980.

[15] D.L MacAdam, "Redetermination of colors for uniform scales," *J. Optical Society of America*, vol. 7, pp. 113–115, 1990.

[16] M.Mahy, L. Van Eycken, and A. Oosterlinck, "Evaluation of uniform color spaces developed after the adoption of CIELAB and CIELUV," *Color research and application*, vol. 19, no. 2, pp. 105–121, April 1994.

[17] S. Takamura and N. Kobayashi, "Practical extension to CIELUV color space to improve uniformity," in *IEEE, ICIP*, 2002, pp. 393–396.

[18] R. W.G. Hunt, "The challenge of our unknown knowns," in *18th Color Imaging Conference*. November 2010, pp. 280–284, IS&T.

[19] D.R.Pant and I. Farup, "Riemannian formulation and comparison of color difference formulas," *Color Res. Appl.(accepted)*, 2011.

[20] D. R. Pant and I. Farup, "Evaluating color difference formulae by Riemannian metric," in *5th European Conference on Colour in Graphics, Imaging, and Vision, CGIV 2010*, Joensuu, Finland, June 2010, p. 497.

[21] H. G. Völz, "Euclidization of the first quadrant of the CIEDE2000 color difference system for the calculation of large color differences," *Color Res. Appl.*, vol. 31, pp. 5–12, 2006.

[22] R. Huertas, M. Melgosa, and C. Oleari, "Performance of a color-difference formula based on OSA-UCS space using small-medium color differences," *J. Optical Society of America*, vol. 23, no. 9, pp. 2077–2084, 2006.

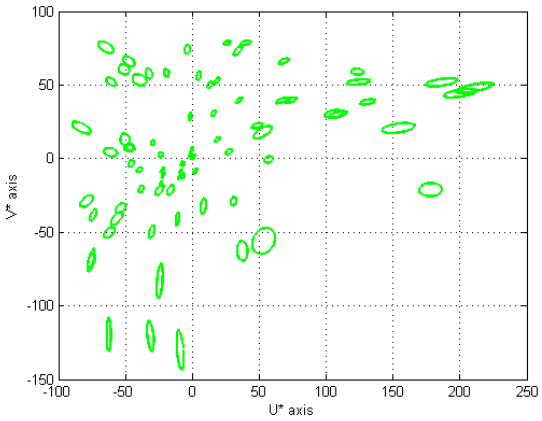

(a) BFD-P ellipses in UCS diagram.

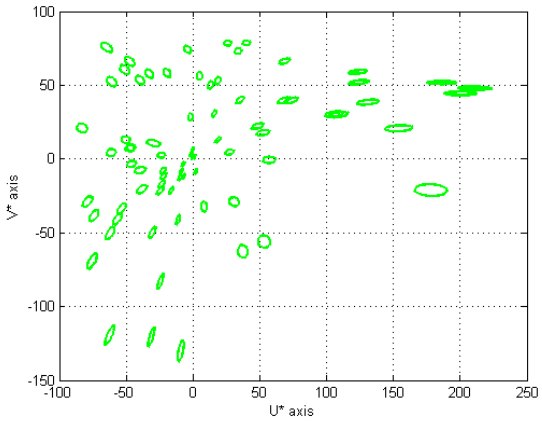

(b) CIEDE00 ellipses in UCS diagram.

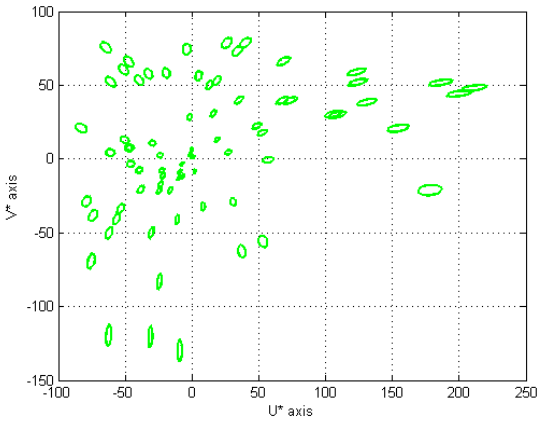

(c) OSA-UCS ΔE_E ellipses in UCS diagram .

Fig. 1. BFD-P and computed OSA-UCS ΔE_E and approximate CIEDE00 ellipses in the u^*v^* chromaticity diagram.

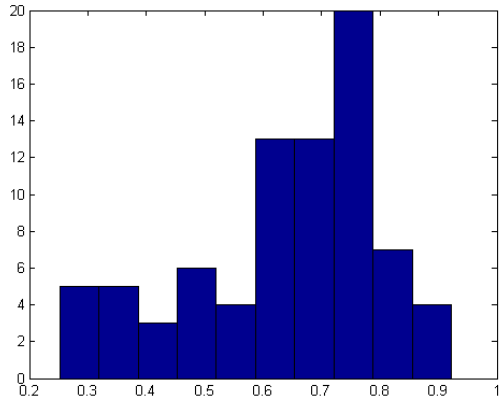

(a) CIEDE00.

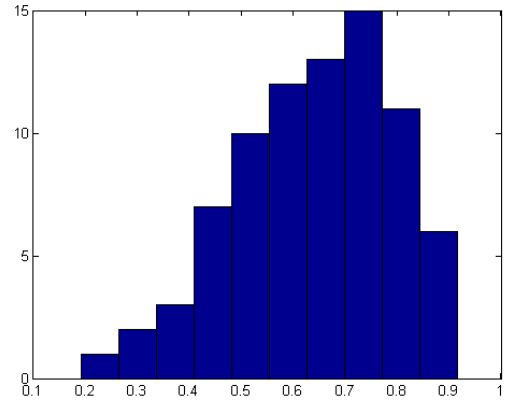

(b) OSA-UCS ΔE_E.

Fig. 2. Histogram of R values of approximate CIEDE00 and OSA-UCS ΔE_E .

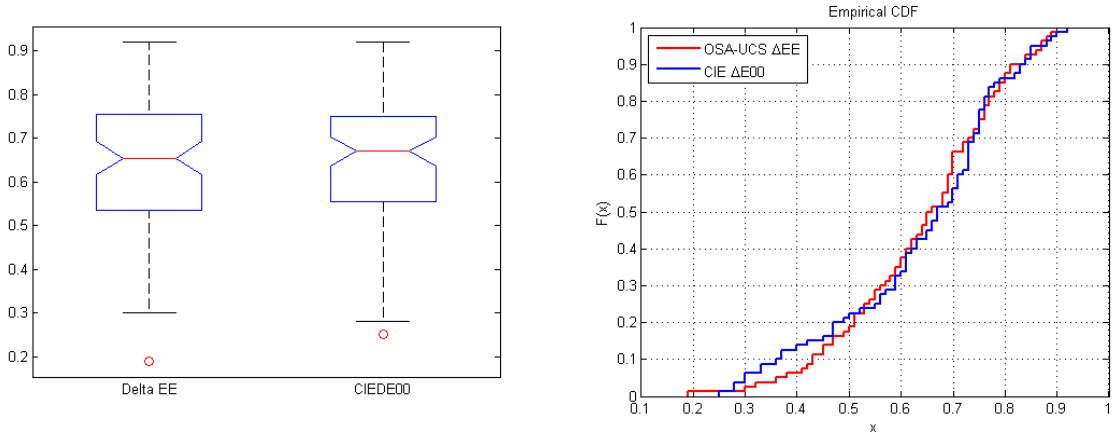

(a) Box plot.

(b) CDF plot.

Fig. 3. Box and CDF plots of R values of approximate CIEDE00 and OSA-UCS ΔE_E .

9

Paper E

Geodesic calculation of color difference formulas and comparison with the Munsell color order system

Dibakar Raj Pant and Ivar Farup

Accepted to publish in

J. Color Research and Application

Geodesic calculation of color difference formulas and comparison with the Munsell color order system

Dibakar Raj Pant[1,2] and Ivar Farup[1]

[1]The Norwegian Color Research Laboratory,
Gjøvik University College, Norway
[2]The Laboratoire Hubert Curien,
University Jean Monnet, Saint Etienne, France

Abstract

Riemannian metric tensors of color difference formulas are derived from the line elements in a color space. The shortest curve between two points in a color space can be calculated from the metric tensors. This shortest curve is called a geodesic. In this paper, the authors present computed geodesic curves and corresponding contours of the CIELAB (ΔE^*_{ab}), the CIELUV (ΔE^*_{uv}), the OSA-UCS (ΔE_E) and an infinitesimal approximation of the CIEDE2000 (ΔE_{00}) color difference metrics in the CIELAB color space. At a fixed value of lightness L^*, geodesic curves originating from the achromatic point and their corresponding contours of the above four formulas in the CIELAB color space can be described as hue geodesics and chroma contours. The Munsell chromas and hue circles at the Munsell values 3, 5 and 7 are compared with computed hue geodesics and chroma contours of these formulas at three different fixed lightness values. It is found that the Munsell chromas and hue circles do not the match the computed hue geodesics and chroma contours of above mentioned formulas at different Munsell values. The results also show that the distribution of color stimuli predicted by the infinitesimal approximation of CIEDE2000 (ΔE_{00}) and the OSA-UCS (ΔE_E) in the CIELAB color space are in general not better than the conventional CIELAB (ΔE^*_{ab}) and CIELUV (ΔE^*_{uv}) formulas.

Introduction

In a color space, color differences are described as the distance between two color points. This distance gives us a quantitative value which in general should agree with perceptual color differences. We can describe such distances from different geometrical points of view. For example, the CIELAB color space is isometric to the Euclidean geometry and the distance is described by the length of a straight line because it has zero curvature everywhere. The distance is no longer the length of a straight line, if we model a color space as a Riemannian space having nonzero curvature. In such a space, the curve having the shortest length or distance between any two points is called a geodesic. The aim of

a color space and a color difference formula is to give a quantitative measure (ΔE) of the perceived color difference correctly. The development of many color spaces and color difference formulas are outcomes of a number of studies of visual color differences based upon the distribution of color matches about a color center [1–5]. Many research works in the past have been continuing to relate theoretical models of color differences with experimental results.

Helmholtz [6] was the first to derive a line element for a color space as a Riemannian space. Schrödinger [7] modified Helmholtz's line element stating that the additivity of brightness is essential for the formulation of the line element. He further argued that surfaces of constant brightness can be derived from the line element in the following way: Suppose that p_1 and p_2 represent the coordinates of two color stimuli in a tristimulus space, p_1 moves away from the origin along a straight line in that space, and p_2 remains fixed. When the geodesic distance between p_1 and p_2 is at minimum, the two given color stimuli are said to be equally bright (which in modern parlance means they are equally luminous). The geodesic between the final p_1 and p_2 is called a constant-brightness geodesic.

Muth et al. [8] used Schrödinger's theoretical conjecture to compute constant brightness color surfaces in the xyY space for FMC1 and FMC2 color difference formulas. The shape of this computed constant brightness surface is consistent with experimental results. Jain [9] determined color distance between two arbitrary colors in the xyY space by computing the geodesics. He also found that geodesics and the constant brightness contours are in agreement with the experimental results of Sanders and Wyszecki [10]. A thorough review of color metrics described with the line element can be found in [11–14].

Wyszecki and Stiles [14] hypothesized that all colors along a geodesic curve originating from a point representing an achromatic stimulus on a surface of constant brightness share the same hue. They further hypothesized that contours of constant chroma can be determined from these geodesics (henceforth called hue geodesics) by taking each point on a chroma contour as the terminus of a hue geodesic such that all the hue geodesics terminate on that chroma contour at the same geodesic distance. This construct has also been used to compute the curvature of color spaces by Lenz at el. [15]. Many other researchers have also pointed out that hue geodesics play a vital role in various color-imaging applications such as color difference preserving maps for uniform color spaces, color-weak correction and color reproduction [15–18].

Hue geodesics and chroma contours of color difference formulas are useful to study the perceptual attributes hue, chroma and lightness predicted by the color difference metric theoretically. A color order system like the Munsell is described in terms of hue, chroma and value to represent scales of constant hue, chroma and lightness. This is analogous to the Riemannian coordinate system. This analogy provides us to compare hue geodesics and chroma contours of a color difference formula in a color space with respect to the Munsell chromas and hues circles computed at a fixed value of lightness which should correspond to the Munsell value. In this sense, in the CIELAB color space, hue geodesics starting from the origin of a^*, b^* at a fixed value of lightness L^* are corresponding to the curves of increasing or decreasing Munsell chroma starting from the same origin at constant hue. In a similar way, chroma contours are closed curves with a constant hue geodesic distance from the achromatic origin. They are also corresponding to changing Munsell hue circles from the origin at the constant

chroma.

The CIELAB and the CIELUV [19] color difference formulas are defined by Euclidean metrics in their own color spaces. The CIEDE2000 [20] is an improved non-Euclidean formula based on the CIELAB color space. The ΔE_E proposed by Oleari [21] is a recent Euclidean color difference formula based on the OSA-UCS color space. However, all these color spaces do not have sufficient perceptual uniformity to fit visual color difference data [22–28]. This leads to difficulty in determining the maximum performance of color difference formulas for measuring visual color differences. Computing hue geodesics and chroma contours of these formulas in a color space help to evaluate their perceptual uniformity theoretically. Similarly, hue geodesics have to be calculated to study distribution of the color stimuli of a color difference formula in a color space. To calculate large color differences, hue geodesics have to calculated [14, 29]. This is even crucial for formulas like the CIEDE2000 because they are developed to measure small color differences, 0–5 ΔE^*_{ab} [20].

In this paper, the authors test the hypothesis described in the fourth paragraph by computing the hue geodesics and chroma contours of four color difference formulas, the CIELAB, the CIELUV, the Riemannian approximation of CIEDE2000 [30] and the OSA-UCS based ΔE_E in the CIELAB color space, and comparing the results to the Munsell color order system. The mathematical construct to compute these hue geodesics and chroma contours using Riemannian metric tensors of each formula are given in the section "The geodesic equation". They are computed at a fixed value of lightness L^*, starting from the origin of the a^*, b^* plane. For the first three color difference metrics above, constant L^* correspond to the constant brightness surface according to Schrödinger's criterion. For the OSA-UCS based ΔE_E it does not correspond to constant brightness due to the definition of the OSA-UCS space. Different hue geodesics and chroma contours of the above four formulas are computed taking three different fixed values of lightness, L^*, corresponding to the Munsell values 3, 5 and 7. The Munsell chromas and hue circles are also plotted in the CIELAB color space at the Munsell values 3, 5 and 7. They are compared with the computed hue geodesics and chromas contours of above mentioned four formulas.

Method

Riemannian Metric

In a Riemannian space, a positive definite symmetric metric tensor g_{ik} is a function that is used to compute the infinitesimal distance between any two points. So, the length of an infinitesimal curve between two points is expressed by a quadratic differential form as given below:

$$ds^2 = g_{11}dx^2 + 2g_{12}dxdy + g_{22}dy^2. \tag{1}$$

The matrix form of Equation (8) is

$$ds^2 = \begin{bmatrix} dx & dy \end{bmatrix} \begin{bmatrix} g_{11} & g_{12} \\ g_{12} & g_{22} \end{bmatrix} \begin{bmatrix} dx \\ dy \end{bmatrix}, \tag{2}$$

and

$$g_{ik} = \begin{bmatrix} g_{11} & g_{12} \\ g_{21} & g_{22} \end{bmatrix} \tag{3}$$

where ds is the distance between two points, dx and dy are differentials of the coordinates x and y and g_{11}, g_{12} and g_{22} are the coefficients of the metric tensor g_{ik}. Here, the coefficient g_{12} is equal to the coefficient g_{21} due to symmetry.

In a two dimensional color space, the metric g_{ik} gives the intrinsic properties of the color space. Specifically, the metric represents chromaticity differences of any two colors measured along any curve of the surface. Riemannian metrics of the CIELAB, the CIELUV, and the OSA-UCS ΔE_E can be derived in a similar way because they are simply identity metrics in their respective color spaces. The Riemannian approximation of CIEDE2000 on the other hand is a non-Euclidean metric, so its Riemannian metric constitute weighting functions, parametric functions and rotation term. The detailed explanation about this as well as the derivation of Riemannian metrics of above color difference formulas can be found in the authors' previous article [30].

Jacobian Transformation

The quantity ds^2 in Equation (1) is called the first fundamental form and it gives the metric properties of a surface. Now, suppose that x and y are related to another pair of coordinates u and v. The metric tensor g_{ik} can be expressed in terms of the new coordinates as g'_{ik}. In analogy with Equation (3), it is written as:

$$g'_{ik} = \begin{bmatrix} g'_{11} & g'_{12} \\ g'_{21} & g'_{22} \end{bmatrix}. \tag{4}$$

Now, the new metric tensor g'_{ik} is related to g_{ik} via the matrix equation as follows:

$$\begin{bmatrix} g'_{11} & g'_{12} \\ g'_{21} & g'_{22} \end{bmatrix} = \begin{bmatrix} \frac{\partial x}{\partial u} & \frac{\partial x}{\partial v} \\ \frac{\partial y}{\partial u} & \frac{\partial y}{\partial v} \end{bmatrix}^T \begin{bmatrix} g_{11} & g_{12} \\ g_{21} & g_{22} \end{bmatrix} \begin{bmatrix} \frac{\partial x}{\partial u} & \frac{\partial x}{\partial v} \\ \frac{\partial y}{\partial u} & \frac{\partial y}{\partial v} \end{bmatrix}, \tag{5}$$

where the superscript T denotes the matrix transpose, and the matrix

$$J = \frac{\partial(x, y)}{\partial(u, v)} = \begin{bmatrix} \frac{\partial x}{\partial u} & \frac{\partial x}{\partial v} \\ \frac{\partial y}{\partial u} & \frac{\partial y}{\partial v} \end{bmatrix} \tag{6}$$

is the Jacobian matrix for the coordinate transformation, or, simply, the Jacobian. Applying the Jacobian method, one can transform color vectors and metric tensors from one color space to another space easily. For example, the CIELUV metric tensor can be transformed into the CIELAB color space by computing the following Jacobians:

$$g_{\Delta E^*_{uv}} = \frac{\partial(X, Y, Z)}{\partial(L^*, a^*, b^*)}^T \frac{\partial(L^*, u^*, v^*)}{\partial(X, Y, Z)}^T I \frac{\partial(L^*, u^*, v^*)}{\partial(X, Y, Z)} \frac{\partial(X, Y, Z)}{\partial(L^*, a^*, b^*)} \tag{7}$$

where $\partial(X, Y, Z)/\partial(L^*, a^*, b^*)$ and $\partial(L^*, u^*, v^*)/\partial(X, Y, Z)$ are the Jacobian metrics and I is an identity matrix in Equation (7). For a detailed derivation of the Jacobians involved, it is referred to the authors'previous paper [30].

The Geodesic Equation

The line element is often written as:

$$ds^2 = g_{ik} dx^i dx^k. \tag{8}$$

Here, Einstein's summation convention which indicates summation over repeated indices, $a^i b_i = \sum_i a^i b_i$ is used. If we consider two points p_1 and p_2, the distance between the two points along a given path is given by the line integral:

$$s = \int_{p_1}^{p_2} ds = \int_{p_1}^{p_2} (g_{ik} dx^i dx^k)^{\frac{1}{2}}. \tag{9}$$

The shortest distance between p_1 and p_2 can be obtained by minimizing s with respect to the path. This path is called the geodesic. Using variational calculus approach and introducing the Lagrangian $L[dx^i/d\lambda, x^i] = \sqrt{g_{ik}\, dx^i/d\lambda\, dx^k/d\lambda}$, Equation (9) in terms of the variation of distance s with path is

$$\delta s = \int_{p_1}^{p_2} \delta L \; d\lambda. \tag{10}$$

where λ is a variable that parametrizes the path. The distance s will be minimum when $\delta s = 0$. From Equation (10) with the criteria of minima, we can obtain the Euler-Lagrange equation in the following form (the detail mathematical derivations can be found in Cohen's text [31]):

$$\frac{\partial L}{\partial x^i} - \frac{d}{d\lambda}\left(\frac{\partial L}{\partial (dx^i/d\lambda)}\right) = 0 \tag{11}$$

From Equation (11), the geodesic equation is derived and is expressed as below:

$$\frac{d^2 x^i}{ds^2} + \Gamma^i_{jk} \frac{dx^j}{ds} \frac{dx^k}{ds} = 0. \tag{12}$$

where Γ^i_{jk} are called Christoffel symbols and are defined in terms of the metric tensor as follows:

$$\Gamma^i_{jk} = \frac{1}{2} g^{i\nu} \left[\frac{\partial g_{j\nu}}{\partial x^k} + \frac{\partial g_{k\nu}}{\partial x^j} - \frac{\partial g_{jk}}{\partial x^\nu} \right]. \tag{13}$$

Here, $g^{i\nu}$ is the inverse of the metric $g_{i\nu}$ satisfying $g^{i\nu} g_{k\nu} = \delta^i_k$. Here, δ^i_k is the Kronecker delta which vanishes for $i \neq k$. Equation (12) can be written in terms of the first order ordinary differential equations as follows:

$$\begin{aligned} \frac{dx^i}{ds} &= u^i \\ \frac{du^i}{ds} &= -\Gamma^i_{jk} u^j u^k \end{aligned} \tag{14}$$

In two dimensions, for $\Gamma^i_{jk}(i, j, k = 1, 2)$, Equation (14) is expressed as:

$$\begin{aligned} \frac{dx^1}{ds} &= u^1 \\ \frac{dx^2}{ds} &= u^2 \\ \frac{du^1}{ds} &= -\Gamma^1_{11}(u^1)^2 - 2\Gamma^1_{12} u^1 u^2 - \Gamma^1_{22}(u^2)^2 \\ \frac{du^2}{ds} &= -\Gamma^2_{11}(u^1)^2 - 2\Gamma^2_{12} u^1 u^2 - \Gamma^2_{22}(u^2)^2 \end{aligned} \tag{15}$$

where, the superscript in italics are indices.

The Geodesic Grid Construction

Differential equations as given in Equation (15) need to be solved to compute the hue geodesics as well as the chroma contours of the CIELAB, the CIELUV, the Riemannized ΔE_{00} and the ΔE_E color difference formulas in the CIELAB color space. Analytical solutions for these equations are complex due to their nonlinear nature. The authors use the Runge-Kutta numerical method for computing the hue geodesics and chroma contours of above color difference formulas in the CIELAB color space. This method gives a solution to increase the accuracy of the integration. The step size is taken 10^{-4} to balance a trade off between rounding error and truncation error. Centered difference formulas are used to calculate the partial derivatives of the metric tensors in the expression for the Christoffel symbols in Equation (14).

Hue geodesics of these color difference formulas start from the origin of a^*, b^* to different directions in the CIELAB color space with a fixed value of L^* and they are spaced from each other at constant intervals. In a similar way, chroma contours start from the a^*, b^* origin. They are also evenly spaced along the hue geodesic distance. The hue geodesics and chroma contours form the geodesic grids of the above four color difference formulas.

Results and Discussion

Geodesic grids of four color difference formulas, the CIELAB, the CIELUV, the Riemannized ΔE_{00} and the ΔE_E are computed and drawn in the CIELAB color space by using the technique described in the previous section. The Munsell color order system is used to compare these computed hue geodesics and chroma contours. Figures 1(a)–1(c) show the Munsell chromas and hue circles at the Munsell value 3, 5 and 7. Figures 2, 3 and 4 show the hue geodesics and chroma contours of the CIELAB, the CIELUV, the Riemannized ΔE_{00} and the ΔE_E computed at $L = 30/50/70$, which correspond to the Munsell value 3, 5 and 7 respectively.

The CIELAB formula is defined as a Euclidean metric in the CIELAB color space, so its hue geodesics and chroma contours are straight lines and circles. They are compared with the Munsell chromas and hue circles at different Munsell values as shown in Figures 2(a), 3(a) and 4(a). The computed hue geodesics intersect the Munsell chromas around yellow, green and blue areas. In the red region of the CIELAB space, the hue geodesics follow the same directions as the Munsell chromas. However, the Munsell chromas are curved at high chroma whereas the hue geodesics of the CIELAB formula are straight in the same region. The chroma contours also vary from the Munsell hue circles at the Munsell value 5 and 7, but at the value 3, the chroma contours are closer to the Munsell hue circles at the a^*, b^* origin and the central region of the CIELAB color space.

The CIELUV hue geodesics and chroma contours tend to agree more with the Munsell chromas and hue circles than the ones predicted by the CIELAB formula. But, the geodesic grids of the CIELUV formula do not cover the Munsell chromas and hue circles due to integration instability. It can be seen in Figures 2(b), 3(b) and 4(b). In this case, hue geodesics predicted by the CIELUV formula intersect the Munsell chromas mostly in the third quadrant of the CIELAB space. This result indicates that the CIELUV hue geodesics and

the Munsell chroma differ in the blue-green region of the CIELAB color space. The CIELUV hue geodesics also follow the curvature pattern of the Munsell chromas, and their directions in the red and yellow regions of the CIELAB space are very close to the Munsell chromas. Chroma contours of the CIELUV formula appear elliptical. They are also similar to the Munsell hue circles at the a^*, b^* origin and the central region. However, they do not comply fully in accordance with the Munsell hue circles in the rest of the CIELAB color space.

The Riemannized ΔE_{00} hue geodesics and chroma contours begin from near the a^*, b^* origin. This is due to the nonexistence of the Riemannian metric at $a^* = b^* = 0$. The detailed discussion about difficulty for getting Riemannian metric of the CIEDE2000 can be found in the article of Pant and Farup [30]. Geodesic grids of the Riemannized ΔE_{00} and their comparison with the Munsell hue and chromas at the different Munsell values are shown in Figures 2(c), 3(c) and 4(c). The hue geodesics are more consistent with the Munsell chromas than the hue geodesics predicted by the CIELAB and the CIELUV metrics. However, they do not follow the curvature pattern of the Munsell chroma in the red and yellow regions of the CIELAB color space. In the blue and violet regions, hue geodesics are sharply curved. They are also changing direction of curvature on their path for intermediate chromas in the CIELAB color space (around $C^* \approx 20$). The chroma contours are elliptical in the central region of the CIELAB color space. Their shapes also diverge from circular to notch on their path in the blue and violet regions. In general, they do not match the Munsell hue circles. The authors found that changing direction of hue geodesics along their path as well as the elliptical shape of chroma contours in the central region are due to the G parameter in the CIEDE2000 formula [20]. Figure 5 shows the hue geodesic and chroma contours of the Riemannized ΔE_{00} setting the value of $G = 0$. This improves the problems of the changing direction of the hue geodesics and the elliptical shape of the chroma contours except in the blue region of the CIELAB space. However, the rotation term of the CIEDE2000 formula is accountable for the sharply curved hue geodesics as well as the shifting of chroma contours in the blue region. This finding suggests that correcting chroma in the blue region of the color space can have a diverse effect on the whole color space.

The OSA-UCS based ΔE_E geodesic grid looks somewhat similar to the CIELUV geodesic grid. Figures 2(d), 3(d) and 4(d) show the ΔE_E hue geodesics and chroma contours. They are following more closely to the direction of the Munsell chromas and hue circles. In the blue region, the hue geodesics intersect the planes of the Munsell chroma. Likewise, the shape of ΔE_E chroma contours are similar to the ones predicted by the CIELUV formula, but they appear to be more correct. Chroma contours are similar to the Munsell hue circles in the achromatic region of the CIELAB color space. In this case also, the ΔE_E predicted chroma contours are not matching the Munsell hue circles in the other parts of the CIELAB color space.

Conclusion

Hue geodesics and chroma contours of color difference metrics can be computed in any desired color space with the known Riemannian metric tensors. This technique is successfully shown by computing geodesic grids of the CIELAB,

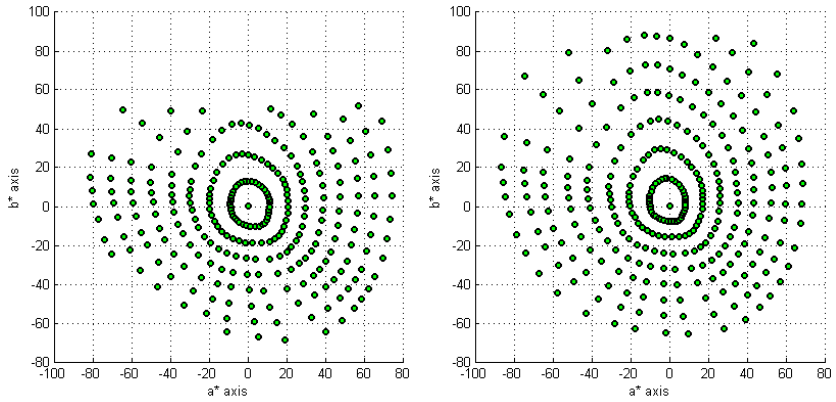

(a) Munsell chromas and hues at value 3. (b) Munsell chromas and hues at value 5.

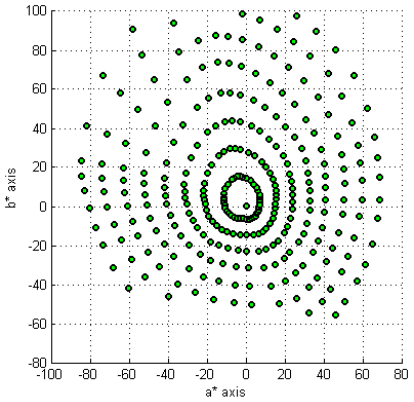

(c) Munsell chromas and hues at value 7.

Figure 1: Munsell chromas and hues at different Munsell values.

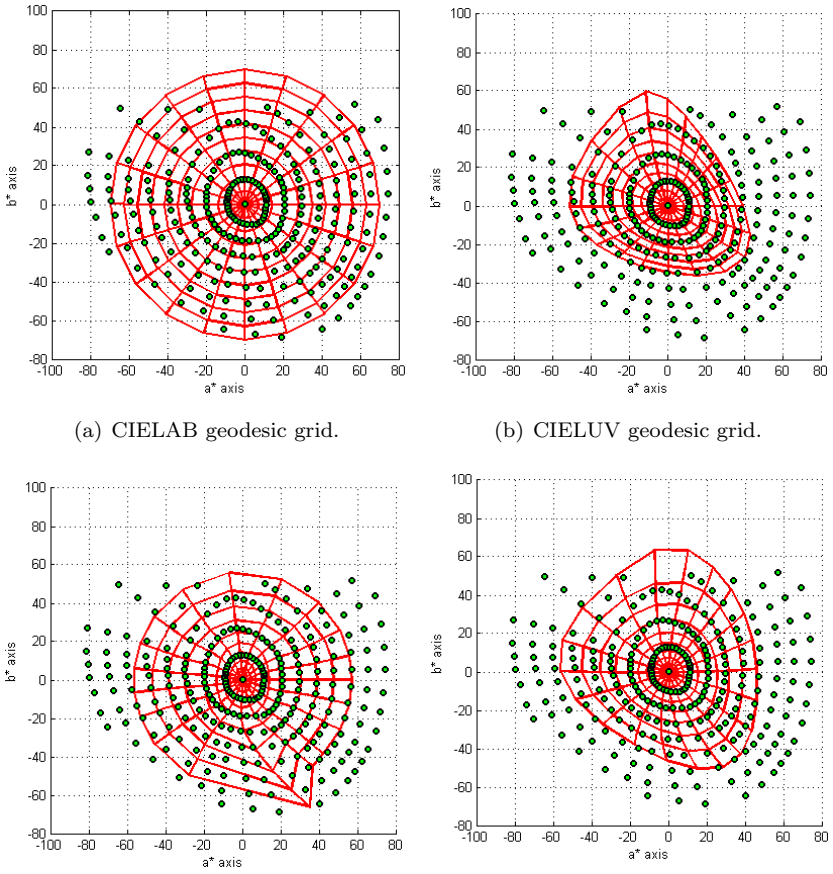

(a) CIELAB geodesic grid.

(b) CIELUV geodesic grid.

(c) Riemannized CIEDE00 geodesic grid.

(d) OSA-UCS ΔE_E geodesic grid.

Figure 2: Computed geodesic grids of CIELAB, CIELUV, Riemannized CIEDE00 and OSA-UCS ΔE_E in the CIELAB space and compared with the Munsell chromas and hues at the Munsell value 3.

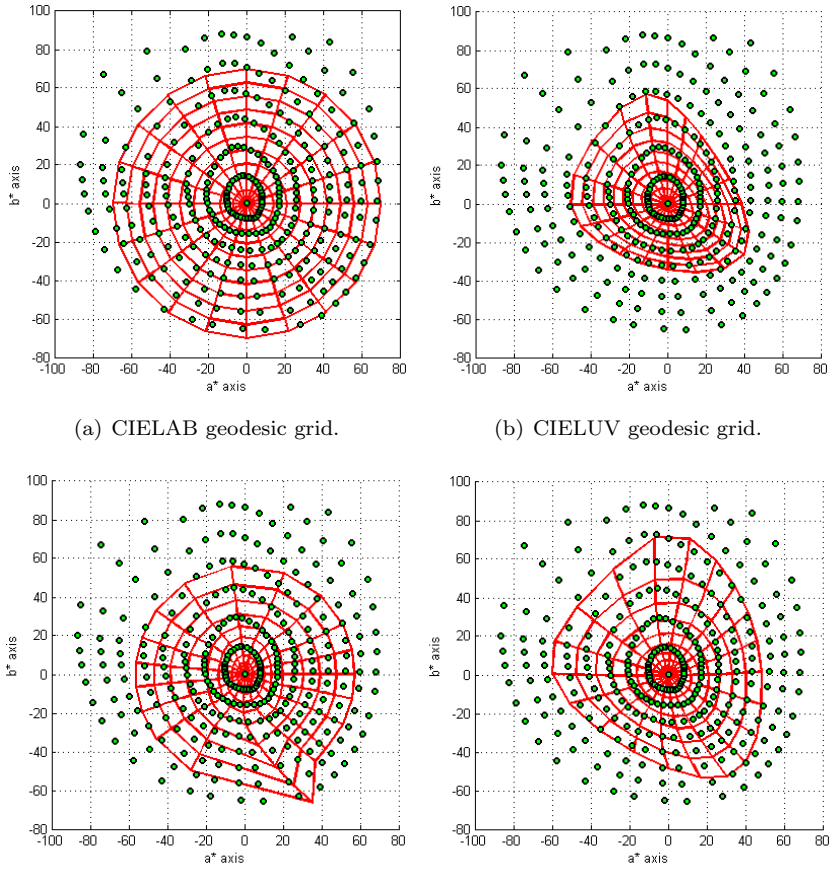

(a) CIELAB geodesic grid.

(b) CIELUV geodesic grid.

(c) Riemannized CIEDE00 geodesic grid.

(d) OSA-UCS ΔE_E geodesic grid.

Figure 3: Computed geodesic grids of CIELAB, CIELUV, Riemannized CIEDE00 and OSA-UCS ΔE_E in the CIELAB space and compared with the Munsell chromas and hues at the Munsell value 5.

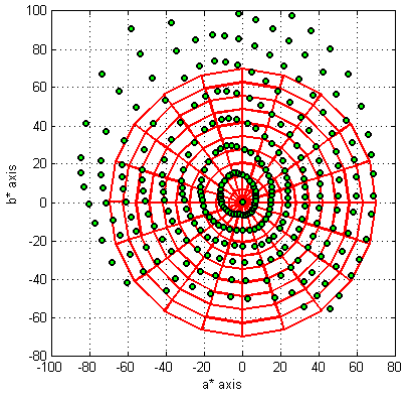

(a) CIELAB geodesic grid.

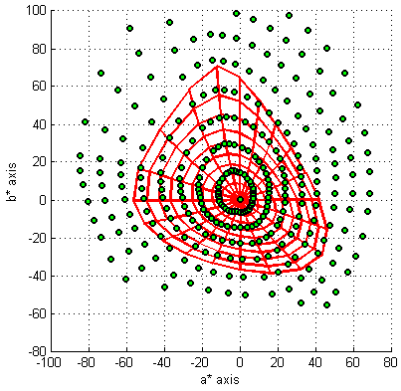

(b) CIELUV geodesic grid.

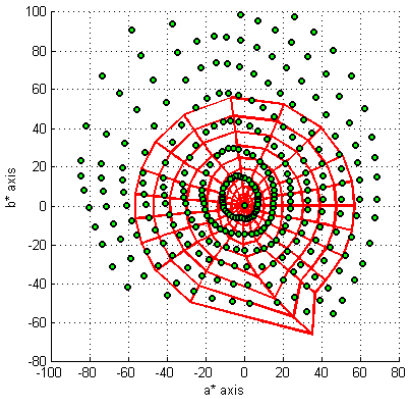

(c) Riemannized CIEDE00 geodesic grid.

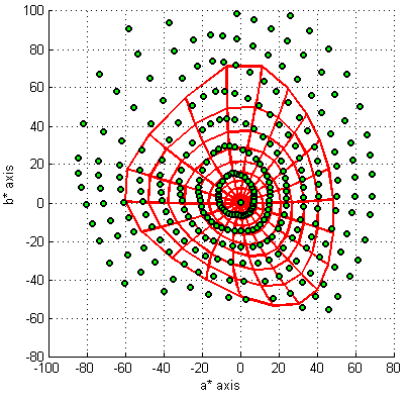

(d) OSA-UCS ΔE_E geodesic grid.

Figure 4: Computed geodesic grids of CIELAB, CIELUV, Riemannized CIEDE00 and OSA-UCS ΔE_E in the CIELAB space and compared with the Munsell chromas and hues at the Munsell value 7.

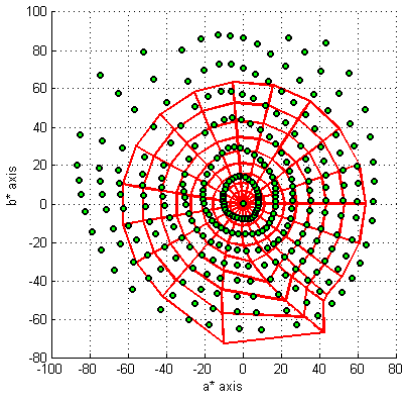

Figure 5: Riemannized CIEDE00 geodesic grid with $G = 0$.

CIELUV, Riemannized CIEDE00 and OSA-UCS ΔE_E color difference formulas with the fixed value of lightness L^* in the CIELAB color space. Comparisons of the geodesic grids of these formulas with the Munsell hues and chromas at the Munsell values 3, 5 and 7 show that none of these four formulas can precisely fit the Munsell data. It is interesting to note that the latest color difference formulas like the OSA-UCS ΔE_E and the Riemannized CIEDE2000 do not show better performance to predict hue geodesics and chroma contours than the conventional CIELAB and CIELUV color difference formulas. These findings also suggest that the distribution of hue geodesics and chroma contours of the above four color difference formulas are weak to predict perceptual color attributes in all over the color space even though their quantitative color difference measures are good.

Acknowledgments

The authors are grateful to the anonymous reviewers for their valuable comments and suggestions.

References

[1] D. MacAdam, "Visual sensitivities to color differences in daylight," J. Optical Society of America **32**, 247–274 (1942).

[2] W. Brown, "Colour discrimination of twelve observers," J. Optical Society of America **47**, 137–143 (1957).

[3] M. R. Luo and B. Rigg, "Chromaticity-discrimination ellipses for surface colours," Color Res. Appl. **11**, 25–42 (1986).

[4] R. Berns, D. H. Alman, L. Reniff, G. Snyder, and M. Balonon-Rosen, "Visual determination of suprathreshold color-difference tolerances using probit analysis," Color Res. Appl. **16**, 297–316 (1991).

[5] K. Chickering, "Optimization of the MacAdam modified 1965 friele color-difference formula," J. Optical Society of America **57**, 537 (1967).

[6] H. von Helmholtz, "Das psychophysische Gesetz auf die Farbunterschiede trichromatischer Auge anzuwenden," Psychol. Physiol. Sinnesorgane **3**, 1–20 (1892).

[7] E. Schrödinger, "Grundlinien einer Theorie der Farbenmetrik im Tagessehen," Annalen der Physik **4**, 397–426 (1920).

[8] E. J. Muth and C. G. Persels, "Constant-brightness surfaces generated by several color-difference formulas," Optical Society of America **61**, 1152–1154 (1971).

[9] A. K. Jain, "Color distance and geodesics in color 3 space," J. Optical Society of America **62**, 1287–1291 (1972).

[10] C. L. Sanders and G. Wyszecki, "Corrleate for lightness in terms of cie-tristimulus values. part i," J. Optical Society of America **47**, 398–404 (1957).

[11] J. Vos and P. Walraven, "An analytical description of the line element in the zone fluctuation model of color vision," J. Vision Research **12**, 1345–1365 (1972).

[12] J. Vos, "From lower to higher colour metrics: a historical account," Clinical and Experimental Optometry **89**, 348–360 (2006).

[13] J. Vos and P. Walraven, "Back to Helmholtz," Color Res. Appl. **16**, 355–359 (1991).

[14] G. Wyszecki and W. Stiles, *Color Science: Concepts and Methods, Quantitative Data and Formula* (John Wiley and Sons, New York, 2000), 2nd ed.

[15] T. Kohei, J. Chao, and R. Lenz, "On curvature of color spaces and its implications," in "5th European Conference on Colour in Graphics, Imaging, and Vision, CGIV 2010," (2010).

[16] J. Chao, I. Osugi, and M. Suzuki, "On definitions and construction of uniform color space," in "2nd European Conference on Colour in Graphics, Imaging and Vision (CGIV 2004)," (2004), pp. 55–60.

[17] J. Chao, R. Lenz, D. Matsumoto, and T. Nakamura, "Riemann geometry for color characterization and mapping," in "In: Proc. CGIV , IS&T, Springfield," (2008).

[18] S. Ohshima, R. Mochizuki, J. Chao, and R. Lenz, "Colour reproduction using riemann normal coordinates," in ""Computational Color Imaging " 2nd International workshop , CCIW," (Springer-Verlag, 2009), pp. 140–149.

[19] CIE, "Recommendations on uniform colour spaces, colour difference equations and psychometric color terms," Tech. Rep. 15, CIE Central Bureau, Vienna (1978).

[20] M. Luo, G. Cui, and B. Rigg, "The development of the CIE2000 colour difference formula," Color Res. Appl. **26**, 340–350 (2001).

[21] C. Oleari, M. Melgosa, and R. Huertas, "Euclidean colour difference formula for small-medium colour differences in log-compressed OSA-UCS space," J. Optical Society of America **26**, 121–134 (2009).

[22] CIE, "Industrial colour difference evaluation," Tech. Rep. 116, CIE Central Bureau, Vienna (1995).

[23] D. Kim and J. Nobbs, "New weighting functions for the weighted CIELAB colour difference formula," in "Proceedings of AIC Colour," (AIC, Kyoto, 1997), pp. 446–449.

[24] CIE, "Improvement to industrial color–difference evaluation," Tech. Rep. 142, CIE central bureau, Vienna (2001).

[25] J. Gay and R. Hirschler, "Field trials for CIEDE2000: Correlation of visual and instrumental pass/fail decisions in industry." Tech. Rep. ISBN 390190621, 25th, The CIE Session, San Diego (2003).

[26] M. Melgosa, R. Huertas, and R. S. Berns, "Performance of recent advanced color difference fromulae using the standardized residual sum of squares index," J. Optical Society of America **25**, pp. 1828–1834 (2008).

[27] P. Urban, M. R. Rosen, and R. S. Berns, "Embedding non-euclidean color spaces into euclidean color spaces with minimal isometric disagreement," Optical Society of America **27** (2007).

[28] R. G. Kuehni, *Color Space and its Division* (John Wiley and Sons, New York, 2003).

[29] V. H. G., "Die Berechnung grosser farbabst ́ande in nichteuklidischen Farbr ́aumen." Die Farbe **44**, 1–45 (1998).

[30] D.R.Pant and I. Farup, "Riemannian formulation and comparison of color difference formulas," Color Res. Appl.(accepted) (2011).

[31] H. Cohen, *Mathematics for Scientists and Engineers* (Prentice-Hall International Editions, 1992).

Part III

Appendix

Appendix A

Detailed Expressions for the Jacobians

The detail expressions of Jacobian metrics are given in this appendix.

A.1 From x, y, Y to X, Y, Z

$$\frac{\partial(X,Y,Z)}{\partial(x,y,Y)} = \begin{bmatrix} \frac{\partial X}{\partial x} & \frac{\partial X}{\partial y} & \frac{\partial X}{\partial Y} \\ \frac{\partial Y}{\partial x} & \frac{\partial Y}{\partial y} & \frac{\partial Y}{\partial Y} \\ \frac{\partial Z}{\partial x} & \frac{\partial Z}{\partial y} & \frac{\partial Z}{\partial Y} \end{bmatrix} = \begin{bmatrix} \frac{Y}{y} & \frac{-xY}{y^2} & \frac{x}{y} \\ 0 & 0 & 1 \\ \frac{-Y}{y} & \frac{(x-1)Y}{y^2} & \frac{1-x-y}{y} \end{bmatrix} \tag{A.1}$$

A.2 From x, y, Y to L, a^*, b^*

$$
\begin{aligned}
(dE^*_{ab})^2 = &\begin{bmatrix} dx \\ dy \\ dY \end{bmatrix}^T \begin{bmatrix} \frac{Y}{y} & \frac{-xY}{y^2} & \frac{x}{y} \\ 0 & 0 & 1 \\ \frac{-Y}{y} & \frac{(x-1)Y}{y^2} & \frac{1-x-y}{y} \end{bmatrix} \times \\
&\begin{bmatrix} 0 & \frac{116}{3}(\frac{1}{Y_r})^{\frac{1}{3}} Y^{\frac{-2}{3}} & 0 \\ \frac{500}{3}(\frac{1}{X_r})^{\frac{1}{3}} X^{\frac{-2}{3}} & \frac{-500}{3}(\frac{1}{Y_r})^{\frac{1}{3}} Y^{\frac{-2}{3}} & 0 \\ 0 & \frac{200}{3}(\frac{1}{Y_r})^{\frac{1}{3}} Y^{\frac{-2}{3}} & \frac{-200}{3}(\frac{1}{Z_r})^{\frac{1}{3}} Z^{\frac{-2}{3}} \end{bmatrix}^T \times \\
&\begin{bmatrix} 1 & 0 & 0 \\ 0 & 1 & 0 \\ 0 & 0 & 1 \end{bmatrix} \begin{bmatrix} 0 & \frac{116}{3}(\frac{1}{Y_r})^{\frac{1}{3}} Y^{\frac{-2}{3}} & 0 \\ \frac{500}{3}(\frac{1}{X_r})^{\frac{1}{3}} X^{\frac{-2}{3}} & \frac{-500}{3}(\frac{1}{Y_r})^{\frac{1}{3}} Y^{\frac{-2}{3}} & 0 \\ 0 & \frac{200}{3}(\frac{1}{Y_r})^{\frac{1}{3}} Y^{\frac{-2}{3}} & \frac{-200}{3}(\frac{1}{Z_r})^{\frac{1}{3}} Z^{\frac{-2}{3}} \end{bmatrix} \times \\
&\begin{bmatrix} \frac{Y}{y} & \frac{-xY}{y^2} & \frac{x}{y} \\ 0 & 0 & 1 \\ \frac{-Y}{y} & \frac{(x-1)Y}{y^2} & \frac{1-x-y}{y} \end{bmatrix} \begin{bmatrix} dx \\ dy \\ dY \end{bmatrix}
\end{aligned}
\tag{A.2}
$$

Here, all Jacobian matrices and their transposes are $\frac{\partial(X,Y,Z)}{\partial(x,y,Y)}^T \frac{\partial(L,a^*,b^*)}{\partial(X,Y,Z)}^T I \frac{\partial(L,a^*,b^*)}{\partial(X,Y,Z)} \frac{\partial(X,Y,Z)}{\partial(x,y,Y)}$.

A.3 From X, Y, Z to L^*, u^*, v^*

$$
\frac{\partial(L^*,u^*,v^*)}{\partial(X,Y,Z)} = \begin{bmatrix} \frac{\partial L^*}{\partial X} & \frac{\partial L^*}{\partial Y} & \frac{\partial L^*}{\partial Z} \\ \frac{\partial u^*}{\partial X} & \frac{\partial u^*}{\partial Y} & \frac{\partial u^*}{\partial Z} \\ \frac{\partial v^*}{\partial X} & \frac{\partial v^*}{\partial Y} & \frac{\partial v^*}{\partial Z} \end{bmatrix}, \tag{A.3}
$$

where the calculations of all partial derivatives are as follows:

$$\frac{\partial L^*}{\partial X} = 0, \tag{A.4a}$$

$$\frac{\partial L^*}{\partial Y} = \frac{116}{3}(\frac{1}{Y_r})^{\frac{1}{3}} Y^{(-2/3)}, \tag{A.4b}$$

$$\frac{\partial L}{\partial Z} = 0, \tag{A.4c}$$

$$\frac{\partial u^*}{\partial X} = 13\left(116\left(\frac{Y}{Y_r}\right)^{(1/3)} - 16\right)\left[\frac{60Y + 12Z}{(X + 15Y + 3Z)^2}\right], \tag{A.4d}$$

$$\begin{aligned}\frac{\partial u^*}{\partial Y} = {} & 13 \times \left(116\left(\frac{Y}{Y_r}\right)^{(1/3)} - 16\right)\left[\frac{-60\mathrm{X}}{(X + 15Y + 3Z)^2}\right] \\ & + \left[\frac{4X}{(X + 15Y + 3Z)}\right]\left(\frac{13 \times 116(\frac{1}{Y_r})^{\frac{1}{3}} Y^{(-2/3)}}{3}\right) \\ & - \left(\frac{4X_r}{X_r + 15Y_r + 3Z_r}\right)\left(\frac{13 \times 116(\frac{1}{\mathrm{Y_r}})^{\frac{1}{3}} \mathrm{Y}^{(-2/3)}}{3}\right),\end{aligned} \tag{A.4e}$$

$$\frac{\partial u^*}{\partial Z} = 13\left(116\left(\frac{Y}{Y_r}\right)^{(1/3)} - 16\right)\left[\frac{-12X}{(X + 15Y + 3Z)^2}\right], \tag{A.4f}$$

$$\frac{\partial v^*}{\partial X} = 13\left(116\left(\frac{Y}{Y_r}\right)^{(1/3)} - 16\right)\left[\frac{-9\mathrm{Y}}{(X + 15Y + 3Z)^2}\right], \tag{A.4g}$$

$$\begin{aligned}\frac{\partial v^*}{\partial Y} = {} & 13\left(116\left(\frac{Y}{Y_r}\right)^{(1/3)} - 16\right)\left[\frac{9\mathrm{X} + 27\mathrm{Z}}{(X + 15Y + 3Z)^2}\right] \\ & + \left[\frac{9\mathrm{Y}}{(X + 15Y + 3Z)}\right]\left(\frac{13 \times 116(\frac{1}{Y_r})^{\frac{1}{3}} Y^{(-2/3)}}{3}\right) \\ & - \left(\frac{9Y_r}{X_r + 15Y_r + 3Z_r}\right)\left(\frac{13 \times 116(\frac{1}{\mathrm{Y_r}})^{\frac{1}{3}} \mathrm{Y}^{(-2/3)}}{3}\right),\end{aligned} \tag{A.4h}$$

$$\frac{\partial v^*}{\partial Z} = 13\left(116\left(\frac{Y}{Y_r}\right)^{(1/3)} - 16\right)\left[\frac{-27\mathrm{Y}}{(X + 15Y + 3Z)^2}\right]. \tag{A.4i}$$

A.4 From $L^{'}$, $a^{'}$, $b^{'}$ to L', C', h'

The Jacobian for this transformation is

$$\frac{\partial(L',C',h')}{\partial(L^{'},a^{'},b^{'})} = \begin{bmatrix} \frac{\partial L'}{\partial L^{'}} & \frac{\partial L'}{\partial a^{'}} & \frac{\partial L'}{\partial b^{'}} \\ \frac{\partial C'}{\partial L^{'}} & \frac{\partial C'}{\partial a^{'}} & \frac{\partial C'}{\partial b^{'}} \\ \frac{\partial h'}{\partial L^{'}} & \frac{\partial h'}{\partial a^{'}} & \frac{\partial h'}{\partial b^{'}} \end{bmatrix} = \begin{bmatrix} 1 & 0 & 0 \\ 0 & \frac{\partial C'}{\partial a^{'}} & \frac{\partial C'}{\partial b^{'}} \\ 0 & \frac{\partial h'}{\partial a^{'}} & \frac{\partial h'}{\partial b^{'}} \end{bmatrix}. \tag{A.5}$$

where the partial derivatives are as follows:

$$\begin{aligned}
\frac{\partial C'}{\partial a^*} &= \frac{\partial C'}{\partial a'} \times \frac{\partial a'}{\partial a^*} \\
\frac{\partial C'}{\partial a'} &= \frac{a'}{\sqrt{a'^2 + b'^2}} \\
\frac{\partial a'}{\partial a^*} &= \frac{\partial a^*}{\partial a^*} + \frac{\partial}{\partial a^*}(Ga^*) = (1+G) + a^* \frac{\partial G}{\partial a^*} \\
\frac{\partial G}{\partial a^*} &= \frac{\partial G}{\partial C^*} \times \frac{\partial C^*}{\partial a^*} \\
&= \frac{a^*}{\sqrt{a^{*2} + b^{*2}}} \frac{\partial G}{\partial C^*} = \frac{a^*}{C^*} \frac{\partial G}{\partial C^*} \\
\frac{\partial G}{\partial C^*} &= -\frac{1}{4} \frac{1}{\sqrt{\frac{C^{*7}}{C^{*7}+25^7}}} \left[\frac{(C^{*7}+25^7)7C^{*6} - C^{*7}(7C^{*6})}{(C^{*7}+25^7)^2} \right] \\
&= -\frac{1}{4} \frac{175 \times 25^6 C^{*5/2}}{(C^{*7}+25^7)^{3/2}} \\
\frac{\partial C'}{\partial a^*} &= \frac{a'}{\sqrt{a'^2 + b'^2}} \left[(1+G) + \frac{a^{*2}}{C^*} \left(-\frac{1}{4} \frac{175 \times 25^6 C^{*5/2}}{(C^{*7}+25^7)^{3/2}} \right) \right]
\end{aligned} \tag{A.6a}$$

$$\begin{aligned}
\frac{\partial C'}{\partial b^*} &= \frac{\partial C'}{\partial b'} \times \frac{\partial b'}{\partial b^*} + \frac{\partial C'}{\partial a'} \times \frac{\partial a'}{\partial b^*} \\
&= \frac{b'}{\sqrt{a'^2 + b'^2}} + \frac{a'}{\sqrt{a'^2 + b'^2}} \left(a^* \frac{\partial G}{\partial b^*} \right) \\
\frac{\partial G}{\partial b^*} &= \frac{\partial G}{\partial C^*} \times \frac{\partial C^*}{\partial b^*} \\
&= \frac{b^*}{C^*} \left(-\frac{1}{4} \frac{175 \times 25^6 C^{*5/2}}{(C^{*7}+25^7)^{3/2}} \right) \\
\frac{\partial C'}{\partial b^*} &= \frac{b'}{\sqrt{a'^2 + b'^2}} + \frac{a'}{\sqrt{a'^2 + b'^2}} \frac{a^* b^*}{C^*} \left(-\frac{1}{4} \frac{175 \times 25^6 C^{*5/2}}{(C^{*7}+25^7)^{3/2}} \right)
\end{aligned} \tag{A.7a}$$

$$\begin{aligned}\frac{\partial h'}{\partial a'} &= \left(\frac{\partial h'}{\partial a'} \times \frac{\partial a'}{\partial a^*}\right) \\ &= \left(\frac{1}{1+(b'/a')^2} \cdot \frac{-b'}{a'^2}\right) \frac{\partial a'}{\partial a^*} \\ &= \frac{-b'}{C'^2} \frac{\partial a'}{\partial a^*} \\ &= \frac{-b'}{C'^2}\left[(1+G) + \frac{a^{*2}}{C^*}\left(-\frac{1}{4}\frac{175 \times 25^6 C^{*5/2}}{(C^{*7}+25^7)^{3/2}}\right)\right]\end{aligned} \tag{A.8a}$$

$$\begin{aligned}\frac{\partial h}{\partial b'} &= \left(\frac{\partial h'}{\partial b'} \times \frac{\partial b'}{\partial b^*}\right) \\ &= \left(\frac{1}{1+(b'/a')^2} \cdot \frac{1}{a'}\right) \\ &= \frac{a'}{C'^2}\end{aligned} \tag{A.9a}$$

A.5 From L_{OSA}, G, J to L_E, G_E, J_E

$$\frac{\partial(L_E, G_E, J_E)}{\partial(L_{OSA}, G, J)} = \begin{bmatrix} \frac{\partial L_E}{\partial L_{OSA}} & \frac{\partial L_E}{\partial G} & \frac{\partial L_E}{\partial J} \\ \frac{\partial G_E}{\partial L_{OSA}} & \frac{\partial G_E}{\partial G} & \frac{\partial G_E}{\partial J} \\ \frac{\partial J_E}{\partial L_{OSA}} & \frac{\partial J_E}{\partial G} & \frac{\partial J_E}{\partial J} \end{bmatrix}, \tag{A.10}$$

where the calculation of all partial derivatives are as follows:

A. DETAILED EXPRESSIONS FOR THE JACOBIANS

$$\frac{\partial L_E}{\partial L_{OSA}} = \frac{10}{a_L + 10 b_L L_{OSA}}, \tag{A.11a}$$

$$\frac{\partial L_E}{\partial G} = 0, \tag{A.11b}$$

$$\frac{\partial L_E}{\partial J} = 0, \tag{A.11c}$$

$$\frac{\partial G_E}{\partial L_{OSA}} = 0, \tag{A.11d}$$

$$\begin{aligned}\frac{\partial G_E}{\partial G} &= -\frac{\partial}{\partial G}\left(\frac{C_E}{C_{OSA}} \cdot G\right) \\ &= -\left(\frac{C_E}{C_{OSA}} + G \cdot \frac{\partial}{\partial G}\left(\frac{C_E}{C_{OSA}}\right)\right)\end{aligned}$$

$$\frac{\partial}{\partial G}\left(\frac{C_E}{C_{OSA}}\right) = \frac{\partial (C_E/C_{OSA})}{\partial C_{OSA}} \cdot \frac{\partial C_{OSA}}{\partial G} \tag{A.11e}$$

$$\frac{\partial (C_E/C_{OSA})}{\partial C_{OSA}} = \frac{C_{OSA}\left(\frac{\partial C_E}{\partial C_{OSA}}\right) - C_E}{C_{OSA}^2} \tag{A.11f}$$

$$\frac{\partial C_E}{\partial C_{OSA}} = \frac{10}{a_c + 10 b_c C_{OSA}} \tag{A.11g}$$

$$\frac{\partial C_{OSA}}{\partial G} = \frac{G}{C_{OSA}} \tag{A.11h}$$

$$\frac{\partial G_E}{\partial G} = -\left(\frac{C_E}{C_{OSA}} + G\left[\frac{C_{OSA}(10/a_c + 10 b_c C_{OSA}) - C_E}{C_{OSA}^2}\right]\frac{G}{C_{OSA}}\right), \tag{A.11i}$$

$$\begin{aligned}\frac{\partial G_E}{\partial J} &= -G \cdot \frac{\partial}{\partial J}\left(\frac{C_E}{C_{OSA}}\right) \\ &= -G \cdot \frac{\partial (C_E/C_{OSA})}{\partial C_{OSA}} \frac{\partial C_{OSA}}{\partial J}\end{aligned}$$

$$\frac{\partial C_{OSA}}{\partial J} = \frac{J}{C_{OSA}} \tag{A.11j}$$

$$= -G\left[\frac{C_{OSA}(10/a_c + 10 b_c C_{OSA}) - C_E}{C_{OSA}^2}\right]\frac{J}{C_{OSA}}, \tag{A.11k}$$

$$\frac{\partial J_E}{\partial L_{OSA}} = 0, \tag{A.11l}$$

$$\frac{\partial J_E}{\partial G} = -J\left[\frac{C_{OSA}(10/a_c + 10 b_c C_{OSA}) - C_E}{C_{OSA}^2}\right]\frac{G}{C_{OSA}}, \tag{A.11m}$$

$$\frac{\partial J_E}{\partial J} = -\left(\frac{C_E}{C_{OSA}} + J\left[\frac{C_{OSA}(10/a_c + 10 b_c C_{OSA}) - C_E}{C_{OSA}^2}\right]\frac{J}{C_{OSA}}\right). \tag{A.11n}$$

In the OSA-UCS space, the coordinates J and G are also related with the lightness function (L_{OSA}). So, to transfer the differential colour vectors $[dL_{OSA}\ dG\ dJ]$ into $[dx_{10}\ dy_{10}\ dY_{10}]$, we have to split the differential lightness vector dL_{OSA} and the differential coordinates dG and dJ in two parts.

A.6 From x_{10}, y_{10}, Y_{10} to L_{OSA}

$$\frac{\partial L_{OSA}}{\partial(x_{10}, y_{10}, Y_{10})} = \frac{\partial L_{OSA}}{\partial Y_0} \begin{bmatrix} \frac{\partial Y_0}{\partial x_{10}} & \frac{\partial Y_0}{\partial y_{10}} & \frac{\partial Y_0}{\partial Y_{10}} \end{bmatrix}, \tag{A.12}$$

$$\frac{\partial L_{OSA}}{\partial Y_0} = 5.9 \left[\frac{1}{3} Y_0^{-2/3} + 0.042 \cdot \frac{1}{3} (Y_0 - 30)^{-2/3} \right] \frac{1}{\sqrt{2}} \tag{A.13a}$$

$$\frac{\partial Y_0}{\partial x_{10}} = Y_{10}(4.4934\, 2x_{10} - 4.2760 y_{10} - 1.3744) \tag{A.13b}$$

$$\frac{\partial Y_0}{\partial y_{10}} = Y_{10}(4.3034 \cdot 2y_{10} - 4.2760 x_{10} - 2.5643) \tag{A.13c}$$

$$\frac{\partial Y_0}{\partial Y_{10}} = (4.4934 x_{10}^2 + 4.3034 y_{10}^2 - 4.2760 x_{10} y_{10} - 1.3744 x_{10} - 2.5643 y_{10} + 1.8103) \tag{A.13d}$$

From x_{10}, y_{10}, Y_{10} to G, J

$$\frac{\partial(G, J)}{\partial(x_{10}, y_{10}, Y_{10})} = \frac{\partial(G, J)}{\partial(L, A, B, C)} \frac{\partial(L, A, B, C)}{\partial(x_{10}, y_{10}, Y_{10})} \tag{A.14}$$

where $\frac{\partial(G,J)}{\partial(L,A,B,C)}$ and $\frac{\partial(L,A,B,C)}{\partial(x_{10},y_{10},Y_{10})}$ are 2×4 and 4×3 Jacobian matrics respectively.

$$\begin{bmatrix} \frac{\partial G}{\partial LOSA} & \frac{\partial G}{\partial A} & \frac{\partial G}{\partial B} & \frac{\partial G}{\partial C} \\ \frac{\partial J}{\partial LOSA} & \frac{\partial J}{\partial A} & \frac{\partial J}{\partial B} & \frac{\partial J}{\partial C} \end{bmatrix} \begin{bmatrix} \frac{\partial L_{OSA}}{\partial x_{10}} & \frac{\partial LOSA}{\partial y_{10}} & \frac{\partial L_{OSA}}{\partial Y_{10}} \\ \frac{\partial A}{\partial x_{10}} & \frac{\partial A}{\partial y_{10}} & \frac{\partial A}{\partial Y_{10}} \\ \frac{\partial B}{\partial x_{10}} & \frac{\partial B}{\partial y_{10}} & \frac{\partial B}{\partial Y_{10}} \\ \frac{\partial C}{\partial x_{10}} & \frac{\partial C}{\partial y_{10}} & \frac{\partial C}{\partial Y_{10}} \end{bmatrix} \tag{A.15}$$

A. DETAILED EXPRESSIONS FOR THE JACOBIANS

Derivation of all partial derivatives of Equation (A.15) is given below:

$$\begin{aligned}\frac{\partial G}{\partial L_{OSA}} &= T_G \frac{\partial S_G}{\partial L_{OSA}} \\ &= T_G \cdot -2 \times 0.764 \\ T_G &= 0.9482[\ln A - \ln(0.9366B)] - 0.3175[\ln B - \ln(0.9807C)]\end{aligned} \tag{A.16a}$$

$$\begin{aligned}\frac{\partial J}{\partial L_{OSA}} &= T_J \frac{\partial S_J}{\partial L_{OSA}} \\ &= T_J \cdot 2 \times 0.57354 \\ T_J &= 0.1792[\ln A - \ln(0.9366B)] + 0.9837[\ln B - \ln(0.9807C)]\end{aligned} \tag{A.16b}$$

$$\begin{aligned}\frac{\partial G}{\partial A} &= S_G \frac{0.9482}{A}; \quad \frac{\partial G}{\partial B} = S_G \frac{-0.9482 - 0.3175}{B}; \quad \frac{\partial G}{\partial C} = S_G \frac{0.3175}{C} \\ \frac{\partial J}{\partial A} &= S_J \frac{0.1792}{A}; \quad \frac{\partial J}{\partial B} = S_J \frac{-0.1792 + 0.9837}{B}; \quad \frac{\partial J}{\partial C} = S_J \frac{-0.9837}{C}\end{aligned} \tag{A.16c}$$

Where, S_G and S_J values are equal to $-2(0.764L_{OSA} + 9.2521)$ and $2(0.5735L_{OSA} + 7.0892)$ respectively.

$$\begin{aligned}&\begin{bmatrix} \frac{\partial A}{\partial x_{10}} & \frac{\partial A}{\partial y_{10}} & \frac{\partial A}{\partial Y_{10}} \\ \frac{\partial B}{\partial x_{10}} & \frac{\partial B}{\partial y_{10}} & \frac{\partial B}{\partial Y_{10}} \\ \frac{\partial C}{\partial x_{10}} & \frac{\partial C}{\partial y_{10}} & \frac{\partial C}{\partial Y_{10}} \end{bmatrix} \\ &= \begin{bmatrix} 0.6597 & 0.4492 & -0.1089 \\ -0.3053 & 1.2126 & 0.0927 \\ -0.0374 & 0.4795 & 0.5579 \end{bmatrix} \begin{bmatrix} \frac{Y_{10}}{y_{10}} & \frac{-x_{10}Y_{10}}{y_{10}^2} & \frac{x}{y_{10}} \\ 0 & 0 & 1 \\ \frac{-Y_{10}}{y_{10}} & \frac{(x_{10}-1)Y_{10}}{y_{10}^2} & \frac{1-x_{10}-y_{10}}{y_{10}} \end{bmatrix}\end{aligned} \tag{A.17}$$

Appendix B

Figures

B.1 BFD-P ellipses in the CIELAB

Figure B.1: BFD-P ellipses in the CIELAB color space - Enlarged 1.5 times.

B.2 Riemannized ΔE_{00} predicted BFD-P ellipses in the CIELAB

Figure B.2: Riemannized ΔE_{00} ellipses having the same center as BFD-P ellipses in the CIELAB color space - Enlarged 1.5 times.

B.3 The OSA-UCS ΔE_E predicted BFD-P ellipses in the CIELAB

B.4 ΔE^*uv predicted BFD-P ellipses in the CIELAB

Figure B.3: The OSA-UCS ΔE_E ellipses having the same center as BFD-P ellipses in the CIELAB color space - Enlarged 1.5 times.

Figure B.4: The ΔE^*uv ellipses having the same center as BFD-P ellipses in the CIELAB color space - Enlarged 1.5 times.